Iceland Liechtenstein Norway grants

Norway grants

Project

Initiative No. EHP-BFNU-OVNKM-4-149-2024

funded under the Fund for Bilateral Relations within the framework of EEA and Norway Grants 2014-2021.

Institute of Structural Mechanics, Faculty of Civil Engineering, Brno University of Technology (BUT)

AND

Dept. of Process, Energy and Environmental Technology, Faculty of Technology, Natural Sciences and Maritime Sciences, Univ. of South-Eastern Norway (USN)

Bilateral cooperation between USN and BUT

Reliability and sustainability of structures

Seminar report

Location and date

Brno, Czech Republic, 23–24/5/2024

Porsgrunn, Norway, 3–5/6/2024

Introduction

This report documents the content and results of the seminars under Initiative No. EHP-BFNU-OVNKM-4-149-2024 funded under the Fund for Bilateral Relations within the framework of EEA and Norway Grants 2014-2021.

The initiative included two two-day seminars held in May 2024 in Brno, Czech Republic, at Brno University of Technology and in June 2024 in Porsgrunn, Norway, at the University of South-Eastern Norway. The seminars aimed to share knowledge and experience in the field of reliability and sustainability of buildings, understand the specific aspects of this issue in each country, establish cooperation between researchers, and create a basis for future joint research, publications, and student exchange.

The seminars comprised lectures by experts from both universities. The list of lecturers and lecture titles is given below. The lecture content can be found in Annexes A-F. Following the lectures, an expert panel was held to discuss theoretical, practical, economic and environmental aspects of reliability and sustainability design and analyses of transport infrastructure and offshore wind turbines.

The second day of seminars was dedicated to technical tours. Visitors visited the experimental laboratories of both universities and the construction sites of the newly built Eifage-Nye Veier E18 motorway.

Summary of the seminars:

Lectures

Hadi Amlashi	*Some aspects on the use of reliability techniques in offshore wind turbine design*	Annex A
Drahomír Novák	*Stochastic assessment of concrete structures: advanced FEM modelling and case studies*	Annex B
Lars Erik Øi	*Cost, size, and structure optimization of CO_2 absorber columns onshore and offshore*	Annex C
David Lehký	*Determination of mechanical fracture parameters using machine learning-based inverse analysis*	Annex D
Mequanent M. Alamnie	*Mechanistic asphalt pavement damage prediction and modelling for Sustainable roads*	Annex E
Lukáš Novák	*Uncertainty quantification in structural mechanics: point estimates and surrogate models*	Annex F

Panel discussion

Theoretical, practical, economic and environmental aspects of reliability and sustainability design and analyses of transport infrastructure and offshore wind turbines.

Technical tours

Brno	*Laboratory of Institute of Physics of Materials, Czech Academy of Science – Fatigue testing of materials.*
Brno	*Laboratory of Institute of Building Testing – Fracture tests of quasi-brittle materials.*
Porsgrunn	*Laboratories of Dept. of Process, Energy and Environmental Technology, USN – Civil, Mechanical, and Process Engineering laboratories.*
Porsgrunn	*Site excursions of Eifage-Nye Veier E18 motorway – cable-stayed bridge and tunnel.*

Lectures

The content of the individual lectures are briefly presented in this section. The lecture slides can be found in Annexes A-F.

Hadi Amlashi

Some aspects of the use of reliability techniques in offshore wind turbine design

The development of offshore wind turbines is considerably more complex than onshore projects due to the challenges posed by remote locations and harsher environmental conditions, particularly in offshore areas with stronger winds. This requires careful consideration of environmental factors and their impacts. In designing support structures for offshore wind turbines, the conventional approach relies on direct calculations of load effects and resistance, supplemented by safety factors and margins. However, it is crucial for the safety format to transparently account for the inherent uncertainties and variability in loads and resistance. Structural reliability methods can be employed to calibrate the safety factors to achieve this goal. This approach is essential to establish a robust support structure for offshore wind turbines. In this first lecture, Hadi Amlashi presented some aspects of using reliability techniques in offshore wind turbine design. The implication of risk and reliability-based design approach and structural design criteria are introduced. When addressing varying load combinations, it is recommended to employ slightly smaller safety factors for wave-induced loads and more prominent safety factors for wind-induced loads within typical moment ratios. The lecture addresses identifying uncertainty measures in load effects and strength specific to offshore wind turbines. It also showcases the proposed methodology for mooring line systems for floating offshore wind turbines.

Drahomír Novák

Stochastic assessment of concrete structures: advanced FEM modelling and case studies

In the second lecture, Drahomír Novák presented an integrated methodology for reliability and durability analysis of structures consisting of several subtopics such as nonlinear finite element method (NLFEM) analysis, uncertainties propagation of Monte Carlo (MC) type, reliability analysis, sensitivity analysis, parameters identification, model updating, surrogate modelling, material degradation aspects and safety formats. Consideration of uncertainties in structural engineering is a growing topic because it provides valuable information on the reliability of structures in time while addressing life-cycle aspects. Utilisation of nonlinear NLFEM and MC type simulation is essential for modelling of the concrete structures like bridges and performing its reliability assessments. The aim of the stochastic analysis is to propagate uncertainties through a computational NLFEM model to gain statistical information from the output as well as information about the sensitivity of the mathematical model to uncertainties in input variables. However, in structural engineering, the mathematical model can be quite complex and uncertainty propagation solved by classical MC approach is very difficult to perform as MC type simulation involves large number of numerical evaluations of structural response. Therefore, advanced statistical and reliability techniques must be applied. Author and his co-workers were active in this field combining nonlinear analysis and reliability approaches for concrete structures, during development an urgent need for efficient combination of several approaches and methods appeared. The lecture focused on several keystones of such integrated approach for a routine complex assessment utilizing developed software tools and practical application of the approach for selected case studies.

Lars Erik Øi

Cost, size, and structure optimization of CO2 absorber columns onshore and offshore

The conventional design of CO2 absorber columns predominantly involves the use of circular steel columns fitted with structured packing. Historically, concrete has been favored for the construction of large-scale structures due to its cost efficiency and robust nature. In recent times, there has been a shift towards the adoption of rectangular concrete shapes as the standard for new land-based CO2 capture projects. Conversely, compact circular steel columns are being recommended for offshore applications, aligning with the specific requirements of such settings. A significant challenge in achieving cost optimization lies in the higher relative costs of process equipment size and weight for offshore applications when compared to land-based projects.

David Lehký

Determination of mechanical fracture parameters using machine learning-based inverse analysis

Due to the increasing worldwide emphasis on the environmental and economic sustainability of material production, much current research is focused on the development of innovative building materials. When studying material behavior, its mechanical fracture properties are determined by conducting laboratory tests. In many cases, attention is focused on analyzing the properties associated with resistance to crack formation and propagation, rather than on the maximum strength of the material. Mechanical fracture parameters help us to understand the relation between the macroscopic response of the specimen and its microstructural evolution during cracking. This is crucial in the design and modeling of newly developed composites. In his lecture, David Lehký introduces artificial neural network (ANN)-based inverse analysis method to identify mechanical fracture parameters from fracture tests. In case of composite materials with the wide range of experimental responses, an ensemble of ANN is recommended to be employed. Lecture also touches the problem of identification of statistical characteristics of parameters. The capabilities of the proposed identification system and software were demonstrated using example of material parameter identification of reinforced concrete wall subjected to shear failure.

Mequanent M. Alamnie

Mechanistic asphalt pavement damage prediction and modelling for Sustainable roads

Asphalt concrete is one of the most important road-building materials that exhibit extraordinary chemical, physical and mechanical properties. It is exposed to variable vehicular and environmental loading. The crucial mechanical properties of asphalt concrete are viscoelastic, viscoplastic, viscodamage (deformability), cracking and fracture properties. Thus, asphalt mixture characterizations are focused on stiffness and stiffness change, fatigue and damage law evolution, permanent deformation (viscoplasticity), and cracks and crack propagation at low temperatures. The mechanistic-empirical (ME) pavement design approach attempts to model these four properties for accurate pavement life prediction. In this lecture, the linear viscoelastic and damage responses (fatigue and rutting) of asphalt concrete were presented. A new damage test procedure (Sequential test procedure) was applied to analyze the damage interaction between the permanent deformation and fatigue. The linear viscoelastic (LVE) properties of asphalt concrete are crucial for mechanistic pavement design. A damage model (fatigue, rutting, or both) takes LVE stiffness as a key parameter. The reliability of pavement structural life prediction relies on the accurate modelling of the associated damage modes as a system, on the robustness of the test methods, and advancement of theories. Based on observations and design experiments, the permanent deformation-fatigue damage interaction sequence dominates the asphalt concrete damage mechanism. Moreover, the Mechanistic pavement design approach is a state-of-the-art design philosophy. This method is founded on the reliability of test methods and holistic (coupling) techniques. The continuum damage mechanics (CDM) theory is the foundation for quantifying the damage. The variables considered in pavement design are many and complicated. Thus, the integration of the reliability approach with the fundamental continuum method can be the way forward to predict pavement life more accurately. Furthermore, a unified damage model can be formulated using the reliability concepts with fundamental constitutive models of asphalt concrete.

Lukáš Novák

Uncertainty quantification in structural mechanics: point estimates and surrogate models

In his lecture, Lukáš Novák addresses topic of uncertainty quantification using surrogate models. Surrogate modeling of costly mathematical models representing physical systems is challenging since it is necessary to fulfill physical constraints in the whole design domain together with specific boundary condition of investigated systems. Moreover, it is typically not possible to create a large experimental design covering whole input space due to computational burden of original models. Therefore, there has been recently a considerable interest in developing surrogate models capable of satisfying physical constraints –spawning an entirely new field of physics-informed machine learning. In this lecture, a recently introduced methodology for the construction of physics-informed polynomial chaos expansion (PC2) that combines the conventional experimental design with additional constraints from the physics of the model was presented. Physical constraints in PC2 can be represented by a set of differential equations and specified boundary condition allowing surrogate model to be constructed more accurately with fewer physics-based model evaluations. Although the main purpose of the PC2 lies in combining data and physical constraints, it is also possible to construct surrogate model only from differential equations and boundary conditions alone without requiring evaluations of the original model. It is well known that a significant advantage of surrogate models in form of polynomial chaos expansions are their possibilities in uncertainty quantification including statistical and sensitivity analysis. Efficient uncertainty quantification by PC2 can be performed through analytical post-processing of a reduced basis filtering out the influence of all deterministic space-time variables. Once the surrogate model with physical constraints is constructed, it is possible to perform realistic reliability analysis to ensure that analyzed physical system will satisfy the given safety requirements.

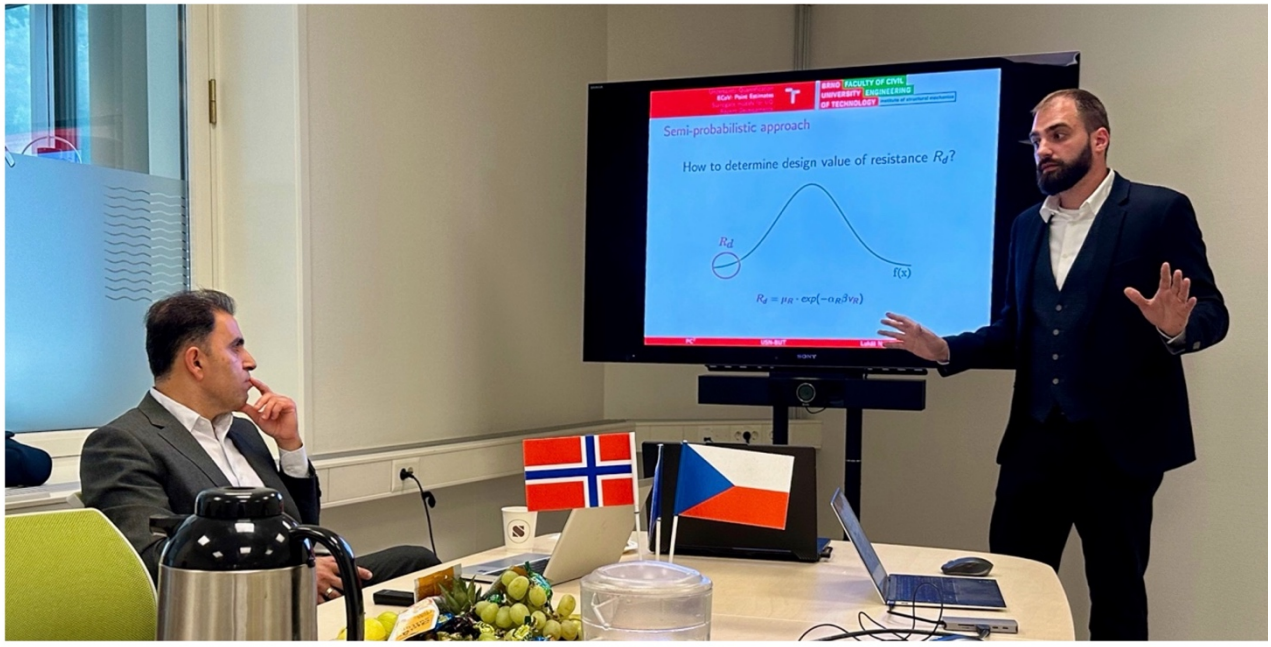

Panel discussion

Theoretical, practical, economic and environmental aspects of reliability and sustainability design and analyses of transport infrastructure and offshore wind turbines were discussed. The presenting experts, together with university staff and students, discussed the topics presented in the lectures and tried to place them in the broader context of sustainability of construction, material resources and climate protection. The topic of CO_2 separation and storage in underwater reservoirs proved to be very attractive. Participants were interested in experimental research in this field, practical applications and challenges for future research. The specifics of the assessment of existing structures in both countries, the specifics of the standards used and the extent to which advanced computing techniques and methods are involved in this activity were also discussed. The need for sharing theoretical and practical knowledge to increase the efficiency of maintenance of transport infrastructure and offshore structures was demonstrated. Surrogate modelling using both data-driven and physics-based models was also a widely debated topic, which has very strong potential in reliability engineering. Also, the application of machine learning-based models and their ability to generalize and adapt to new data is proving to be a very promising research direction in engineering. The panel discussion ended with an invitation to technical tours, which presented some parts of the experimental research necessary to validate the developed methods and software tools or to obtain data of computational models.

Technical tours

On the second day of the seminars there were technical tours, the course of which is described in this section.

Czech Academy of Science, Brno, Czech Republic

Laboratory of Institute of Physics of Materials – Fatigue testing of materials

During the visit to the Institute of Physics of Materials, Czech Academy of Science, the participants were shown three laboratories – low cycle fatigue and high cycle fatigue laboratories and creep laboratory.

The main interest of the low cycle fatigue group is the study of fatigue damage mechanisms, interaction of low cycle fatigue with creep at elevated temperatures, structural changes and damage evolution in high temperature symmetric and asymmetric loading, cracking and fatigue fracture of laminate composites, effect of the coatings on the cyclic plasticity and fatigue life of advanced materials, and short crack growth kinetics in advanced steels. Some basic theoretical backgrounds were presented to the participants together with the example of low fatigue tests performed on selected machines including MTS 809 axial–torsional test system, MTS 880 servo-hydraulic testing machine for thermo-mechanical fatigue, etc.

The research activities in the high cycle fatigue group are focused on the study of the nature and quantitative description of the fatigue processes in all fatigue stages. The main goal of the research is to contribute to better understanding of cyclic plasticity at low amplitudes, crack initiation and threshold values of fatigue crack propagation and to the fracture-mechanical description of the fatigue crack behavior. Theoretical and experimental studies are focused on the relation between microstructure, microstructure evolution during damage progress, and macroscopic fatigue and fatigue/creep properties. The numerical estimation of the fracture parameters and simulations of the fracture behavior are an important part of the research as well. The formulation of crack stability criteria for non-homogenous materials, notches and layered structures is a live issue studied in the group. Owing to this, the spectrum of studied materials is rapidly increasing. At present non-metallic materials such as polymers, polymer or ceramic based composites and advanced building materials are being analyzed.

The last visited laboratory focuses on creep tests and study of processes occurring upon creep deformation of materials. The research infrastructure of the Institute provides a unique capacity of almost 40 creep devices suitable for identification of creep characteristics, such as the time until rupture, creep rate or overall creep elongation. Both tension and compression experiments are possible, under controlled load and stress, within the temperature range from 20°C to 1,000°C (commonly). The two most recently installed devices enable carrying out experiments at the temperature up to 1,400°C, either in vacuum or in protective (modified) atmosphere. There are also devices for the small punch test available.

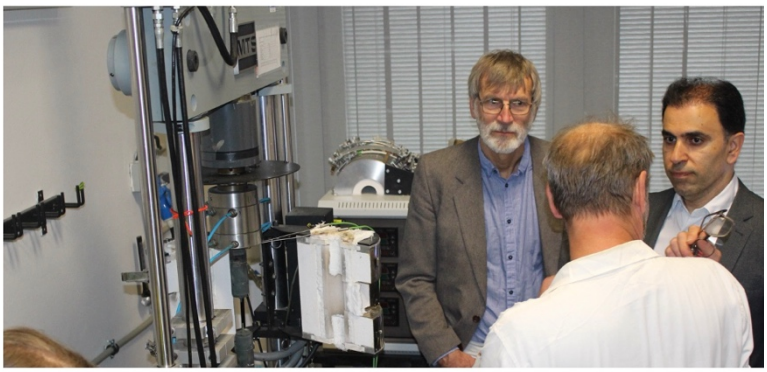


MTS
880
Material
Test System

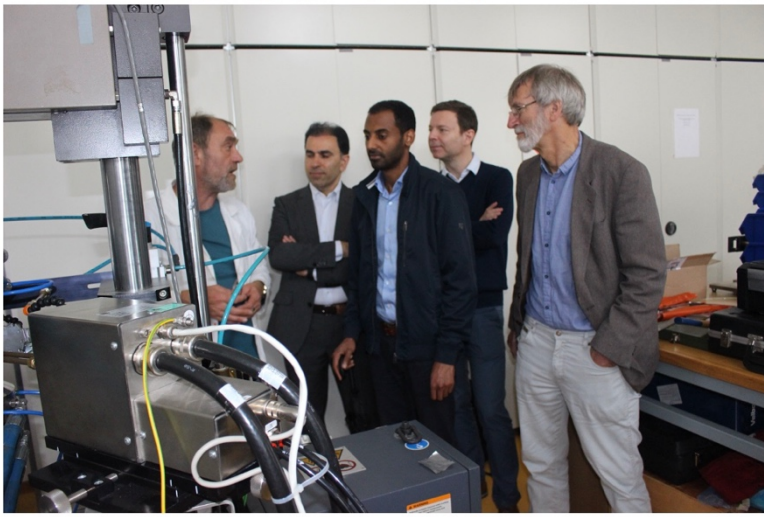

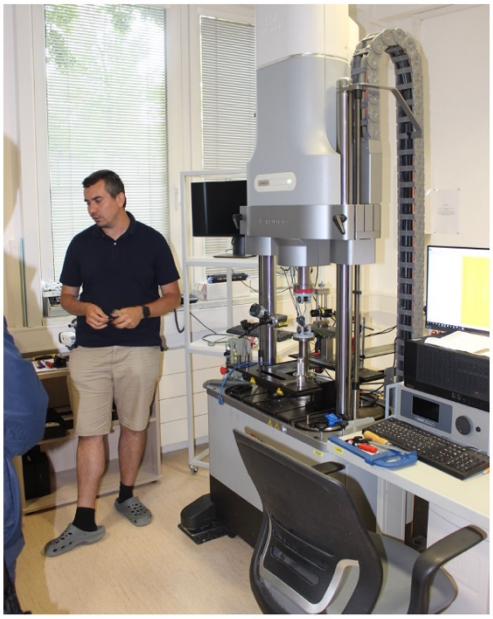

Brno University of Technology, Brno, Czech Republic

Laboratory of Institute of Building Testing – Fracture tests of quasi-brittle materials

Theoretical and practical aspects of testing fracture parameters of quasi-brittle materials were presented to the participants in the laboratory of the Institute of Building Testing. This institute is focused on the research and development of diagnostic and test methods in the field of civil engineering, assessment and evaluation of existing structures, laboratory and field testing of structural units, elements, components, details, and models, including specific properties of building materials. One of the groups focuses on testing of mechanical fracture parameters of specimens with edge notch loaded in a suitable test configuration such as three-point bending test or wedge splitting test. Theoretical details of evaluation of test records and identification of material parameters using inverse analysis were presented in one of the seminar lectures. In lab, testing machine and related measuring equipment was introduced followed by video demonstration of loading a notched specimen in three-point bending configuration. Participants were able to see development of strains at the vicinity of the notch and a development of magistral crack and surrounding fracture process zone. Aspects of accurate measuring of displacements and recording of post-peak behavior were discussed.


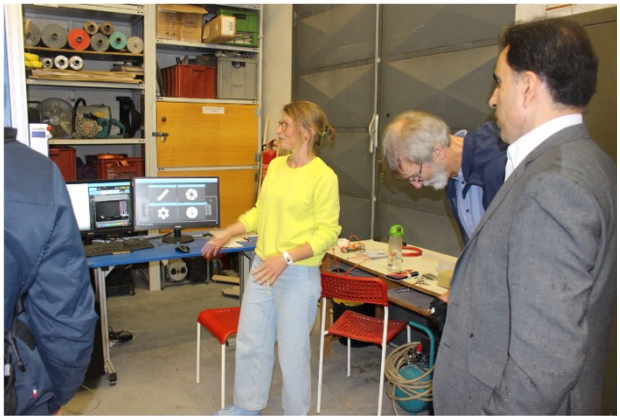

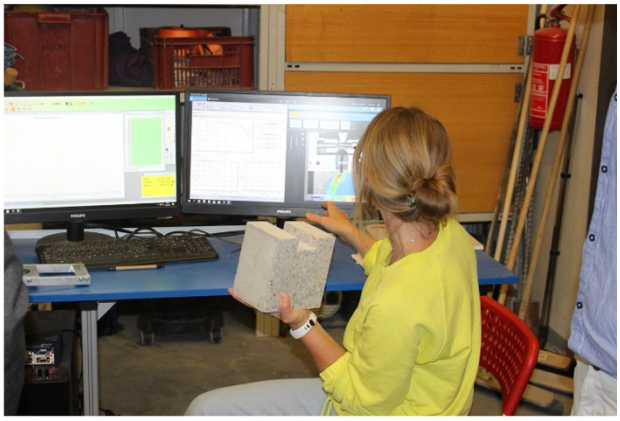

University of South-Eastern Norway, Porsgrunn, Norway

Laboratories of Dept. of Process, Energy and Environmental Technology

Participants visited three different laboratories at USN, Porsgrunn. At first, participants visited the USN's process laboratories, where research projects focused on capturing and analysing carbon dioxide (CO_2) and its environmental impacts were conducted in collaboration with industrial partners. The primary areas of interest include studying mechanisms of amine degradation, assessing various types of amines for their CO_2 absorption capabilities, and developing advanced techniques for accurately analysing CO_2 absorption processes. The equipped laboratory has multiple instruments and apparatus to support the research efforts. These include a gas chromatograph with mass spectrometer (GC-MS) for precise molecular analysis, a rheometer for highly accurate viscosity measurements, a density meter for density determinations, an equilibrium cell for in-depth studies of reaction equilibriums, a Raman spectrometer for molecular and structural analysis, various reactors and autoclaves for experimental setups, as well as multiple gas chromatographs equipped with flame ionisation (FID) and thermal conductivity (TCD) detectors for comprehensive gas analysis. The visit is then followed by a tour of the chemical processing hall that serves as a central space for a wide range of experimental setups dedicated to research in fields such as CO_2 capture, catalysis, and multiphase flow. In the multiphase flow section, researchers have access to state-of-the-art equipment, including ECT/ERT and Gamma meters, enabling precise and detailed analysis of fluid behaviour. The research areas span various topics, including biological purification processes and powder technology. A fully equipped Venturi rig with a Coriolis meter, Gamma meter, and ultrasonic level sensors allows for comprehensive and accurate measurement of various parameters. The facility has a compressed air compressor, providing researchers with the necessary utilities to support their research.

During the visit, the participant had the opportunity to explore the civil engineering lab, which is equipped with tools such as a press and bending rig used for testing the strength of wood and concrete. The lab also contains specialised equipment like bucket drills, wing drills, cone apparatuses for geotechnical investigations, levelling binoculars, plane lasers, total stations, and GNSS equipment for surveying and GIS.

At last, participants visited the mechanical lab of the mechanical department at USN. The lab is equipped to conduct material testing, including tensile testing, deflection, impact toughness, hardness measurement, and microscopy. Additionally, the lab is furnished with equipment for fluid mechanics tasks, such as a pipe resistance calculation rig, a pump curve calculation rig, and a 3D printer capable of producing photopolymer models using UV light. A cooling system with an output of up to 20 kW has been installed in connection with thermodynamics. The central workshop has a lathe, milling machine, sheet metal shears, plate crackers, column drills, Tig, Mig, gas and stick welding, plasma cutting equipment, and other mechanical tools. This workshop fabricates experimental equipment for bachelor's, master's, and PhD levels.




Eifage-Nye Veier E18 motorway, Norway

Site excursions – cable-stayed bridge and tunnel

In the second part, participants visited the new Eifage-Nye Veier E18 motorway. A project manager in Nye-Veier first welcomed them at the site. The "Nye Veier e18 Rugtvedt – Langangen" project is a 17-kilometre expansion of the E18 motorway strategically positioned within the Greenland region. Anticipated to open in 2026, the project will boast a four-lane configuration designed to accommodate a maximum speed limit of 110 km/h. The project involves building six bridges, with the Grenland Bridge as the main focus, and adding two more bridges in the Language area. The planned infrastructure includes six tunnels, covering a total distance of 9 kilometres and an additional 4.2 kilometres of purpose-built daytime roadway. The zoning plan for this motorway has been formally approved, and Eiffage is the contractor constructing it for Nye-veier, the project owner. Two new twin bridges are being built over Langangsfjord, each 400 meters long and with 50-meter-high pillars. The bridges are being designed using the highest BIM standards available.

Conclusions

The seminars aimed to share knowledge and experience in the field of reliability and sustainability of buildings, to understand the specific aspects of this issue in each country, to establish cooperation between researchers and to create a basis for future joint research, publications and student exchange. All parts of the seminar were very beneficial for both sides. The topics of the lectures raised great interest among the audience, which was confirmed by the subsequent panel discussion, where not only the details of the subtopics were discussed, but their setting in a broader engineering-social context. The follow-up technical tours then appropriately complemented the theoretical aspects with a practical component. The participants thus had the opportunity to see the issues in their entirety.

In addition to research and engineering topics, experts from both countries also discussed the possibilities of cooperation in education, student exchange, support for employee mobility, etc. It can be concluded that the joint activity fulfilled its purpose and started cooperation, which both partner institutions are interested in further developing.

Annexes

Annex A
Hadi Amlashi **–** *Some aspects on the use of reliability techniques in offshore wind turbine design*

Annex B
Drahomír Novák – *Stochastic assessment of concrete structures: advanced FEM modelling and case studies*

Annex C
Lars Erik Øi – *Cost, size, and structure optimization of CO_2 absorber columns onshore and offshore*

Annex D
David Lehký – *Determination of mechanical fracture parameters using machine learning-based inverse analysis*

Annex E
Mequanent M. Alamnie – *Mechanistic asphalt pavement damage prediction and modelling for Sustainable roads*

Annex F
Lukáš Novák – *Uncertainty quantification in structural mechanics: point estimates and surrogate models*

Annex A

Hadi Amlashi

Some aspects on the use of reliability techniques in offshore wind turbine design

Some aspects on the use of reliability techniques in offshore wind turbine design

by Hadi Amlashi

Associate professor in structural mechanics, USN

Brno, 23.05.2024

University of South-Eastern Norway

Contents

University of South-Eastern Norway

Relationships between structural failure and safety

Structural failure scenario	Mitigation	Safety measures
Inadequate safety margin to cover normal inherent uncertainties	Appropriate design criteria, such as Sufficient safety factors or increased characteristic loads	Structural reliability analysis
Gross error or lack of proper checks or inefficiency during design, fabrication, installation or operation	QA/QC in engineering and project management processes	Risk analysis
Unknown phenomena	Firsthand Experience and knowledge gain	Lesson learned (case by case basis)

University of South-Eastern Norway

Risk and reliability methods

- What is it?
  - *How to account for the uncertainties in the predicted behaviour under extreme and cyclic load conditions and inspection.*
- Generally classified in to two:
  - Structural Reliability Analysis (SRA)
    - *Determine the failure probability considering fundamental variability, and natural and man-made uncertainties due to lack of knowledge.*
  - Quantitative Risk Analysis (QRA)
    - *Estimation of likelihood of fatalities, environmental damage, or loss*

Structural design criteria

- Structural design criteria refer to serviceability and safety:
  - *Serviceability*: Service experiences and operational issues, i.e., accidental actions and abnormal (SLS and ALS)
  - *Safety*: normal design conditions considering loads and strength,. i.e., ultimate and fatigue limit states (ULS, FLS)

- How to ensure adequate structural safety?
  - *Proper design, load and response monitoring and condition monitoring during its design lifetime.*

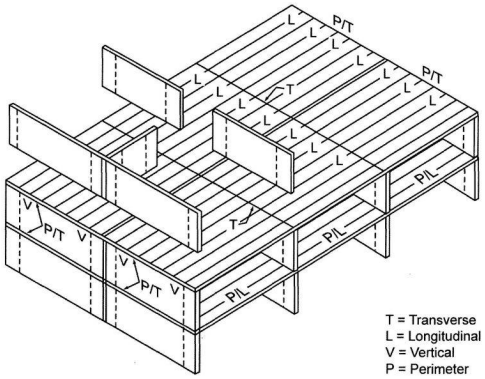

Structural reliability analysis

- Design equation: $R_d > L_d$
  or in partial safety factors format: $\gamma_L L_c = \frac{R_c}{\gamma_R}$

- $P_f = P[g(\boldsymbol{X}) \leq 0] = \int_{g(\boldsymbol{X})\leq 0} f_{\boldsymbol{X}}(\boldsymbol{x}) d_{\boldsymbol{x}}$

  Reliability Index $\beta = \Phi^{-1}(P_f)$

- Methods for calculating the probability of failure:
  - *First-order Reliability Method (FORM)*
  - *Second-order Reliability Method (SORM)*
  - *Monte Carlo Simulations*
  - *Etc.*

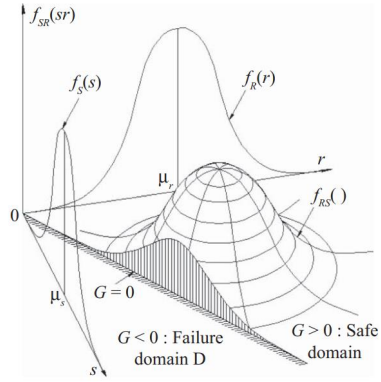

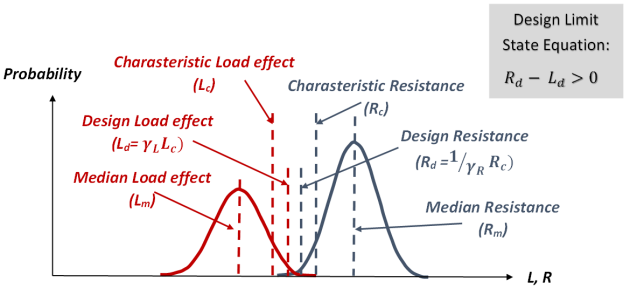

Offshore wind turbines

- Nearly 80% of offshore wind turbines are of the type *monopile supported offshore wind turbines*.
- Reducing the uncertainty in the design of the support structure can significantly contribute to reducing the LCOE, as it can reduce the safety factors.
- What is the implied safety level for support structures defined in design codes, such as IEC 61400-1 (IEC, 2019) and DNV-ST-0126 (DNV, 2021)?

Major sources of uncertainty in offshore wind turbine

- *Wind turbine*: Structural, mechanical and electrical systems, production, installation, operation and maintenance, etc.
- *Wind*: Turbulence intensity, Wind shear, Coherence, Wind load model, etc.
- *Wave and current*: Long-term environmental description (load model, wave kinematics, spectrum, spreading) , wave-wind-current directionalities, etc.
- *Pile-soil interaction*: Soil model (damping and stiffness), scouring, etc.
- Simplified (mathematical) models
- Both *model and parameter uncertainty* are important

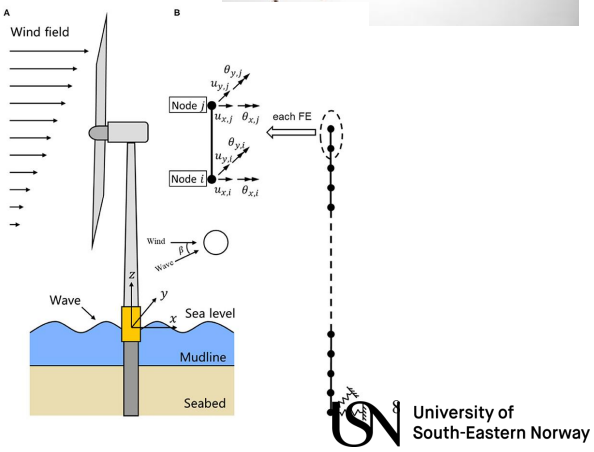

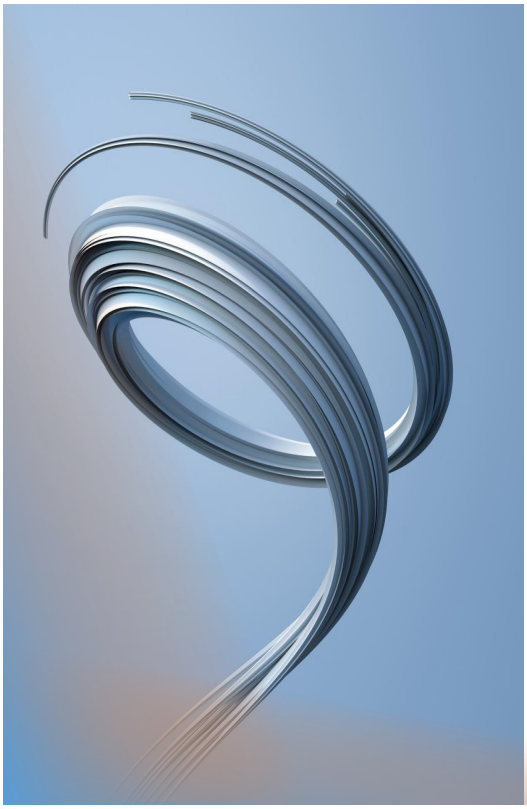

Wind model uncertainty

- Medium-fidelity models like the Kaimal spectrum or Mann model Vs. high-fidelity methods based on computational fluid mechanics, such as large eddy simulations (LES), and measurements.
- Differences in wind shear profiles and coherent structures has a significant impact on the predicted tower fore-aft bending moments, as well as tower torsion and blade root moments
- The effect of turbulence intensity should also be notified.

Wave model uncertainty

- Linear or second-order or higher-order wave kinematics at different sea states
- Differences in responses due to use of Pierson-Moskowitz or JONSWAP wave spectrum
- The directionality of environmental loads in operational conditions is important, since aerodynamic damping is significant for in-line wind and negligible in the cross-wind direction.
- Differences in computer codes for OWTs gives different model uncertainties due to different structural models, implementation of aerodynamic loads and discretization of the hydrodynamic loads, etc.

Maximum fore-aft bending moment wave-to-wind ratio

- Expected value of Maximum fore-aft bending moment for wind load only (*Mv*), wave load only (Myy,w) and relative ration of Myy,w/Myy,v (Env. Condition Set 1., short-term statistics, Barreto et al. 2020) - Fully-coupled aero-hydro-servo-elastic nonlinear time-domain response analysis
- The relative bending moment of $M_{yy,w}/M_{yy,v}$ varies between ***0.2-0.6*** depending on environmental condition

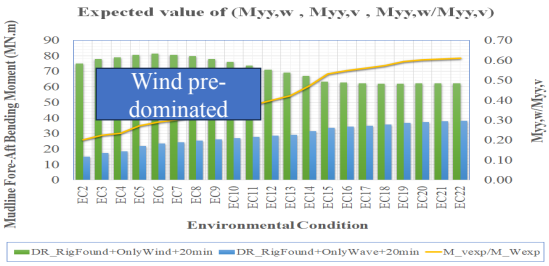

- Representative ULS design load combination cases for the monopile tower global bending (IEC 61400-3-1):

Load combinations $\varphi_w = 1$

#	Wind	Wave	Wind-Wave Directionality (misalignment)
LC1	U1	W1	ϕ = 0°
LC2	U2	W4	ϕ = 0°
LC3	U2	W4	ϕ = 90°
LC4	U3	W2	ϕ = 0°
LC5	U4	W4	ϕ = 0°

Uncertainty due to long-term extreme response extrapolation Effect of short-term simulation time

- Modified Environmental Contour Method

$$F_{X_{1h,50yr}}(\xi) = \left[F_{X_{1h,short-term|u_w,H_s,T_p}}(\xi|u_{N_0},H_{N_0},T_{N_0})\right]^{50/N_0}$$

- 10min simulation length introduces high uncertainty in the long-term extrapolation (50 years) around rated and cut-out wind speeds.

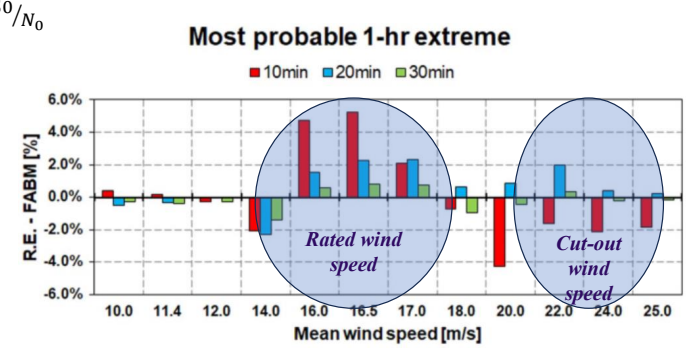

Resistance of support structure

- Resistance formulation for ultimate limit state :

$$M_u = \frac{F_y}{6}\left(1 - 0.84\frac{F_y}{E}\frac{D}{t}\right)(D^3 - (D-2t)^3)$$

- Required characteristic capacity:

$$\boldsymbol{M_{u,true}} = \frac{M_{u,true}}{M_{u,given\ par}} . \frac{M_{u,given\ par}}{M_{u,actual\ par}} . \frac{M_{u,actual\ par}}{M_{u,charc}} . M_{u,charc}$$

- True bending strength for the tower:

$$M_{u,true} = \hat{\chi}_{m,given\ par} \cdot \hat{\chi}_{m,actul\ par} \cdot \hat{\chi}_{m,charc} \cdot \gamma_r \cdot (\gamma_w M_{wc} + \gamma_v M_{vc})$$

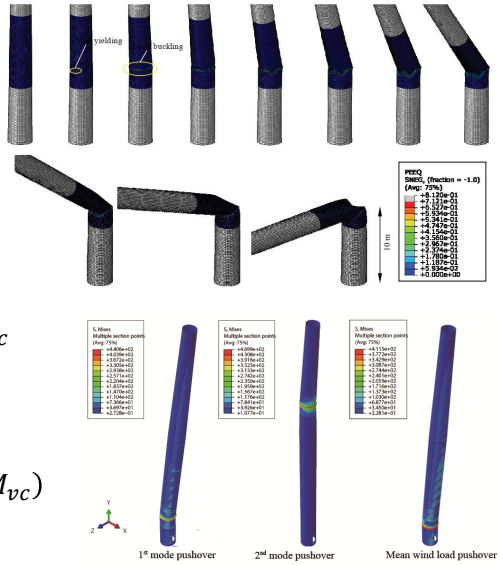

Reliability formulation for monopile-supported offshore wind turbine

$$g(\boldsymbol{X}) = M_{FA,u,req.} - \left(\varphi_w M_{FA,wt} + M_{FA,vt}\right)$$
$$= \hat{\chi}_{m,given.par}\hat{\chi}_{m,actual.par}\hat{\chi}_{m,charc}M_{FA,uc}$$
$$- \left(\varphi_w \hat{\chi}_{w,nl} B_{flex} B_{sim} \hat{\chi}_{w,stat.} \hat{\chi}_{w,lin.} \hat{\chi}_{w,env.} M_{FA,wc}\right.$$
$$\left. + \hat{\chi}_{v,nl.} \hat{\chi}_{v,stat.} \hat{\chi}_{v,aero.} \hat{\chi}_{v,env.} \hat{\chi}_{v,geo.} M_{FA,vc}\right)$$

Design equation: $M_{yy,uc} = \gamma_r(c.\gamma_w + \gamma_v)M_{yy,vc}$

where: $c = M_{yy,wc} / M_{yy,vc}$

Reference case: $c = 0.5$ & $(\gamma_r, \gamma_w, \gamma_v) = (1.35, 1.35, 1.35)$

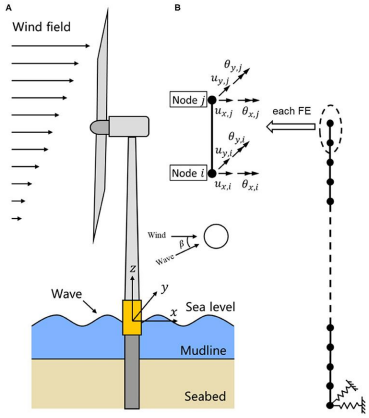

Sensitivities:

- ***Bias due to the Simulation time***
- ***Flexibility in the foundation***

Reliability formulation for monopile-supported offshore wind turbine

Random variable	Uncertainty due to	Distribution	Mean	CoV
$\hat{\chi}_{m,given\ par}$	Given resistance parameters	Normal	1.0	0.1
$\hat{\chi}_{m,actul\ par}$	Actual resistance parameters	Normal	1.0	0.1
$\hat{\chi}_{m,charc.}$	Characteristics resistance	Lognormal	1.1	0.15
$\hat{\chi}_{v,nl.}$	Wind nonlinearities	Normal	0.9	0.15
$\hat{\chi}_{v,stat.}$	Wind statistics	Gumbel	1.05	0.10
$\hat{\chi}_{v,aero.}$	Wind linear prediction	Normal	1.0	0.1
$\hat{\chi}_{v,env.}$	Wind environmental prediction	Normal	0.9	0.1
$\hat{\chi}_{v,geo.}$	Secondary (geometry-related) loads	Normal	0.9	0.1
$\hat{\chi}_{w,nl}$	Wave nonlinearities	Normal	0.9	0.15
$\hat{\chi}_{w,stat.}$	Wave statistics	Gumbel	1.05	0.10
$\hat{\chi}_{w,lin.}$	Wave linear prediction	Normal	1.0	0.1
$\hat{\chi}_{w,env.}$	Wave environmental prediction	Normal	1.0	0.15
φ_w	Load combination factor	---	1.0	---
c	Normalized bending moment ($M_{yy,wc}/M_{yy,vc}$)	---	0.2 (0.5)	---
γ_r	Resistance safety factor	---	1.35	---
γ_w	Wave load factor	---	1.35	---
γ_v	Wind load factor	---	1.35	---

Implied Safety level in Offshore Wind Turbines

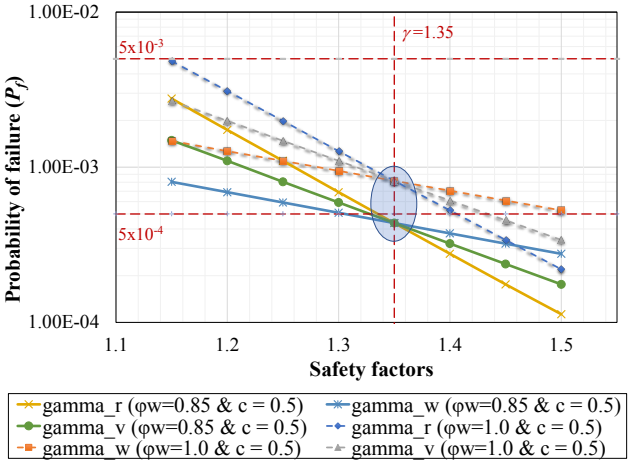

$M_{yy,wc}/M_{yy,vc} = 0.5$
Solid lines: $\varphi_w = 0.85$; Dashed lines: $\varphi_w = 1.0$

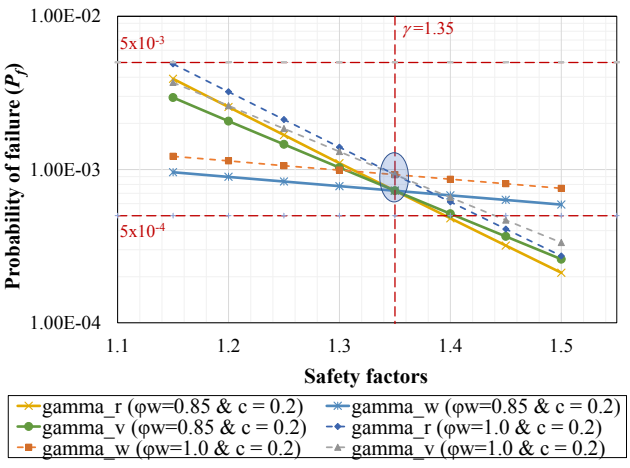

$M_{yy,wc}/M_{yy,vc} = 0.2$
Solid lines: $\varphi_w = 0.85$; Dashed lines: $\varphi_w = 1.0$

Annual failure probabilities - Sensitivity to the model uncertainty in *wave nonlinearity prediction*

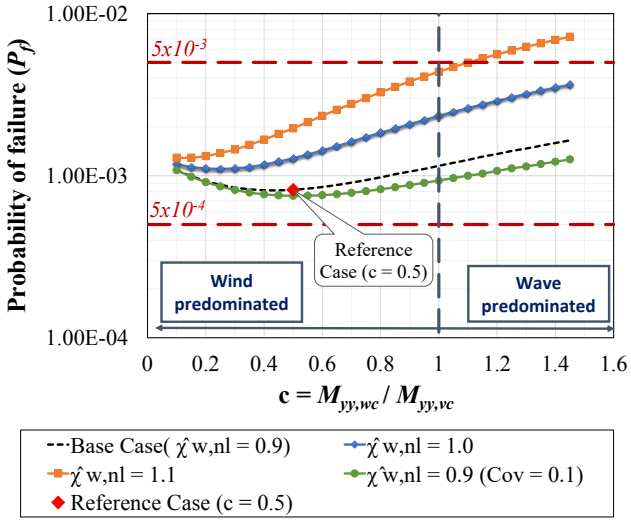

Annual failure probabilities - Sensitivity to the model uncertainty in *wave statistics prediction*

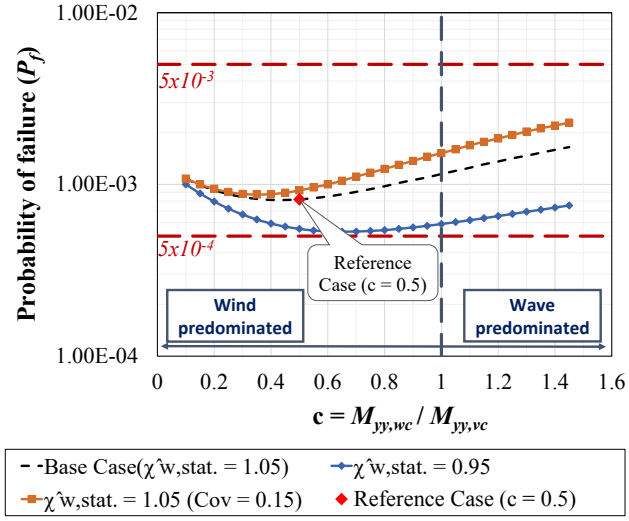

Annual failure probabilities - Sensitivity to the *correlation between the nonlinearity in wind and wave environmental load prediction*

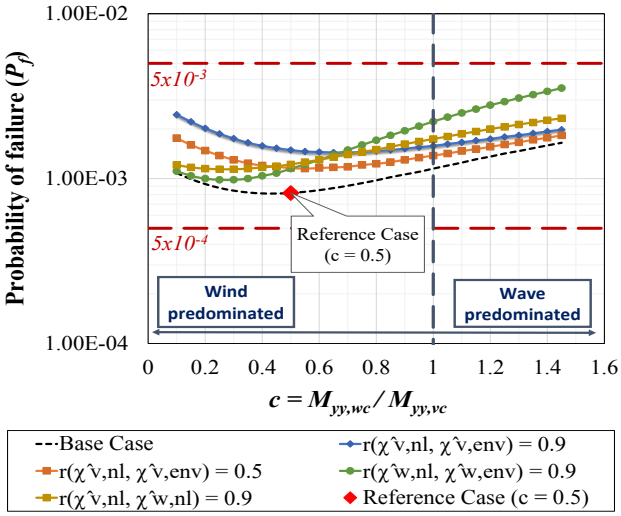

Annual failure probabilities - Sensitivity to the model uncertainty in *wind nonlinearity prediction*

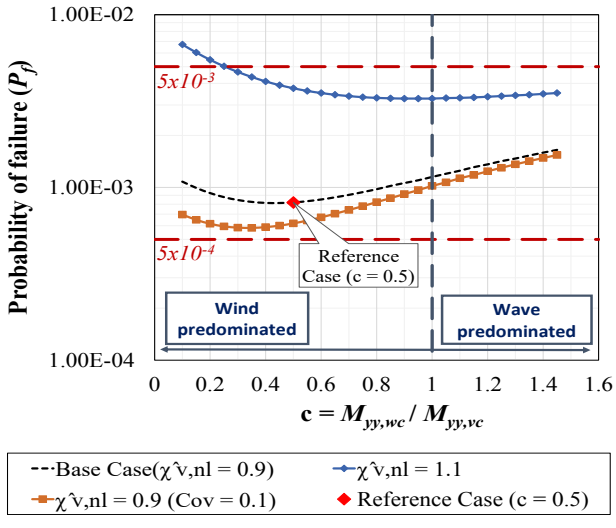

Annual failure probabilities - Sensitivity to the model uncertainty in *wind statistics prediction*

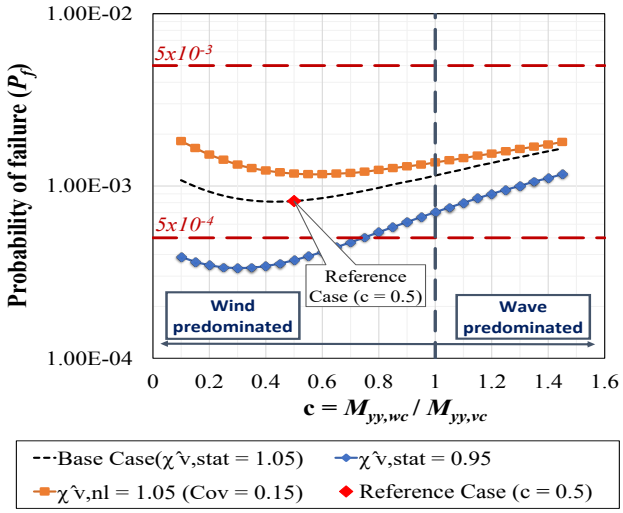

Annual failure probabilities - Sensitivity to wind safety factor, *Bias due to the Simulation time*

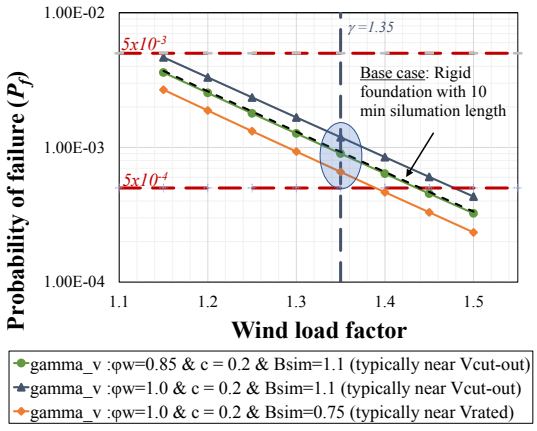

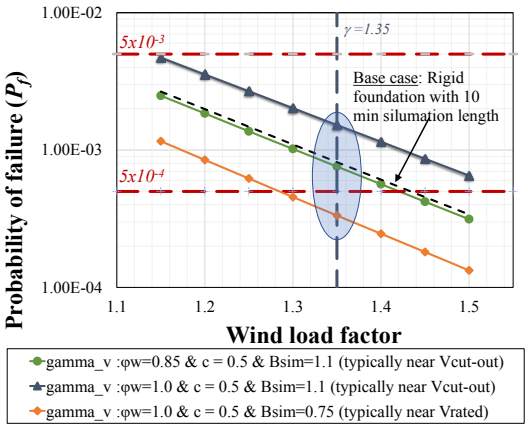

moment ratio of 0.2

moment ratio of 0.5

The effect of simulation length is less pronounced compared to the case with c=0.5 due to the wave-to-wind moment ratio, i.e., wind-dominated design.

Annual failure probabilities - Sensitivity to wave safety factor, *Bias due to the Simulation time*

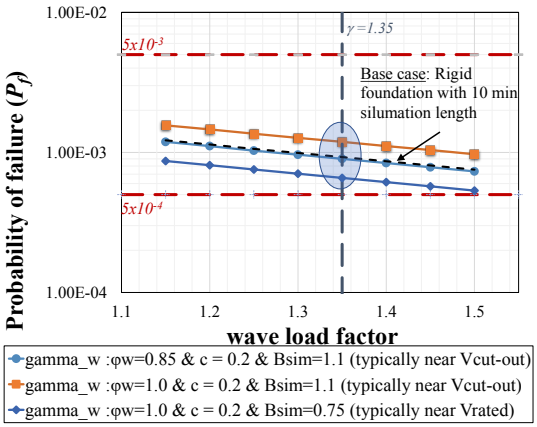

moment ratio of 0.2

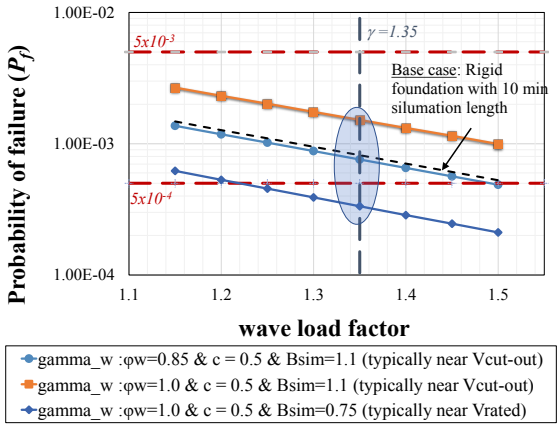

moment ratio of 0.5

Annual failure probabilities - Sensitivity to resistance safety factor, *moment ratio of 0.5, Bias due to the Simulation time*

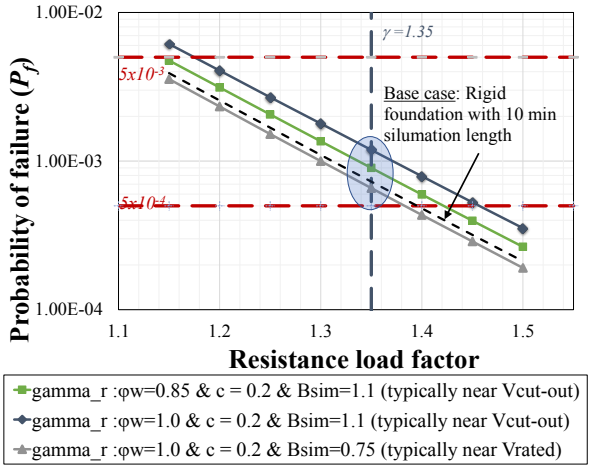

moment ratio of 0.2

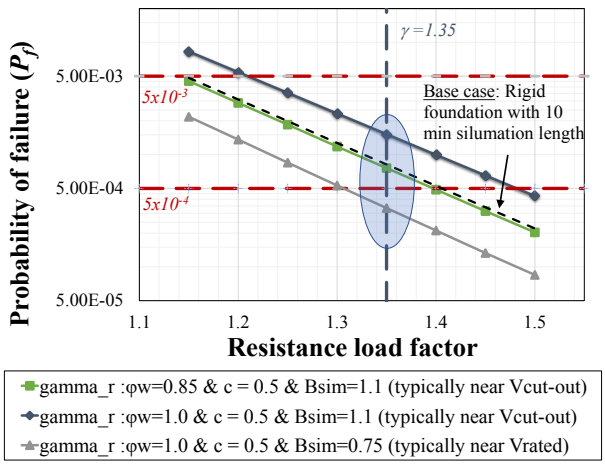

moment ratio of 0.5

Annual failure probabilities as a function of wave to wind moment ratio

When wave bending moment predominates, the bias on response extrapolation near cut-out wind speed (B_{sim}=1.1) will increase the failure probability, while the bias on response extrapolation near rated wind speed (B_{sim}=0.75) conservatively reduces the implied failure probability

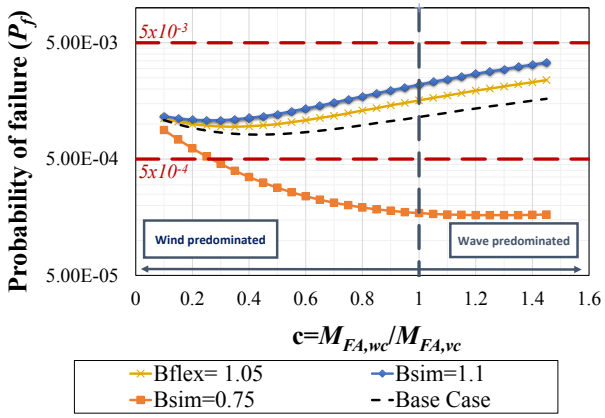

Implied safety levels in the mooring systems under different ULS design load conditions

- Structural safety in DNV standard for FWTs is ensured by use of a consequence class methodology:
  - *Consequence Class 1 (CC1);* in which failure is assumed unlikely to lead to an unacceptable event such as loss of life, collision with an adjacent structure, or environmental damages
  - *Consequence Class 2 (CC2);* in which failure may well lead to an unacceptable event such as those stated above.

$$R_c = \gamma_r(\gamma_{mean}T_{mc} + \gamma_{dyn}T_{dync})$$

Limit state	Load factor	CC1	CC2
ULS	γ_{mean}	1.3	1.5
ULS	γ_{dyn}	1.75	2.2
ALS	γ_{mean}	1.00	1.00
ALS	γ_{dyn}	1.10	1.25

Reliability formulation for mooring systems for ULS

- Ultimate limit state function for the mooring lines can be expressed by the tension:

$$g(\hat{\mathbf{X}},\hat{\mathbf{Z}}) = R(\hat{\mathbf{X}}) - \left(T_m(\hat{\mathbf{X}}) + T_{dyn}(\hat{\mathbf{X}},\hat{\mathbf{Z}})\right)$$

$$P_f = P[g(\boldsymbol{X}) \le 0] = P\left[\boldsymbol{R}_m - \left(\boldsymbol{T}_m + \boldsymbol{T}_{dyn}\right) \le 0\right]$$

$$R_c = \gamma_r\left(k\gamma_{mean} + \gamma_{dyn}\right)T_{dync}$$

$$k = T_{mc}/T_{dync}$$

The limit-state equation can then be written as:

$$g(\boldsymbol{X}) = R_{c,true} - \left(T_{m,true} + T_{dyn,true}\right)$$

$$R_{c,true} = \hat{\chi}_{R_m}.\hat{\chi}_{R_{sys}}.\hat{\chi}_{R_{c,comp}}.R_{c,comp}$$

$$T_{m,true} = \hat{\chi}_{mean}T_{mc}$$

$$T_{dyn,true} = \hat{\chi}_{stat,LF}\hat{\chi}_{dyn,LF}\hat{\chi}_{dyn,WF}T_{dync}$$

sub-indices mean, stat., LF and WF refer to uncertainties due to mean tension characteristic, Low frequency statistical, Low Frequency load modelling, Wave Frequency load modelling, respectively.

Reliability formulation for mooring systems for ULS

Random variable	Uncertainty due to	Distribution	Mean	SD
$\hat{\chi}_{Rm}$	Tension capacity model prediction	Normal	1.0	0.05
$\hat{\chi}_{Rsys}$	System effect	Extreme Value Distribution	μ_{EVD}	σ_{EVD}
$\hat{\chi}_{Rc,comp}$	Characteristics resistance	Lognormal	1.0	0.05
$\hat{\chi}_{mean}$	Mean tension load model	Normal	1.0	0.15
$\hat{\chi}_{stat,LF}$	Statistical prediction in LF	Normal	1.0	0.4
$\hat{\chi}_{dyn,LF}$	Dynamic load prediction in LF	Normal	1.0	0.05
$\hat{\chi}_{dyn,WF}$	Dynamic load prediction in WF	Gumbel	0.9	0.05
k	Normalized (relative) tension load (T_m/T_{dync})	---	Varies btw 0.1-2.0 (Typical values used: 0.2, 1.0 & 2.0)	---
γ_r	Resistance safety factor	---	1.0	---
γ_{mean}	Mean tension load factor	---	CC1: 1.3 CC2: 1.5	---
γ_{dyn}	Dynamic tension load factor	---	CC1: 1.75 CC2: 2.2	---

Annual probability of failure as a function of mean tension safety factor (γ_{mean}) with $\gamma_{dyn} = 1.75$ for CC1 and $\gamma_{dyn} = 2.2$ for CC2

Sensitivity to relative mean to dynamic tension loads of k = 0.2 and k = 1.0. The case for ULS with Consequence Class 1 and k = 2 and ULS offshore NORMOOR single safety factor are also shown for comparison.

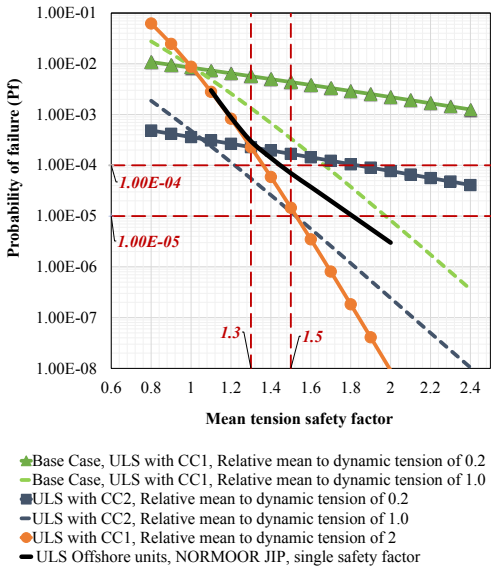

Annual probability of failure as a function of dynamic tension safety factor (γ_{dyn}) with $\gamma_{mean} = 1.3$ for CC1 and $\gamma_{mean} = 1.5$ for CC2

Sensitivity to relative mean to dynamic tension loads of k = 0.2 and k = 1.0. The cases for ULS with Consequence Class 1 and k = 2 and ULS offshore NORMOOR safety factors are also shown for comparison.

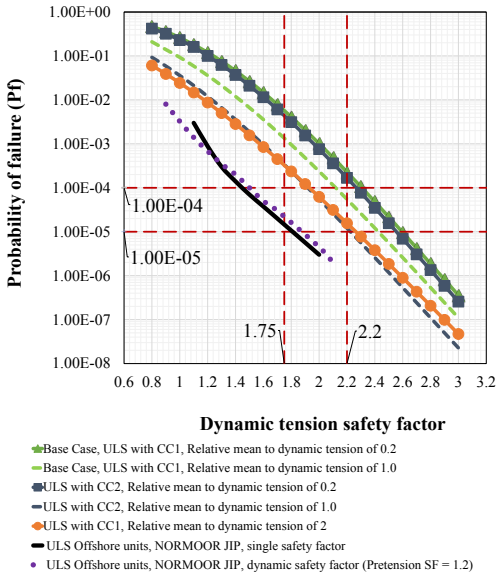

Safety level as a function of mean to dynamic tension load (k) with sensitivity study on the number of components in a segment

the number of components in a segment beyond 100 has very limited effect on the implied reliability level

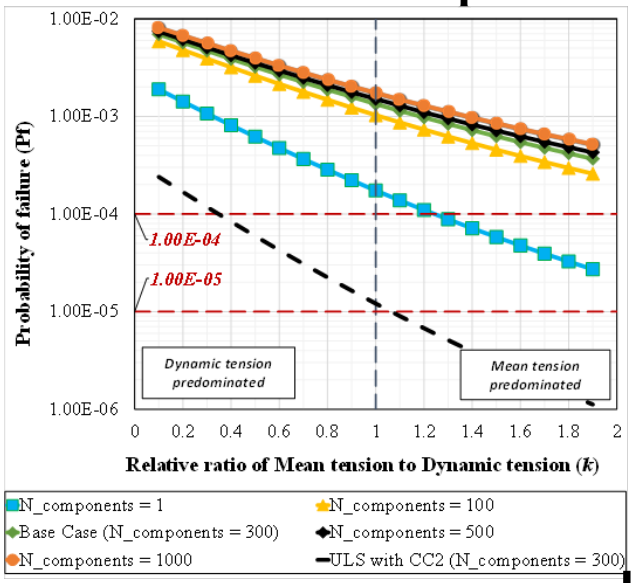

Conclusions

- For monopile-supported offshore wind turbines:
  - Safety level generally corresponds to the probability level of the order 5×10^{-3} to 5×10^{-4}.
  - The implied failure probability depends on the wave to wind moment ratio.
  - Differentiated safety factors for different wind and wave load combinations will provide a unified safety level across a wide range of load combination, wind predominate vs. wave predominate
  - Slightly smaller safety factors for wave-induced loads and larger for the wind-induced loads for a typical moment ratio range of 0.2-0.5 to obtain a unified safety level
  - The implied safety level in current design codes can further be harmonized especially accounting for bias in calculation of wind and wave statistics, effect of simulation time on long-term response and bias in the Inclusion of monopile bottom flexibility
- For mooring line systems:
  - The implied safety level for CC1 is not satisfactory across a range of mean-to-dynamic tension ratio (k= 0.1-2.0) when comparing to the nominal target level (10^{-4}).
  - The implied safety for design of mooring systems according to CC2 are, however, generally acceptable as compared to the nominal target value (10^{-5}).

Advancing Reliability-Based Design

Data Collection

More comprehensive data on the relative magnitude of wave and wind loads for larger wind turbines is needed to improve the statistical models and reliability estimates.

Soil-Structure Interaction

The influence of pile-soil interaction on the reliability level should be further investigated, as the response of rigid and flexible foundations can differ significantly.

Design Code Refinement

Ongoing efforts to refine design codes, such as IEC 61400-3-1, should continue to ensure transparent and explicit safety requirements based on reliability principles.

Collaborative Research

Interdisciplinary collaboration between researchers, engineers, and industry stakeholders is crucial to advance the reliability-based design of offshore wind turbines.

University of South-Eastern Norway

Embracing the Complexity

1

Comprehensive Modeling

Offshore wind turbine design requires advanced numerical modeling to accurately capture the complex interactions between wind, waves, and the supporting structure.

2

Uncertainty Quantification

Careful assessment and transparent representation of uncertainties in loads, load loads, load effects, and structural resistance are essential for reliable design. design.

3

Reliability-Based Approach

Adopting a reliability-based design approach, with explicit safety requirements, requirements, ensures the desired safety level for offshore wind turbine structures. structures.

University of South-Eastern Norway

Towards a Sustainable Future

Reliability-Based Design	Transparent Safety Requirements	Advancing Design Codes	Collaborative Research
Accounting for uncertainties in loads and resistance	Explicit safety factors based on target reliability levels	Continuous refinement of design standards	Interdisciplinary efforts to address complex challenges
Ensuring the desired safety level for offshore wind turbines	Optimizing the balance between safety and cost-effectiveness	Adapting to evolving industry needs and technological advancements	Driving innovation and sustainable growth in offshore wind energy

References

1. *Hadi Amlashi, Zhiyu Jiang, Madjid Karimirad,* Ultimate limit state safety format requirement for mooring lines of floating wind turbines, IOWTC2023-119493, Proceedings of ASME 2023 5th International Offshore Wind Technical Conference, IOWTC2023, December 18-19, 2023, The Exeter University, Exeter, United Kingdom
2. *Hadi Amlashi, Madjid Karimirad, David Barreto*, Comparative structural reliability analysis of monopile-supported offshore wind turbines: considering the effect of flexible foundation and simulation time on long-term extreme response extrapolation, ICASP14, 14th International Conference on Application of Statistics and Probability in Civil Engineering, 9th-13th July 2023, Trinity College Dublin, 2023, http://www.tara.tcd.ie/bitstream/handle/2262/103325/submission_206.pdf?sequence=1&isAllowed=y
3. *Hadi Amlashi*, Monopile-Supported Offshore Wind Turbine Ultimate Limit State Design Format from A Structural Reliability Point' of View – Impact of Uncertainties in Loads and Strength on The Implied Safety Level, OMAE 2023, 42nd International Conference on Ocean, Offshore & Arctic Engineering, Melbourne, Australia, June 11–16, 2023, https://asmedigitalcollection.asme.org/OMAE
4. *Hadi Amlashi, Madjid Karimirad, David Barreto,* Implied safety level in design codes for monopile offshore wind turbines: parametric study on the effect of partial safety factors, International Conference on Marine Structures, April 03-06, 2023, Gothenburg, Sweden, DOI: https://doi.org/10.1201/9781003399759
5. DNV-ST-0119, Floating wind turbine structures, Edition June 2021, Det Norske Veritas, Høvik, Norway, 2021
6. IEC 61400-3-2, Part 3-2: Design requirements for floating offshore wind turbines, Edition 1.0, International Electrotechnical Commission, Geneva, Switzerland, (2019)
7. DNV-OS-E301, Position mooring, Edition July 2021
8. *Mathisen, J.; Okkenhaug, S.; Larsen*, On the probability distribution of mooring line tensions in a directional environment, OMAE2011-50104, Rotterdam, 2011
9. *Barreto, D, Karimirad, M, & Ortega, A. "Influence of Wind Shear Uncertainty in Long-Term Extreme Responses of an Offshore Monopile Wind Turbine." Proceedings of the ASME 2020 39th International Conference on Ocean, Off-shore and Arctic Engineering. Volume 2A: Structures, Safety, and Reliability. Virtual, Online. August 3–7, 2020. V02AT02A061,ASME.*
10. *Hørte, T.; Okkenhaug, S.* NORMOOR- JIP – PHASE 2: Summary and Recommendations from Phase I and II, ULS and ALS Joint Industry Project Report No.: 2017-0900, Rev. 1, 2017IEC 61400-3-2, Part 3-2: Design requirements for floating offshore wind turbines, Edition 1.0, International Electrotechnical Commission, Geneva, Switzerland, (2019)
11. *Sørensen JD, Toft HS.* Probabilistic Design of Wind Turbines. Energies. 2010; 3(2):241-257
12. *Sørensen, J.D.; Toft, H.S.* Safety Factors-IEC 61400-1 ed. 4-Background Document; Technical Report, DTU Wind En-ergy-E-Report- 0066(EN); Technical University of Den-mark (DTU): Lyngby, Denmark, 2014.

Annex B

Drahomír Novák

Stochastic assessment of concrete structures: advanced FEM modelling and case studies

Stochastic assessment of concrete structures: advanced FEM modelling and case studies

Drahomír NOVÁK (and many co-workers)

Brno University of Technology
Faculty of Civil Engineering
Institute of Structural Mechanics

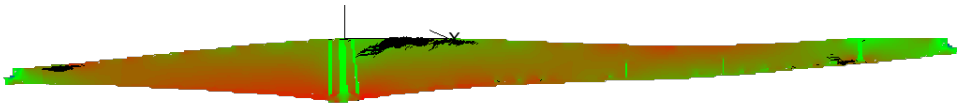

Bilateral cooperation between USN and BUT Reliability and sustainability of structures

Complexity: Nonlinearity + uncertainty + degradation + metamodeling +….

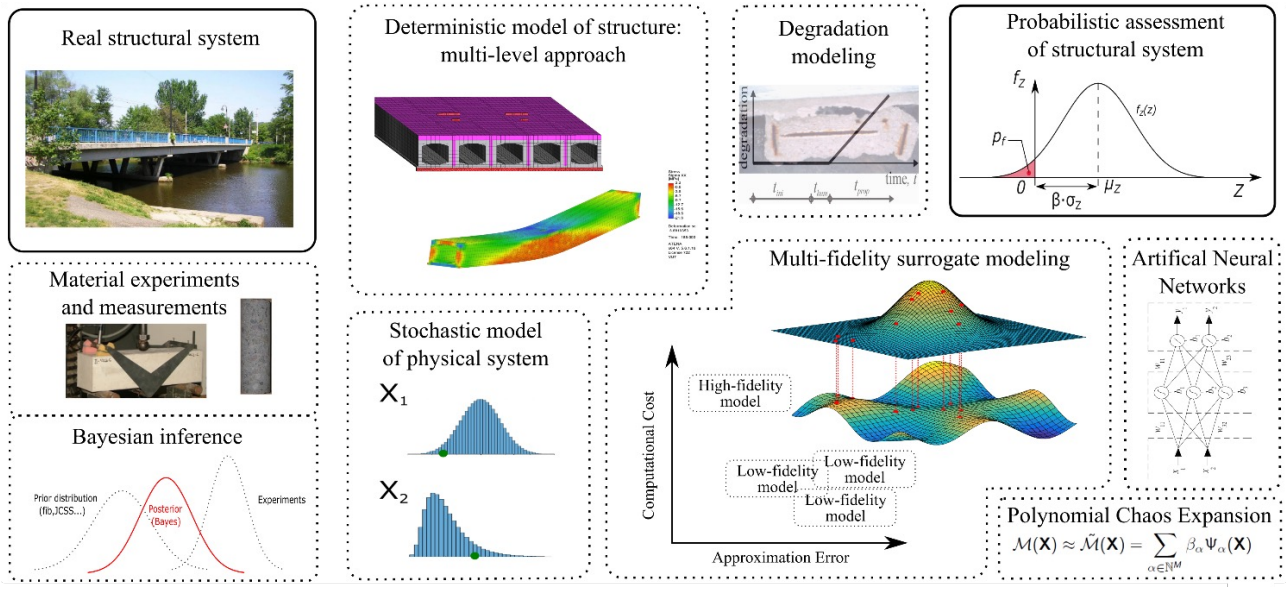

Outline

- The aim
- Deterministic model
  - Nonlinear fracture mechanics
  - ATENA software
  - Material parameters identification
- Stochastic model
  - Uncertainties simulation
  - FReET software – statistical, sensitivity, reliability analyses
- Degradation modelling
  - Carbonation of concrete, corrosion of reinforcement
  - FReET-D software
- Meta-modelling
  - ANN surrogate modelling
  - Polynomial chaos expansion
- Safety formats
- Examples – case studies
- Conclusions

DETERMINISTIC MODEL: Nonlinear FEM – ATENA software

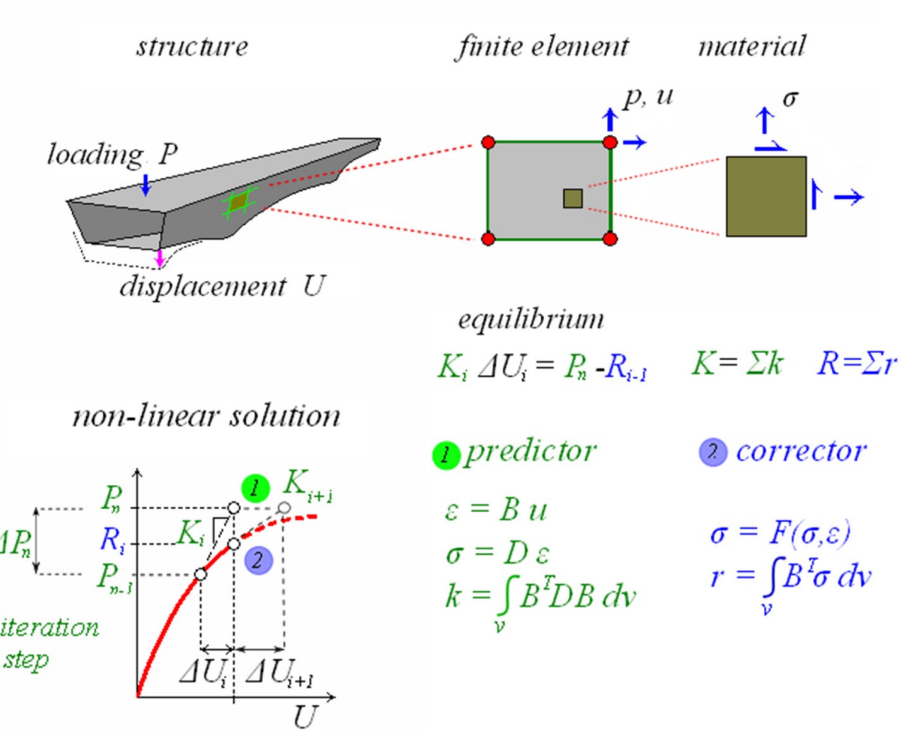

Nonlinear FEM simulation

Materials Models for Concrete

Plasticity
Damage mechanics
Microplane models

Uniaxial law

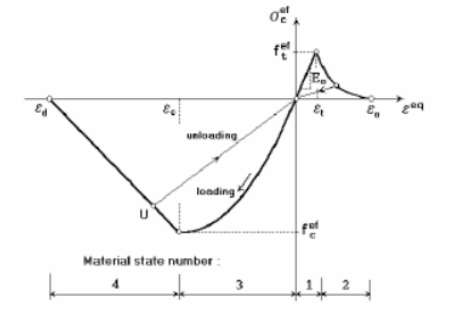

Bi-axial criterion

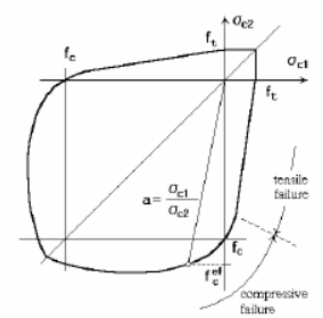

Kupfer 1969

3D failure surface

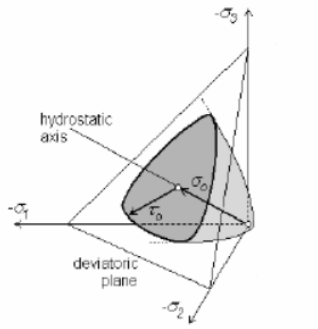

Menetrey Willam, ACI 1995

Nonlinear FEM simulation

Crack band method – correct energy dissipation during the fracturing process

concrete in tension

tensile cracks
post-peak behavior
fracture energy

crack band method

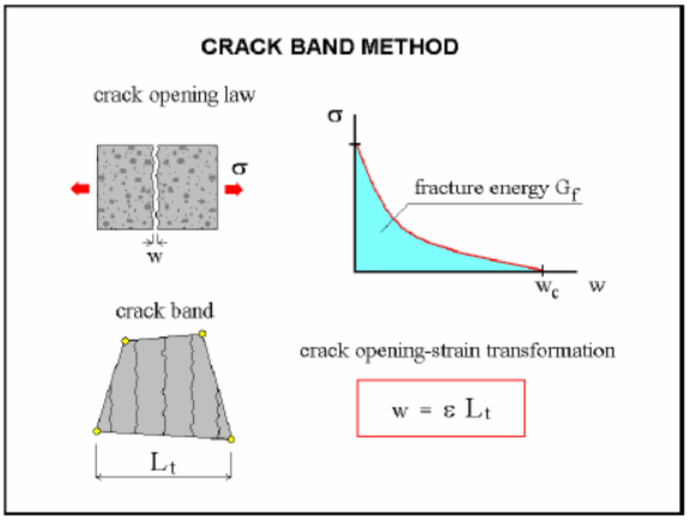

Realistic crack patterns prediction

Tunnel segments – damage of reinforced concrete

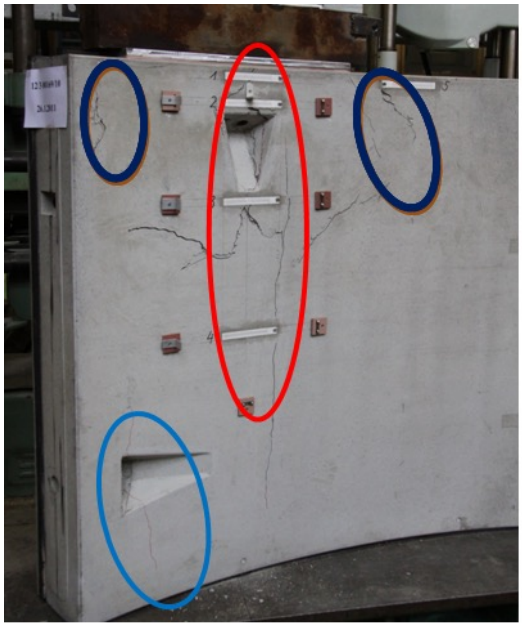

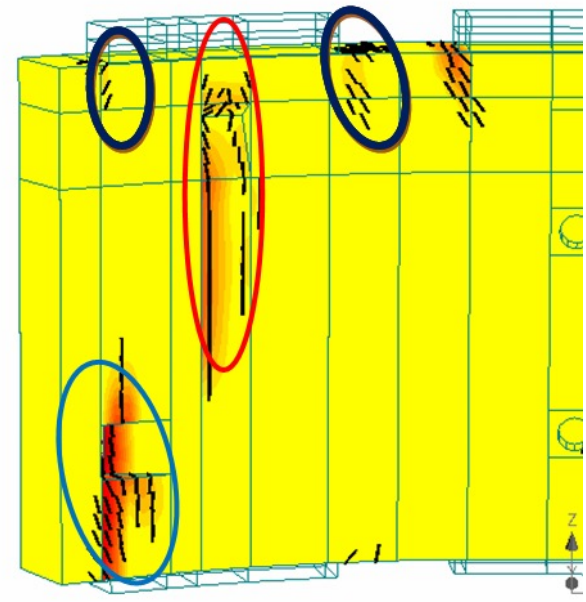

Material parameters identification: fracture-mechanical parameters

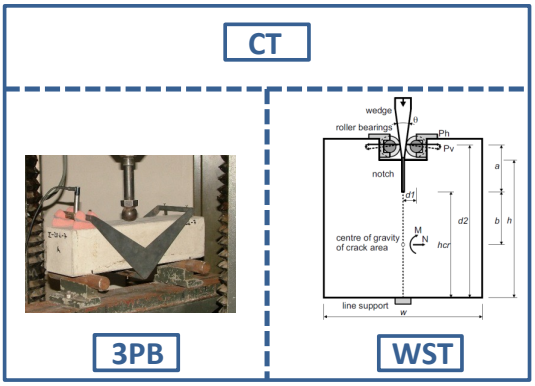

+

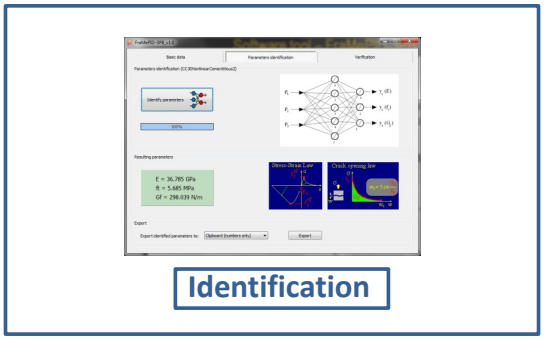

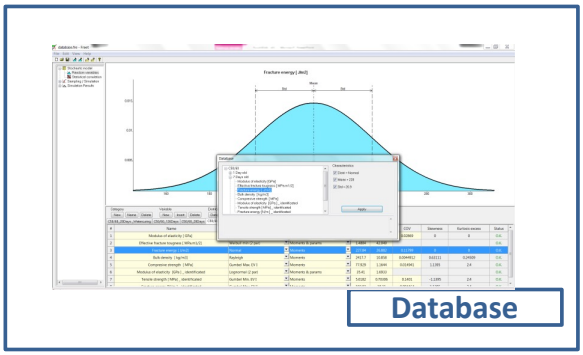

- Compressive strength
- Tensile strength
- Modulus of elasticity
- Fracture energy
- Etc.

Scheme of inverse analysis

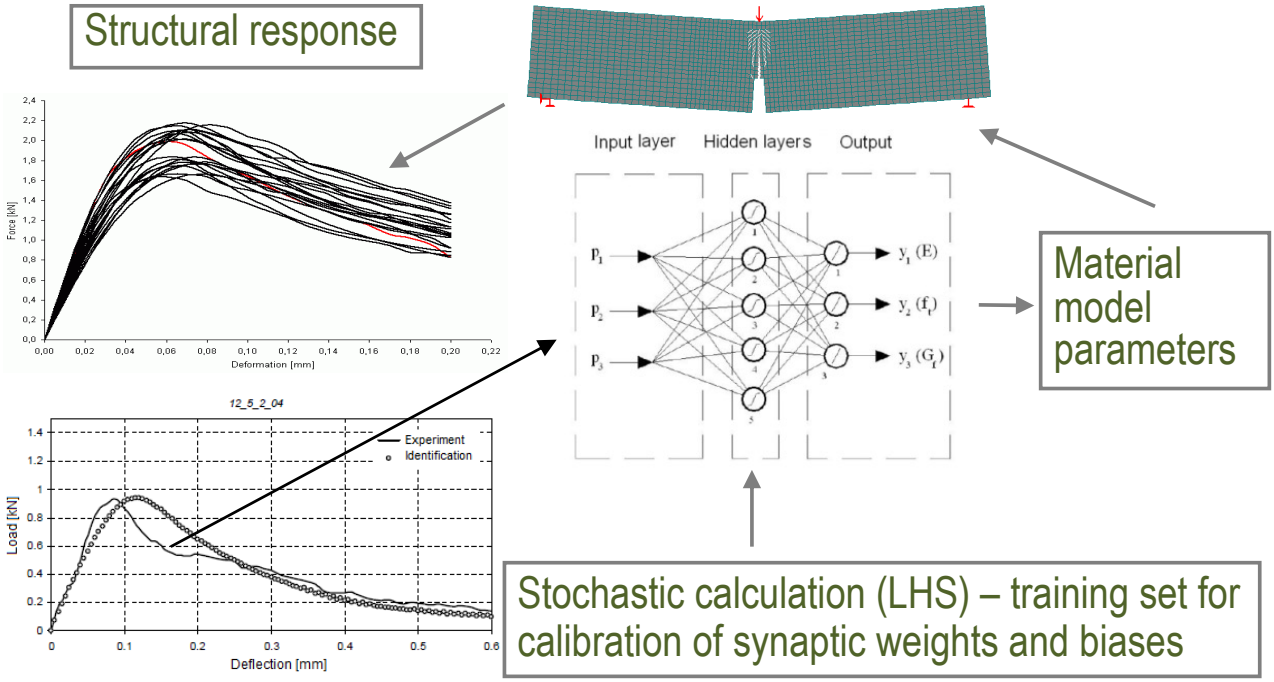

Deterministic and probabilistic approach

Deterministic

- Safety factors format
- The level of structural reliability is not determined !
- Nonlinearity – safety factors problematic !

Probabilistic

- Parameters as random variables/fields, statistical correlation
- Design with respect to target reliability level – reliability is determined
- Nonlinearity – leads to global safety factor

STOCHASTIC MODEL: Uncertainties simulation – FReET software

Feasible Reliable Engineering Tool – FReET, version 1.6:

- multipurpose probabilistic software for statistical, sensitivity and reliability analysis of engineering problems;
- allows to simulate uncertainties of the problem at random variables level (typically in civil/mechanical engineering – material properties and loading, geometrical imperfections);

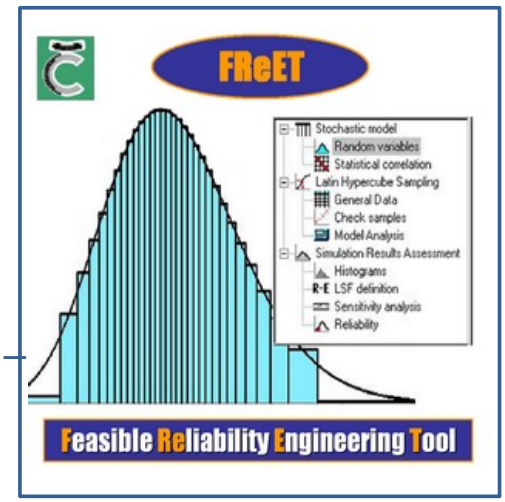

Motivation

- Uncertainties are involved in every part of the system Structure – Load – Environment, probabilistic assessment of civil infrastructure systems
- Random response Z is a function of basic random variables (or random fields) **X**: $Z = g(\mathbf{X})$

where function g(**X**) represents a computational model

Statistical analysis
Reliability analysis
Sensitivity analysis

$$\mu_g = \int g(\mathbf{X}) f_{\mathbf{X}}(\mathbf{X}) \, \mathrm{d}\mathbf{X}$$

$$p_f = \mathrm{P}(Z \le 0)$$

- **Computationally intensive problems/nonlinear FEM!**

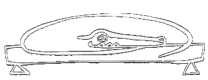

Uncertainty simulation
Small-sample simulation of Monte Carlo type

Latin Hypercube Sampling

$$y_i = \frac{\int_a^b y \cdot f(y)\ \mathrm{d}y}{\int_a^b f(y)\ \mathrm{d}y} = N_{Sim} \int_a^b y \cdot f(y)\,\mathrm{d}y$$

where $a = \frac{i-1}{N_{Sim}}$ $b = \frac{i}{N_{Sim}}$

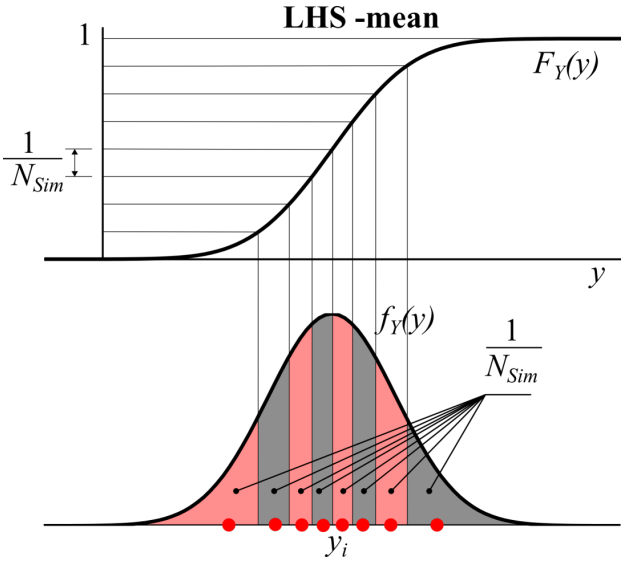

- takes mean value of each interval = interval centroid

Uncertainty simulation
Small-sample simulation of the Monte Carlo type

LHS-mean

- sample averages equal exactly the mean values of variables;
- variances of the sample sets are much closer to the target values compared to other selection schemes;
- for some probability density functions (including e.g. Gaussian, Exponential, Laplace, Rayleigh, Logistic, Pareto, etc.) the integral can be solved analytically;
- for others, the extra effort of doing the numerical integration is definitely worthwhile.

Uncertainty simulation
Small-sample simulation of the Monte Carlo type

Imposing statistical correlation

- Correlation matrices:
  - prescribed (target) – **T**
  - generated (actual) – **A**
- Difference matrix (error matrix):

$$\mathbf{E} = \mathbf{T} - \mathbf{A}$$

⇩

- a suitable norm of the matrix E defined as an objective function: minimum among all possible rank combinations.
- There exist $(N_{sim}!)^{N_{var}-1}$ possibilities

⇩

simulated annealing

x_1	y_1	…	z_1
x_2	y_2	…	z_2
x_3	y_3	…	z_3
x_4	y_4	…	z_4
x_5	y_5	…	z_5
x_6	y_6	…	z_6
x_7	y_7	…	z_7
x_8	y_8	…	z_8
…	…	…	…
x_{NSim}	y_{NSim}	…	z_{NSim}

Nonparametric rank-order based sensitivity analysis
A small-sample simulation of the Monte Carlo type

Sensitivity analysis:

- Nonparametric rank-order correlation between input variables and output response variable.

Kendall tau:

$$\tau_i = \tau\left(q_{ji}, p_j\right), \quad j = 1, 2, \ldots, N$$

Spearman's coefficient of correlation:

$$r^s = 1 - \frac{6\sum_{i=1}^{n} d_i^2}{n(n-1)(n+1)}$$

- Robust – uses only orders.
- Additional result of LHS simulation, no extra effort.
- Bigger correlation coefficient = high sensitivity.
- Relative measure of sensitivity (-1, 1).

variable values

simulation	input variable		result
1	x_1	y_1	g_1
2	x_2	y_2	g_2
3	x_3	y_3	g_3
4	x_4	y_4	g_4
5	x_5	y_5	g_5
6	x_6	y_6	g_6
⋮	⋮	⋮	⋮

⟹

orders

simulation	input variable		result
1	p_{11}	p_{21}	q_1
2	p_{12}	p_{22}	q_2
3	p_{13}	p_{23}	q_3
4	p_{14}	p_{24}	q_4
5	p_{15}	p_{25}	q_5
6	p_{16}	p_{26}	q_6
⋮	⋮	⋮	⋮

Uncertainty simulation
A small-sample simulation of the Monte Carlo type

Reliability analysis:

- Simplified – rough estimates, as constrained by extremally small number of simulations (10–100)!
- Cornell safety index.
- Curve fitting.
- FORM, importance sampling, response surface…

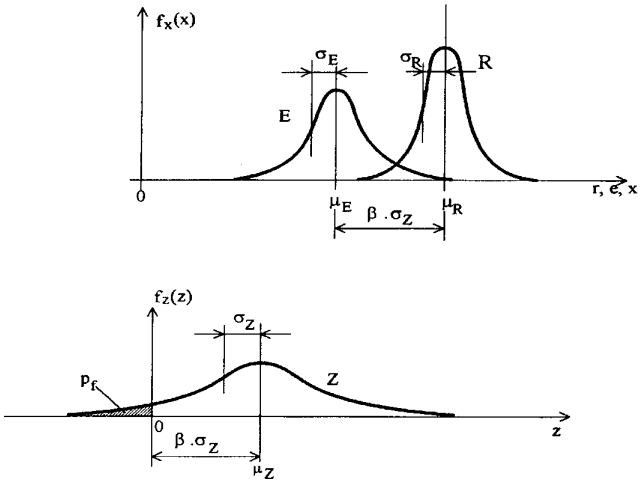

FReET software

„Random variables“ window:

- friendly Graphical User Environment;
- 30 probability distribution functions (PDF), mostly 2-parametric, some 3-parametric, two 4-parametric (Beta PDF and normal PDF with a Weibullian left tail);
- unified description of random variables with the optional use of statistical moments or parameters or a combination of moments and parameters;
- PDF calculator.

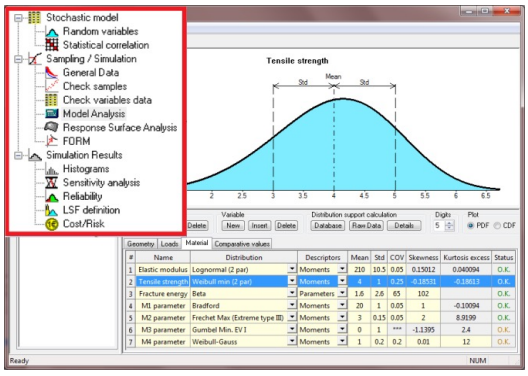

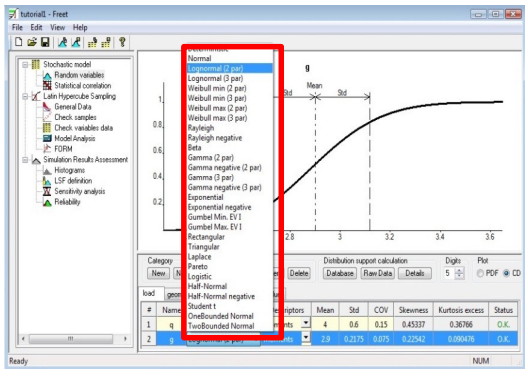

FReET software

„Statistical correlation“ window:

- visualization in both Cartesian and parallel coordinates;
- also a weighting option.

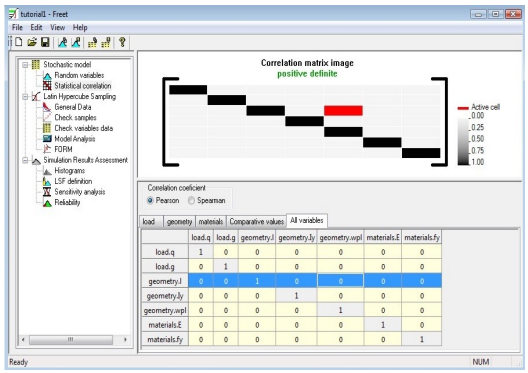

„Limit state/response functions“ window:

- closed form (direct), using the implemented Equation Editor (simple problems);
- numerical (indirect), using a user-defined DLL function that can be prepared in practically any programming language (C++, Fortran, Delphi, etc.);
- general interface to third-party software using user-defined *.BAT or *.EXE programs based on input and output text communication files;
- multiple response functions assessed in the same simulation run.

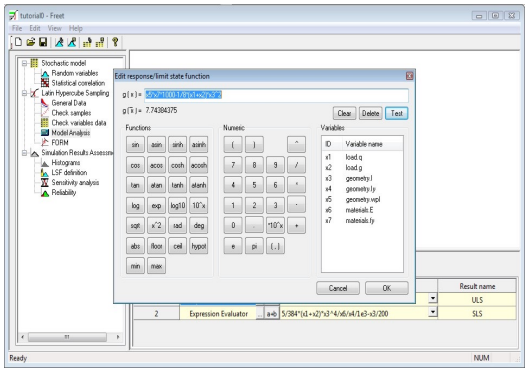

FReET software

„Reliability“ window:

- histograms of output variables;
- sensitivity analyses;
- reliability estimates by various simulation and approximation methods;
- limit state functions;
- parametric studies;
- cost/risk assessment.

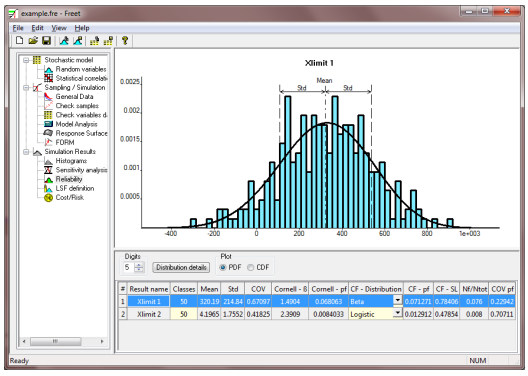

Probabilistic techniques:

- crude Monte Carlo simulation;
- Latin Hypercube Sampling (3 alternatives);
- Hierarchical Latin Hypercube Sampling;
- First Order Reliability Method (FORM);
- Curve fitting;
- Simulated Annealing employed for correlation control over inputs;
- Bayesian updating;

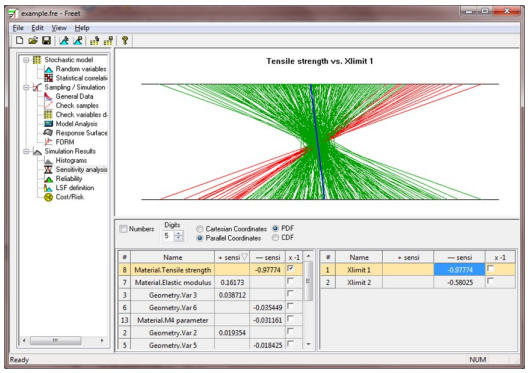

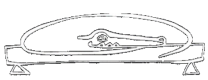

Random fields

Extensions in modeling of uncertainties

Random distribution of material properties along the structure: Spatial variability

material properties

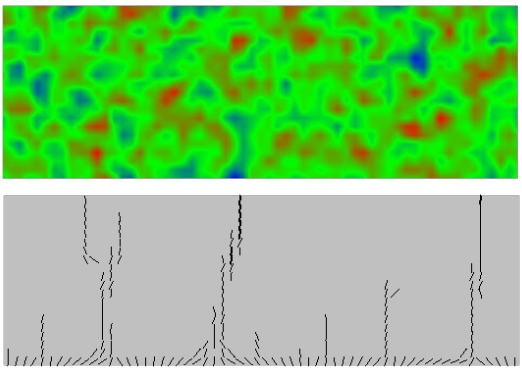

horizontal strains

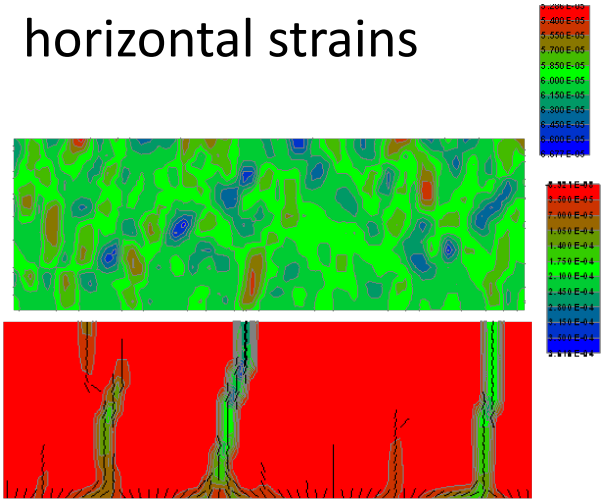

SARA software

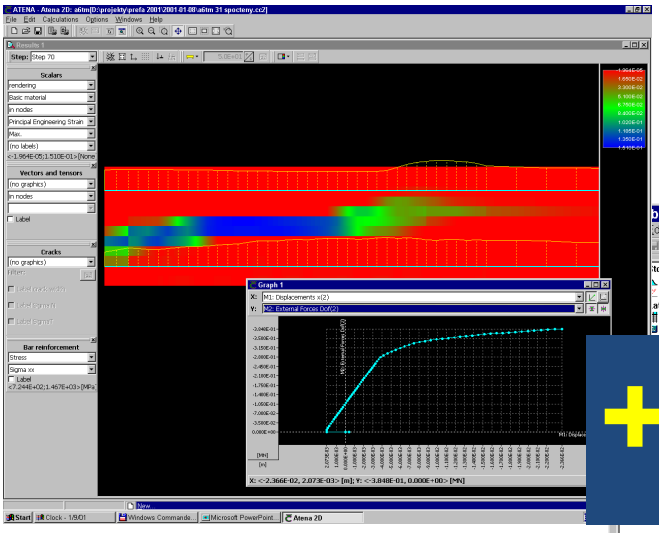

nonlinear fracture mechanics software ATENA

probabilistic software FReET

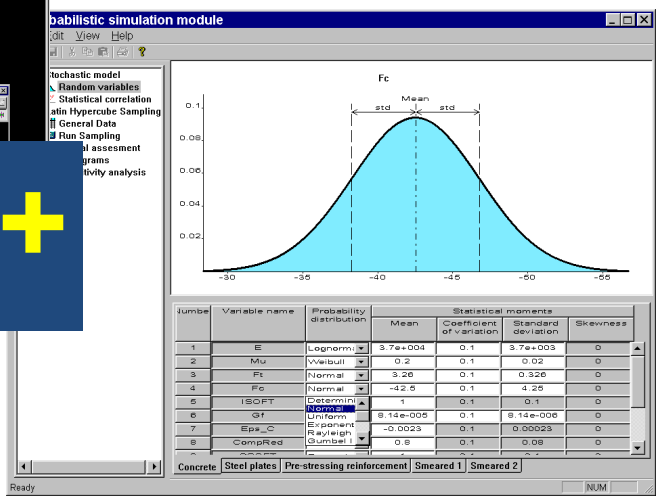

META-MODELLING

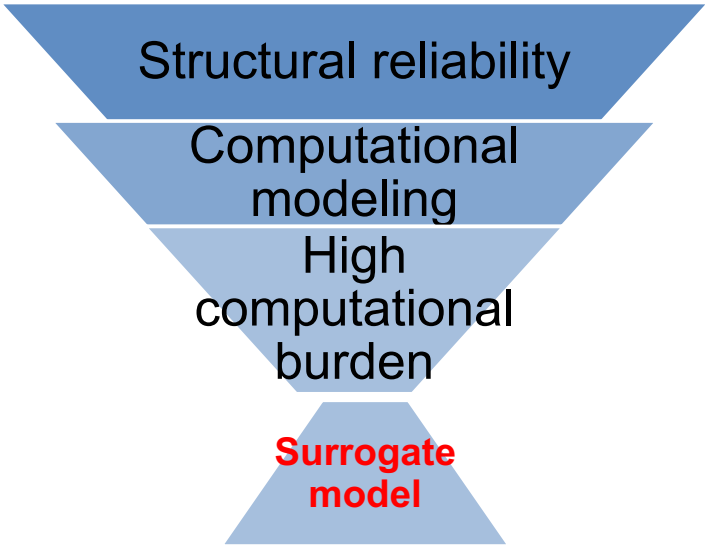

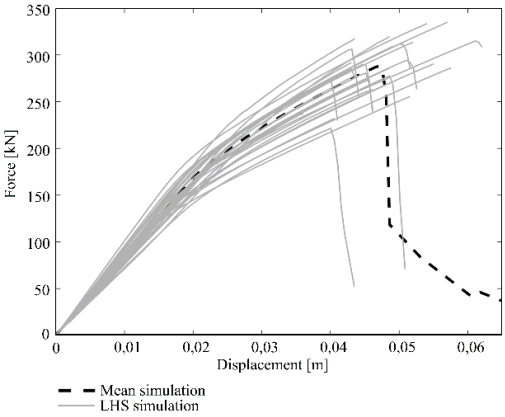

ANN surrogate model

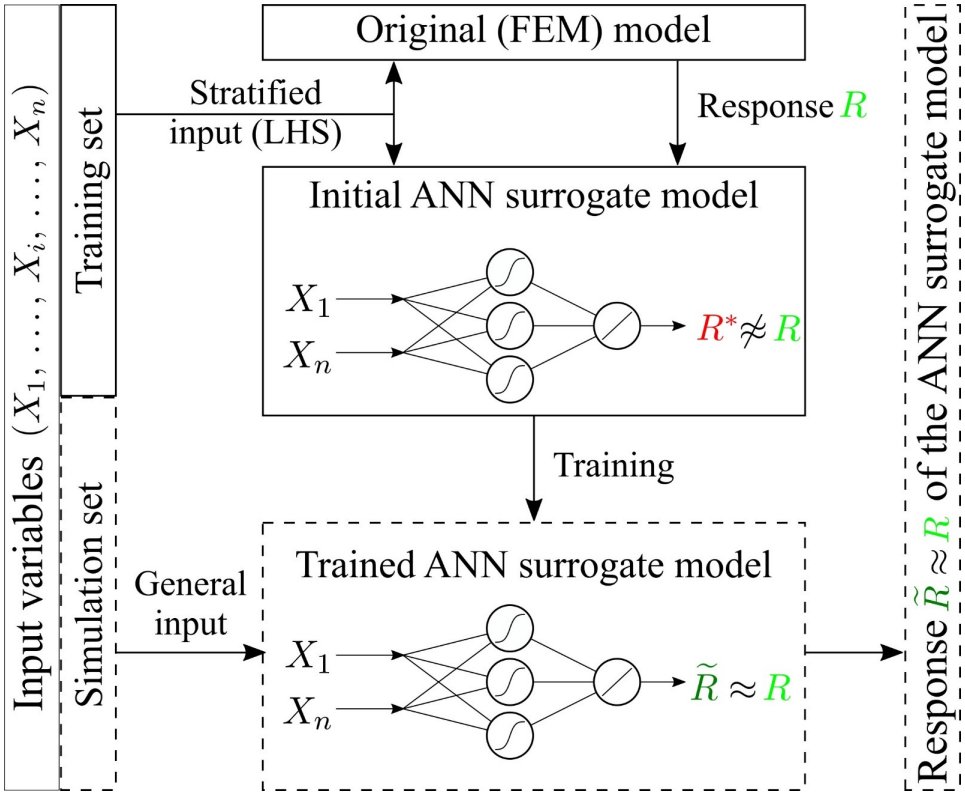

Polynomial chaos expansion (PCE)

$$Y = \mathcal{M}(\mathbf{X}) = \sum_{\boldsymbol{\alpha} \in \mathbb{N}^M} \beta_{\boldsymbol{\alpha}} \Psi_{\boldsymbol{\alpha}}(\mathbf{X})$$

- β_α deterministic coefficients to be computed (Least Square Regression)
- $\Psi_\alpha(\mathrm{X})$ basis of multivariate polynomials is orthonormal with respect to the joint distribution function (Hermite polynomials)
- *M* represents size of stochastic model (Curse of Dimensionality)
- Efficient algorithm for Sparse PCE was employed (9 terms) – Least Angle Regression

DEGRADATION MODELLING

- Increasing age of structures leads to material degradation significantly influencing durability, serviceability and ultimate capacity limit states and decreasing service life
- Significant role for planning reconstruction or demolition of structures – prognosis in time needed
- Main stressors: Carbonation of concrete and corrosion of reinforcement

Limit states and reliability levels

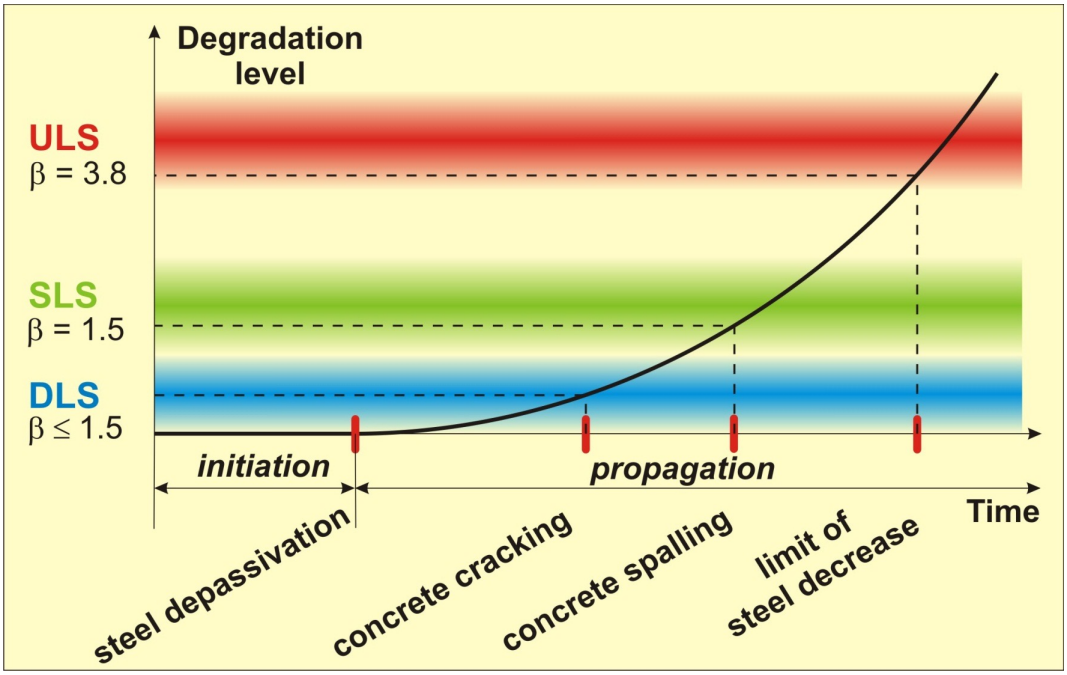

ULS = Ultimate Limit State SLS = Serviceability LS DLS = Durability LS

FReET-D module

Feasible **Re**liable **E**ngineering **T**ool for **D**egradation – **FReET–D**:

- module of the software FReET;
- combination of analytical models and simulation techniques for assessing the potential degradation of newly designed as well as existing concrete structures;
- models for carbonation, chloride ingress, reinforcement corrosion, sulphide, acid and frost attack;
- Around 50 models which can be used in stochastic way

SAFETY FORMATS

- How to determine design value of resistence using NLFEA? Nonlinear behaviour and uncertain material parameters!

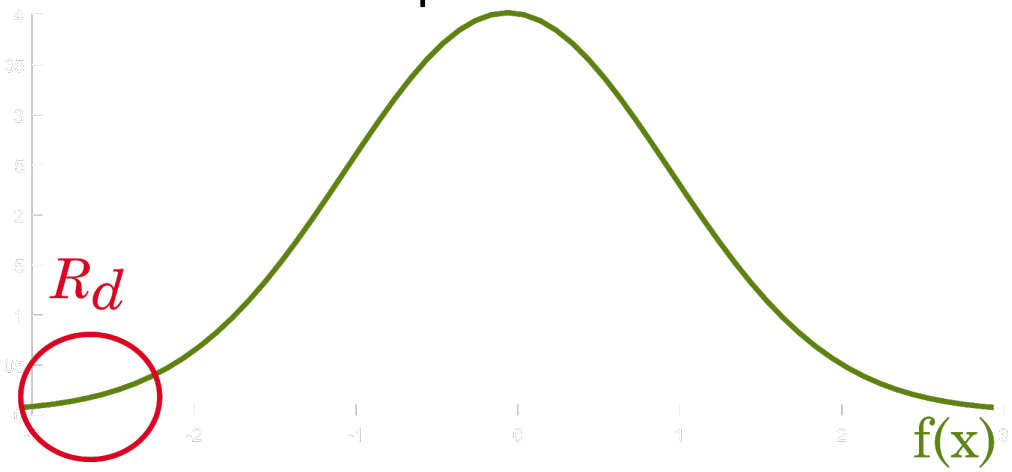

Design value of resistance R_d

Design value ?

- **Ultimate limit state represented by critical value of force applied during experiment (peak of LD diagram)**
- **Design value by:**
  - **fully probabilistic approach – design value for Probability = 0.0012 (Eurocode)**
  - **classical calculation using partial safety factors**
  - **ECOV method**

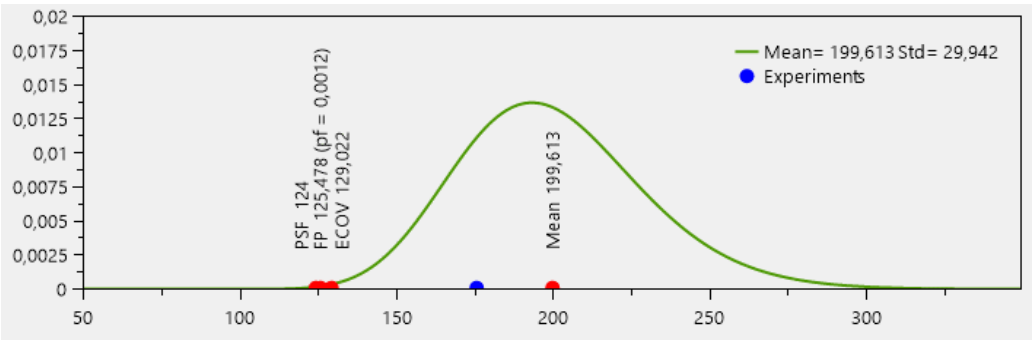

Safety formats for NLFEA

- **Partial Safety Factor method :** $R_d = R(f_{cd}, f_{yd,})$
  - material characteristics are extremely low
  - possibility of unrealistic behaviour
  - only **one** NLFEA is needed

- **Global safety format EN 1992-2:** $\mathbf{R_d = \frac{R(f_{ym}, \tilde{f}_{cm}, \dots)}{1.27}}$ $\mathbf{\tilde{f}_{cm} = 0.843 \cdot f_{ck}}$
  - NLFEA with mean values
  - application of global safety factor on result
  - reduced mean value of concrete characteristic because of its higher variability
  - only **one** NLFEA is needed

ECoV for NLFEA

Another **global safety factor** approach via estimation of coefficient of variation:

$$R_d = \frac{R_m}{exp\left(\alpha_R \beta v_f\right)}$$

- **ECoV by Červenka:**
  - **2** x NLFEA needed (R_m & R_k) $\quad v_f = \frac{1}{1{,}65} ln\left(\frac{R_m}{R_k}\right)$
- **ECoV by Schlune:**
  - **(N+1)** x NLFEA needed $\quad v_f \approx \frac{1}{R_m} \sqrt{\sum_{i=1}^{N} \left(\frac{R_m - R_{\Delta fi}}{\Delta_{fi}} \sigma_{fi}\right)^2}$
  - reduced mean values $f_{\Delta i}$ $\quad f_{\Delta i} = f_{mi} \cdot exp\left(-(\alpha_R \beta)/\sqrt{2} \cdot v_{fi}\right)$

Semi-probabilistic approach

$$R_d = \mu_R \cdot exp(-\alpha_R \beta_n v_R)$$

- **L**atin **H**ypercube **S**ampling for estimation of moments of response function
- approximation by surrogate model (Polynomial Chaos Expansion, ANN etc.)
- A simple **numerical quadrature** method to estimate moments of function R by Rosenblueth

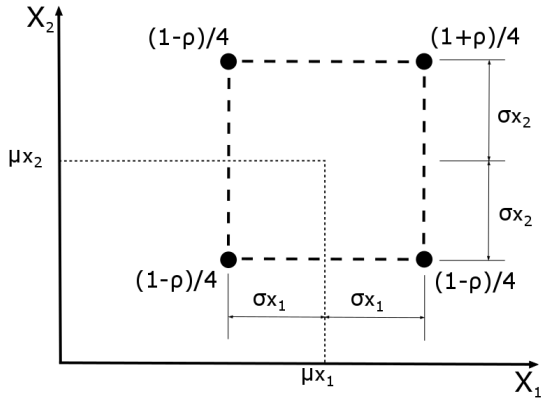

Design value of Response

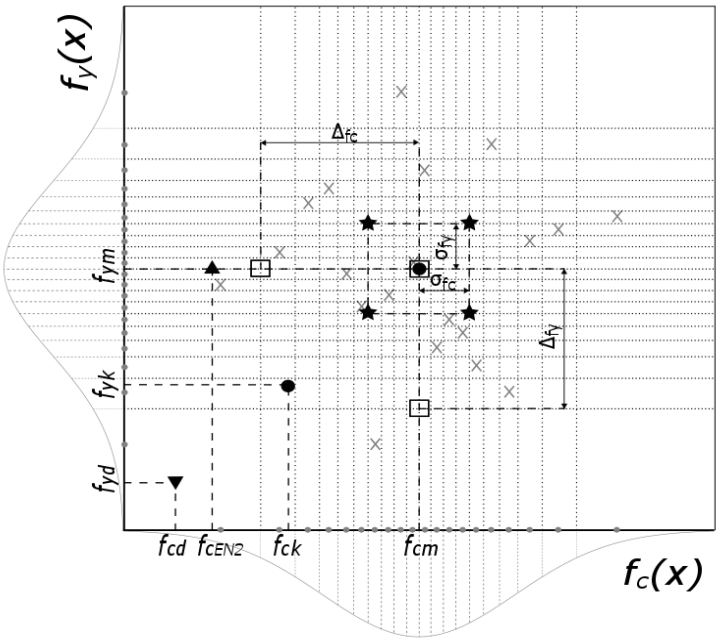

n	SAMPLING POINTS
x	Latin Hypercube Sampling
1	Partial Safety Factor
1	EN 1992 - 2
2	ECoV by Červenka
3	ECoV by Schlune et al.
4	Numerical Quadrature

Design value ? Left tail of PDF

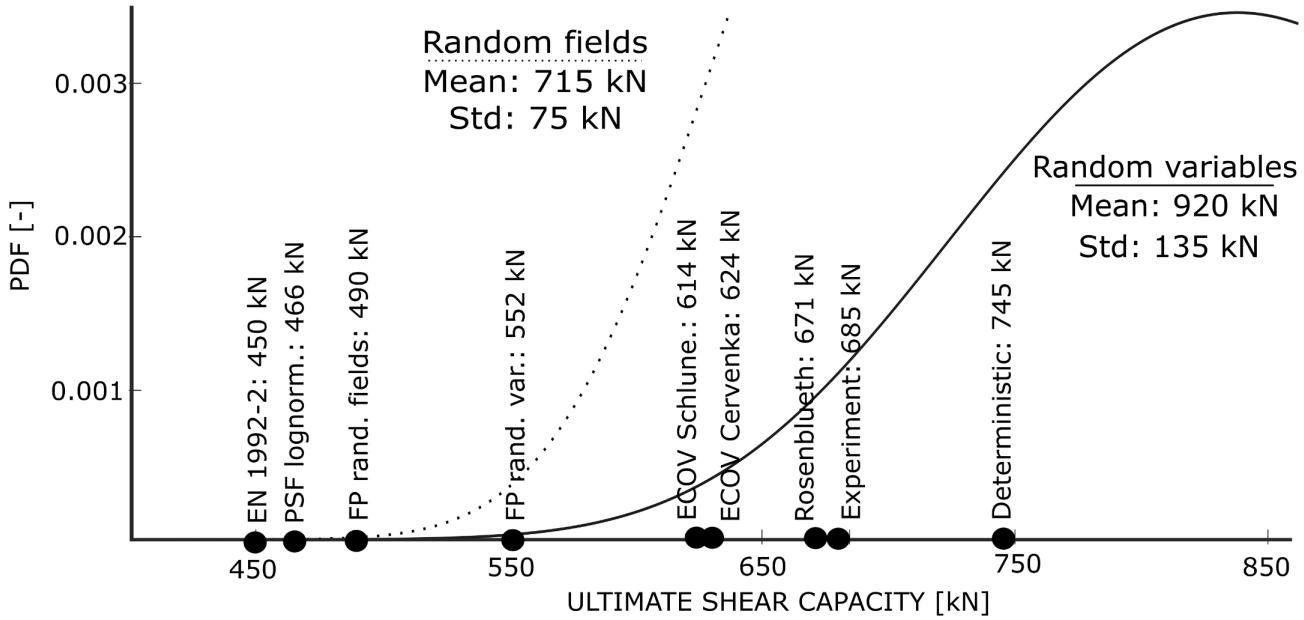

EXAMPLES: SELECTED CASE STUDIES OF CONCRETE STRUCTURES/BRIDGES

Application: S33.24 bridge in Austria

- Jointless bridge
- Casting in the end of March 2009
- Testing after 28 days
- Material parameters identification

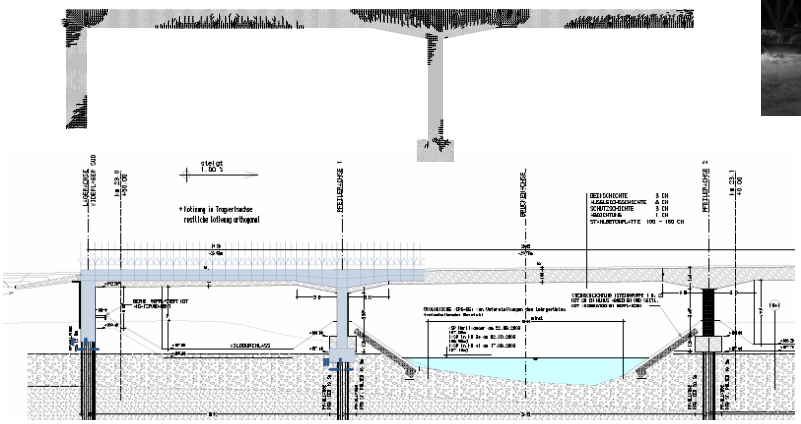

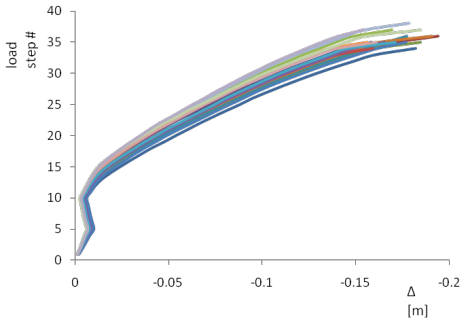

Application: S33.24 bridge in Austria

Selected parameters of steel:

	Symbol	Unit	Mean	Coeff. Of Variation	PDF	Source
Elastic Modulus	E	Gpa	210	0.03	LN	Literature
Yield stress	f_y	Mpa	475	0.07	LN	Literature

Variable	E	f_y
E	1.0	**0.60**
f_y	0.59	1.0

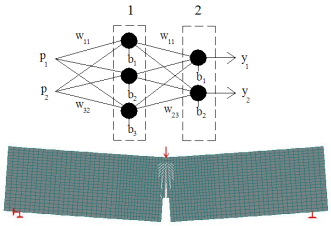

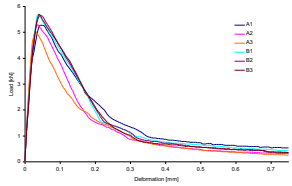

Selected parameters of concrete:

	Symbol	Unit	Mean	Coeff. of Variation	PDF	Source
Elastic Modulus	E	Mpa	39500	0.1	N	Identification
Poisson's ratio	v	-	0.20	0.05	LN	Literature
Tensile strength	f_t	Mpa	2.90	0.09	Weibull	Identification
Compressive strength	f_c	Mpa	-28.90	0.1	LN	Literature
Specific fracture energy	G_f	N/m	178.00	0.13	Weibull	Identification
Uniaxial compressive strain	ε_c	-	0.0018	0.15	LN	Literature
Reduction of strength	c_{Red}	-	0.80	0.06	Rect.	Literature
Critical comp. displacement	w_d	m	-0.0005	0.1	LN	Literature
Specific material weight	ρ	MN/m³	0.023	0.1	LN	Literature

Variable	E	f_t	f_c	G_f	ε_c
E	1.0	**0.69**	**-0.9**	**0.5**	**0.9**
f_t	0.70	1.0	**-0.78**	**0.89**	**0.61**
f_c	-0.86	-0.76	1.0	**-0.61**	**-0.89**
G_f	0.52	0.87	-0.60	1.0	**0.49**
ε_c	0.85	0.61	-0.88	0.47	1.0

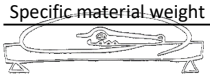

Application: S33.24 bridge in Austria

ULS: g(X) = R(X) - E(X)

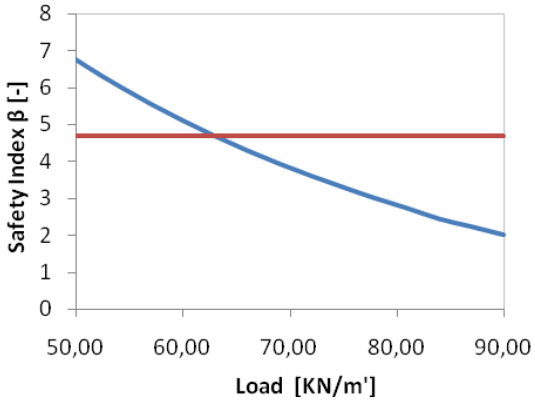

Eurocode:

β = 4.7 for one year period

Pf = 1.5E-6.

SLS: g(X) = Wlim(X) - W(X)

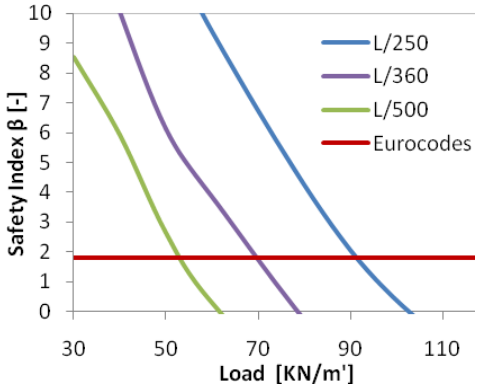

Eurocode: β = 1.8

deflection limit of span: L/250 or L/500

US Standard Specifications: L/360 or L/500

Application: railway sleeper

- pre-stressed railway sleeper (ŽPSV a.s.)
- model in ATENA 3D
- random dominant concrete parameters
- LHS simulations with imposed statistical correlation – 30 realizations
- probability of maximal crack width

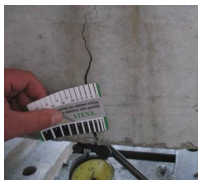

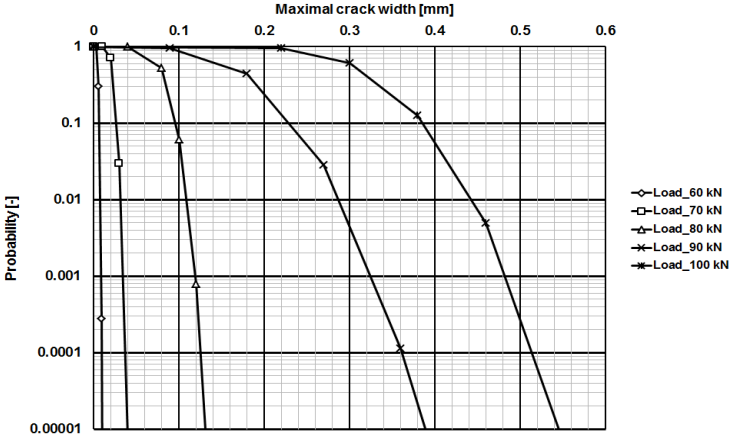

Case study: Kristineberg bridge

Bridge Nr. 2-2043-15
E4 Kristineberg, Stockholm

The reinforced concrete bridge has a two-span frame structure. Total bridge length is 26 m; bridge deck has a width of 7 m. The bridge deck has inclination 2.5% in both longitudinal and transverse directions. There are two lateral abutments and one intermediate support. The abutments have a significant inclination with respect to road axis and they have a different shape and size.

Case study
Deterministic model

3D Model

Geometry

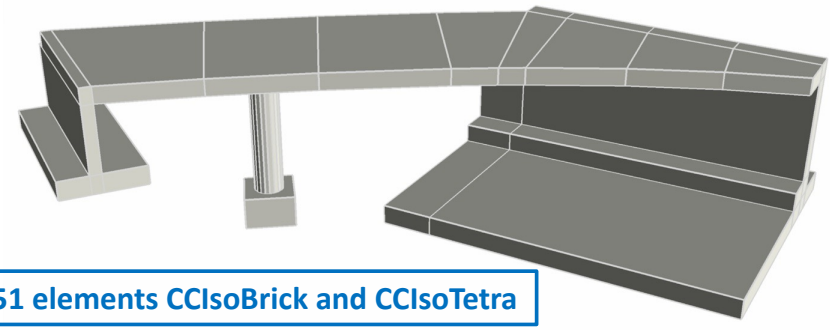

FE mesh **11 351 elements CCIsoBrick and CCIsoTetra**

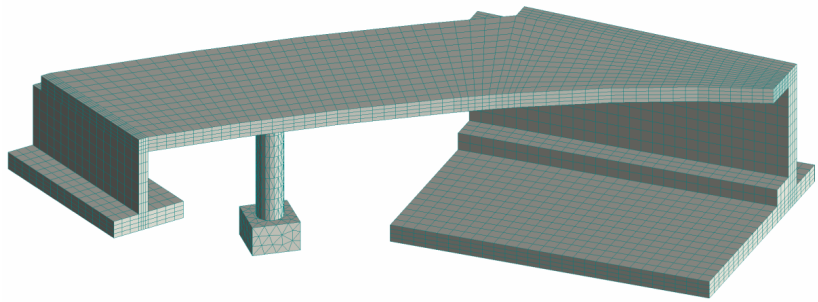

Material parameters (concrete, reinforcement) based on laboratory experiments.

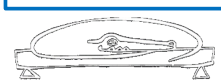

Case study
Stochastic model

Random parameters of concrete and steel

Element	Cube strength (28 days) [MPa]
Foundation 1	58.8
Foundation 2	54.6
Foundation 3	59.6
Support 1	54.4
Support 2	54.0
Support 3	40.7
Top desk	41.2

	Mean	Unit	COV	PDF
Concrete C 35/45				
Elastic modulus	For each part of the structure determined based on cube strength from Tab. 1 using material model CC3DNonLinCementitious		0.1	Lognormal (2par)
Tensile strength			0.2	Lognormal (2par)
Compressive strength			0.15	Lognormal (2par)
Fracture energy			0.25	Weibull min (2 par)
Mass density	2300	kg/m^3	0.05	Normal
Steel (B505B)				
Elastic modulus	200	GPa	0.07	Lognormal (2par)
Yield strength	552	MPa	0.07	Lognormal (2par)
Ultimate strength	621	MPa	0.07	Lognormal (2par)
Limit strain	0.05	-	0.07	Normal

Case study
Stochastic model – chosen results

Example of graphical output

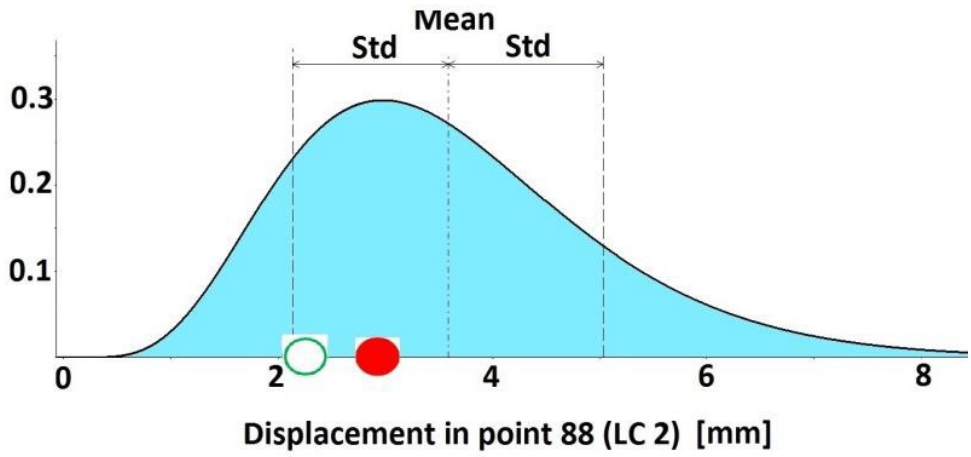

Experiment (empty green symbol), deterministic simulation (full red symbol) and PDF of perpendicular displacement for selected monitoring point – Nr. 88, loading case 2.

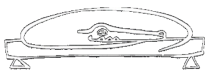

Case study
Deterministic model

Cracks in concrete deck (max 0.285 mm)

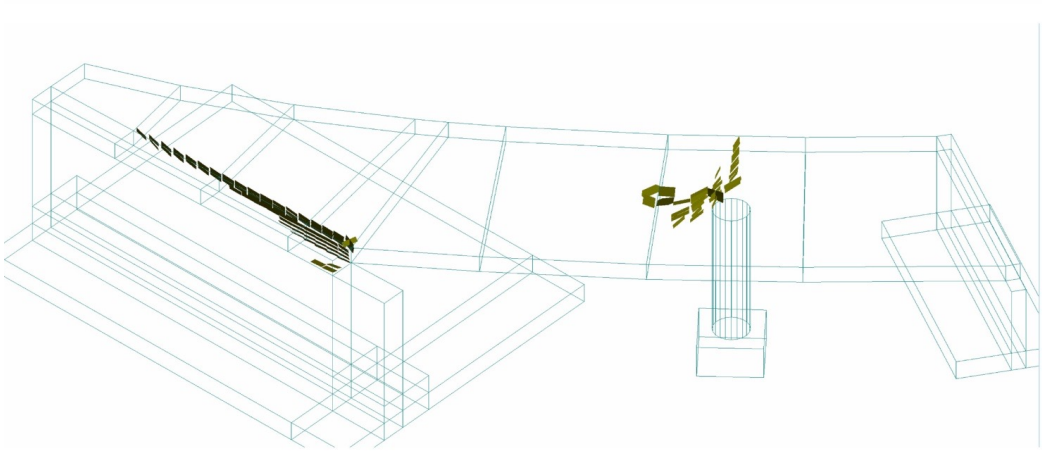

Load case 2

Case study
Stochastic model – chosen results

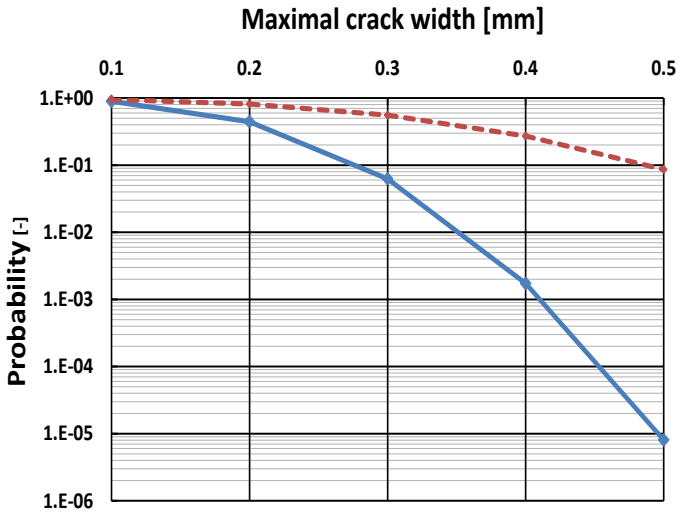

Probability of exceedance of crack width (full blue/broken red line – loading case 1/2).

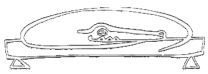

Toronto shear tests
(June 2015) span 19 m, height 4m

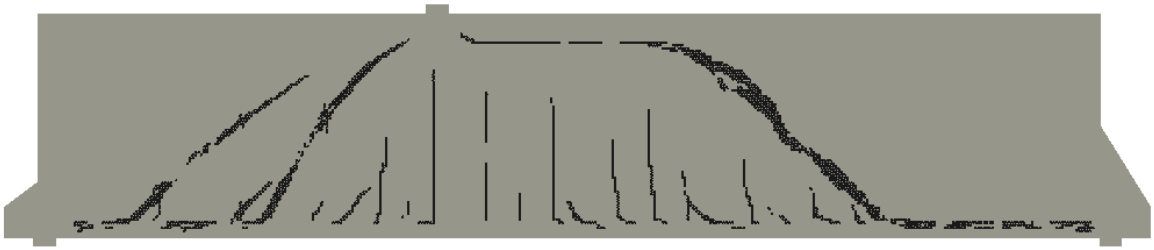

Collins, M.P., et al.: Challenge of Predicting the Shear Strength of Very Thick Slabs. Concrete International, V.37,No.11, Nov. 2015,

Succesfull prediction

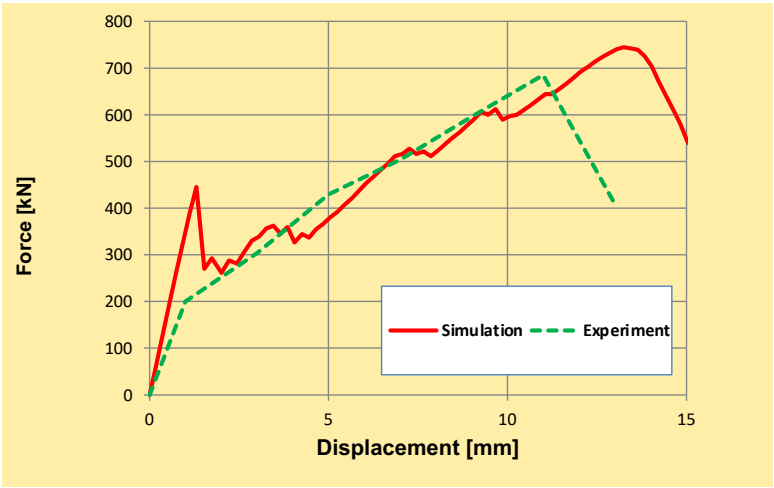

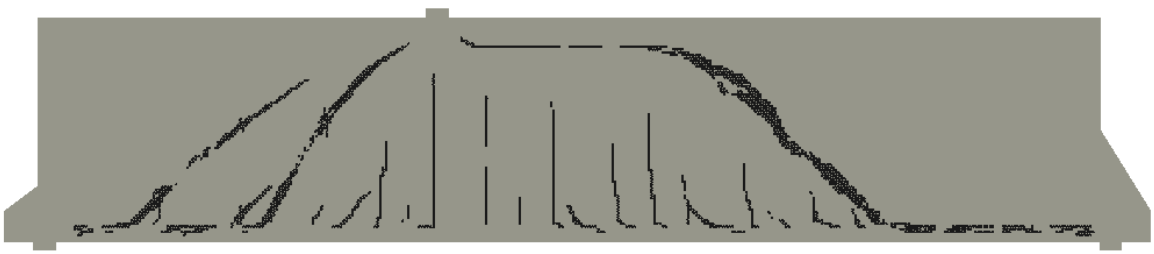

Toronto shear tests
Influence of uncertainties ?

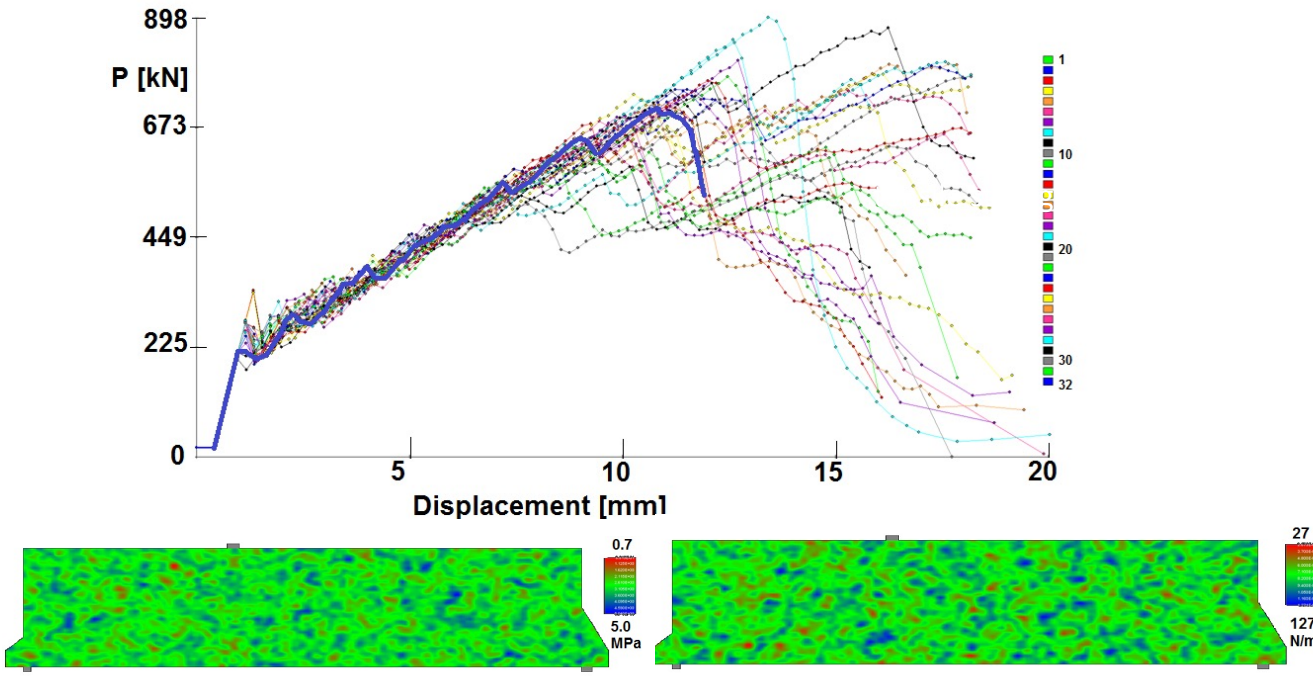

tensile strength random field

fracture energy random field

Degradation

- Increasing age of structures leads to material degradation significantly influencing durability, serviceability and ultimate capacity limit states and decreasing service life
- Significant role for planning reconstruction or demolition of structures – prognosis in time needed
- Main stressors: Carbonation of concrete and corrosion of reinforcement

Limit states and reliability levels

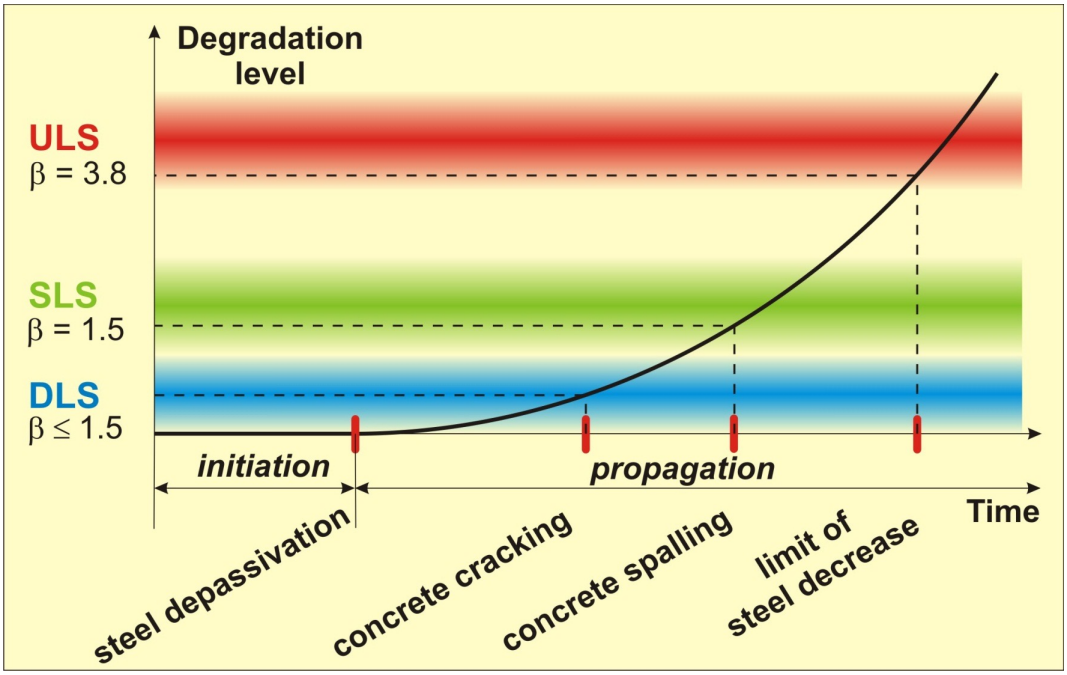

ULS = Ultimate Limit State SLS = Serviceability LS DLS = Durability LS

Service life

The service life can be assessed based on different levels of limit state function modeling:

1) durability limit states based on phenomenological models for concrete carbonation and corrosion of reinforcement – level 1
2) ultimate limit states at the level of critical structural element – level 2
3) ultimate limit states at the level of global behavior of structure – level 3

For the global structural modeling advanced computational models are needed, where aspects of nonlinear behavior of concrete and degradation modeling are combined

FReET-D module

Feasible **Re**liable **E**ngineering **T**ool for **D**egradation – **FReET–D**:

- module of the software FReET;
- combination of analytical models and simulation techniques for assessing the potential degradation of newly designed as well as existing concrete structures;
- models for carbonation, chloride ingress, reinforcement corrosion, sulphide, acid and frost attack;
- can serve for design or performance-based specification.

Case study
Degradated reinforced concrete arch bridge

over the Morava river in Czech Republic

Built in 1940

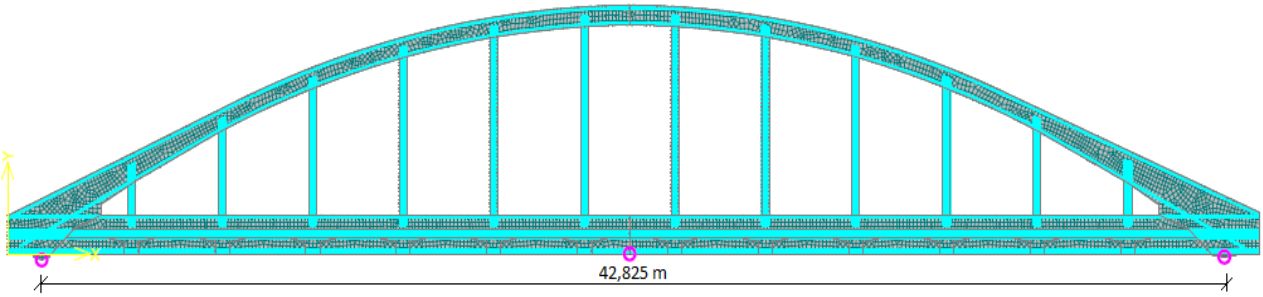

Concrete arch bridge

Detailed in-situ inspection was carried out (cut probes and radiographic inspection):

- Geometry of individual parts
- Type and position of reinforcement
- Level of degradation

cracks in arch

corrosion in bar

Significant cracks in left arch and significant corrosion of reinforcement after depassivation of concrete in vertical pull bars.

Basic random variables

Variable	Symbol	Unit	PDF	Mean	COV
Concrete					
Modulus of elasticity	E_c	[GPa]	Lognormal	$E_{c,m}$	0.15
Tensile strength	f_{ct}	[MPa]	Lognormal	$f_{ct,m}$	0.30
Compression strength	f_c	[MPa]	Lognormal	$f_{c,m}$	0.06
Steel reinforcement					
Yield strength	f_y	[MPa]	Normal	$f_{y,m}$	0.07
Geometry					
Reinforcement area	A_s	[mm^2]	Normal	A_s	0.02
Deviation of reinf. location	y	[m]	Rectangular	0	± 0.02 m
Carbonation of concrete					
Unit content of cement	c	[kg/m^3]	Normal	300	0.03
Unit content of water	w	[kg/m^3]	Normal	190	0.03
Corrosion of reinforcement					
Initial bar diameter	d_i	[mm]	Deterministic	Variable	
Time to corrosion initiation	t_i	[mm]	Deterministic	Variable according to calculated depth of carbonation	

Source: destructive and non-destructive tests + adopted from literature (JCSS probabilistic model code, FReET-D documentation)

Level 1: Durability limit state of girder

- Limit state for depassivation of reinforcement due to carbonation of concrete cover:

$$Z(t) = c - d(t)$$

$d(t)$ is carbonation depth of concrete in time t,
c is concrete cover

- Models for carbonation depth according to Morinaga (Carb3) and Kishitani (Carb7)
- Target reliability index β_n = 1.3

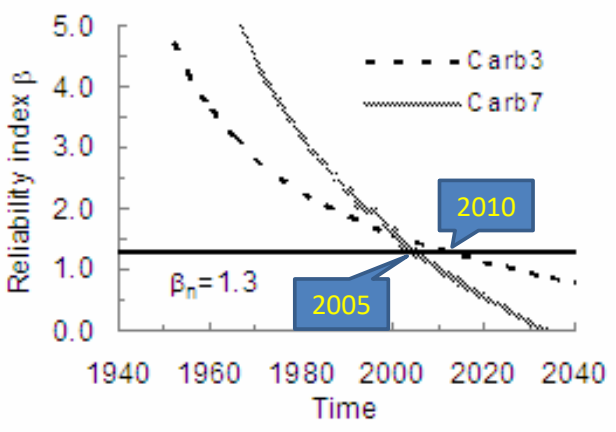

Level 2: Ultimate limit state of pull bar

- Ultimate load-bearing of highly deteriorated pull bar has been analyzed. Time dependent limit state function:

$$Z(t) = A_s(t) f_y - N(t)$$

$A_s(t)$ *is* area of reinforcement, f_y is yield stress of steel,
N is axial force in bar, t is time.

- Model Corr1 for steel corrosion

$$d(t) = \begin{cases} d_i & t \le t_i \\ \psi \left| d_i - 0.0116 i_{corr} R_{corr} (t - t_i) \right| & t_i < t \le t_i + \dfrac{d_i}{0.0116 i_{corr} R_{corr}} \\ 0 & t > t_i + \dfrac{d_i}{0.0116 i_{corr} R_{corr}} \end{cases}$$

- Target reliability β_n = 3.8

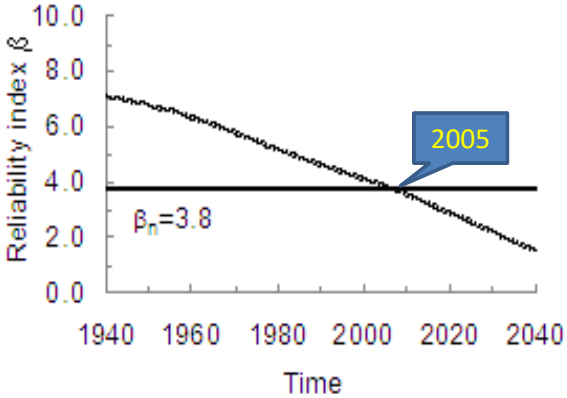

Level 3: Global level

- Ultimate load-bearing of the whole structure using stochastic nonlinear FEM analysis has been analyzed.
- Target reliability index $\beta_n = 3.8$
- Model Corr1 for steel corrosion

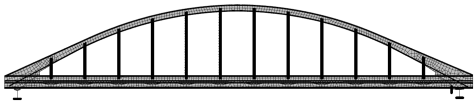

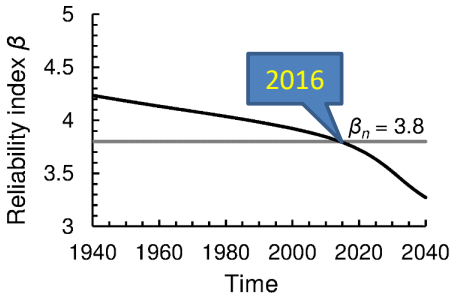

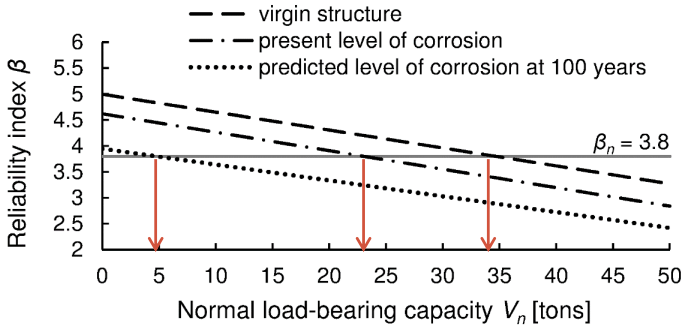

Shear resistance of prestressed girders: Probabilistic design

- **Oberndorfer Wien**
- **Experiments on fracture-mechanical parameters of concrete, database of fracture-mechanical parameters**
- **Experiments of scaled prestressed concrete girders**
- **Deterministic computational model of pre-stressed concrete girders.**
- **Stochastic model**
- **Probabilistic design**

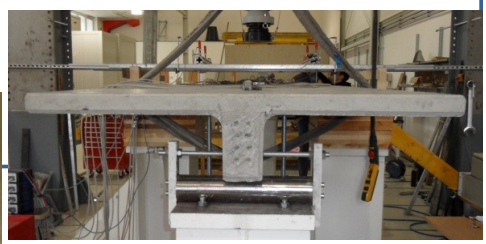

Experiment: fracture-mechanical parameters of concrete

CT

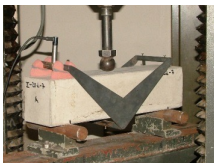

3PB

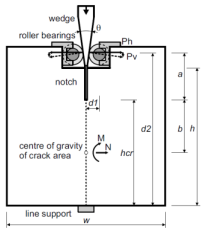

WST

+

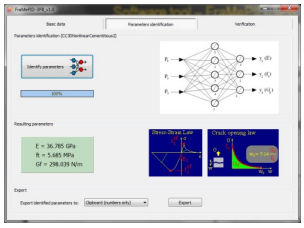

Identification

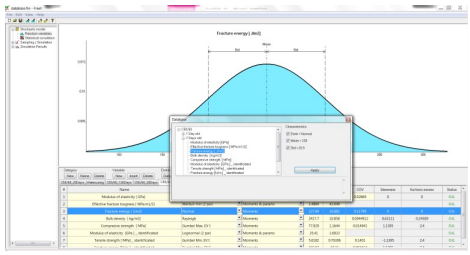

Database

More concrete mixes:

- C40/50
- C50/60
- …

Different ages of testing:

- 1 day
- 7 days
- 28 days
- 126 days

Scheme of inverse analysis

Structural response

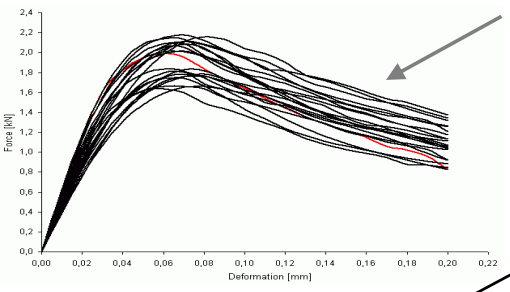

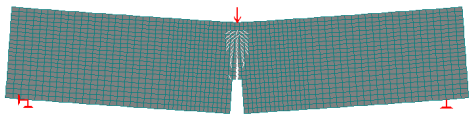

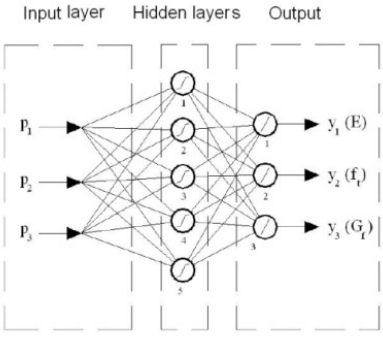

Material model parameters

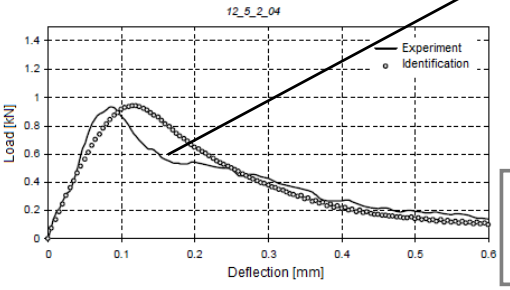

Stochastic calculation (LHS) – training set for calibration of synaptic weights and biases

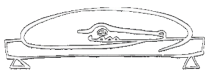

Database of fracture-mechanical parameters of selected concrete in FReET software

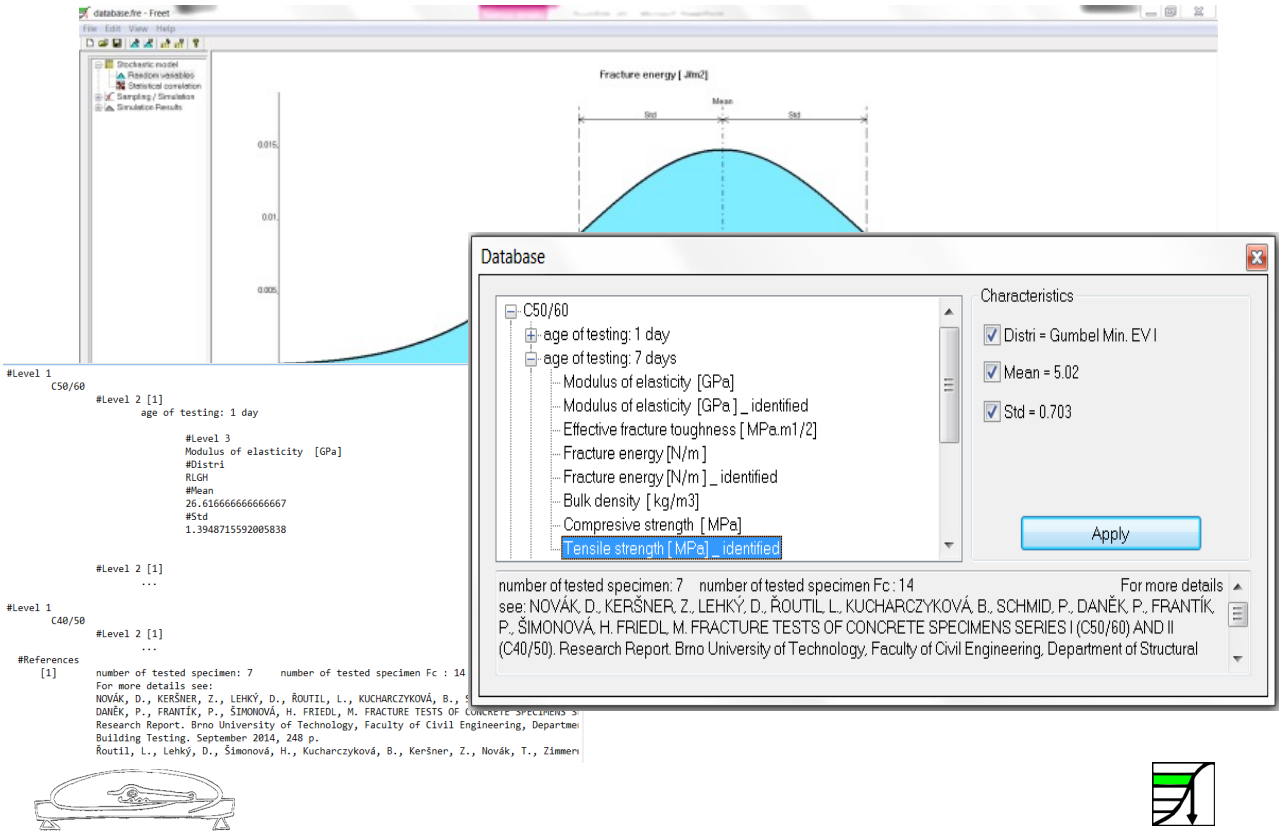

Experiment: scaled pre-stressed girders

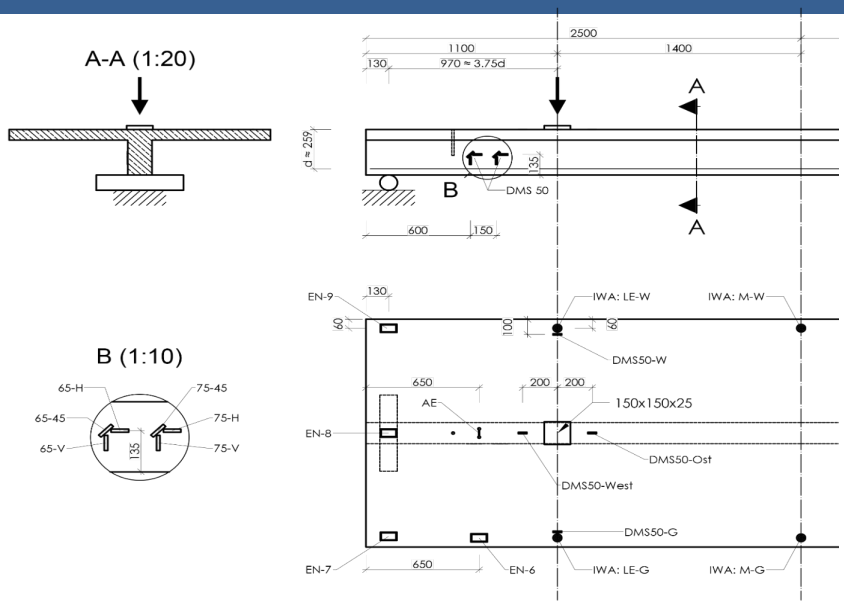

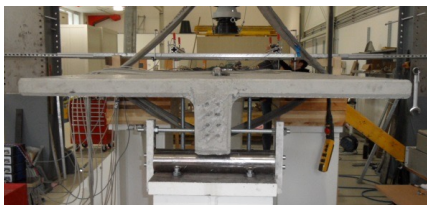

Basic geometry:
length 5 m, beam flange 1.5 m, thickness 0.07 m, beam web 0.14 m wide and 0.23 m high

Experiment: scaled pre-stressed girders

Scheme of loading during experiment

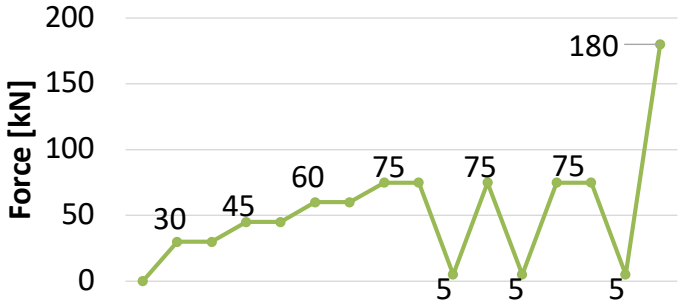

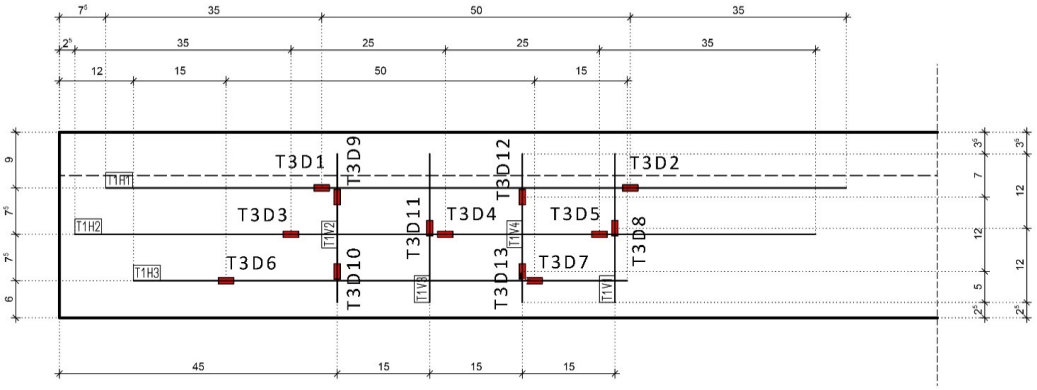

Internal strain monitors layout

Deterministic computational model

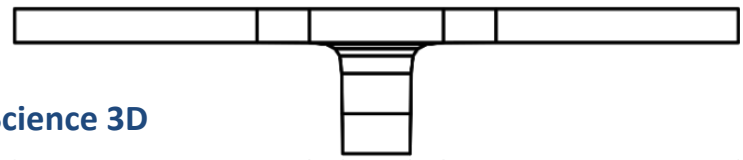

ATENA Science 3D

It is necessary to model transition radius between web and flange according to drawings of form provided by manufacturer.

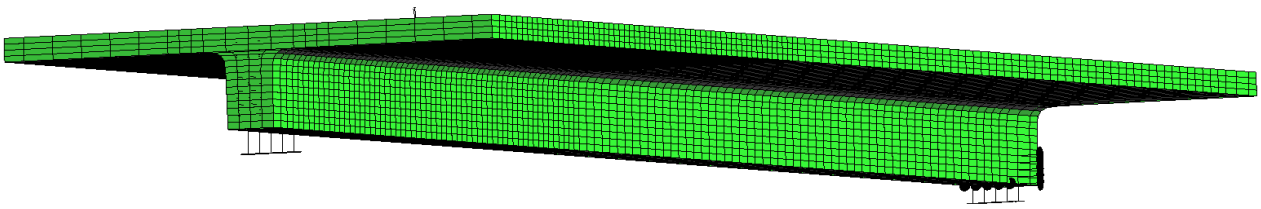

Regular hexagonal FE mesh composed of 24714 finite elements was generated in the program GID.

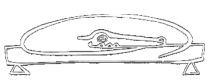

Deterministic computational model

The beam was continuously pre-stressed with 83.5 kN by a six cables St 1570/1770

Two different approaches have to be use simultaneously for applying prestressing losses:

A) **Reduction of prestressing itself –** due to difference of E module value at time of prestressing and time of experiment (also due to relaxation of tendons);

B) **Application of temperature load** – in order to capture effect of creep and shrinkage (value of corresponding temperature load was calculated according to FIB Model Code 2010).

Deterministic computational model

Numerical model of destructive test described above shows very good agreement with experiment in all aspects.

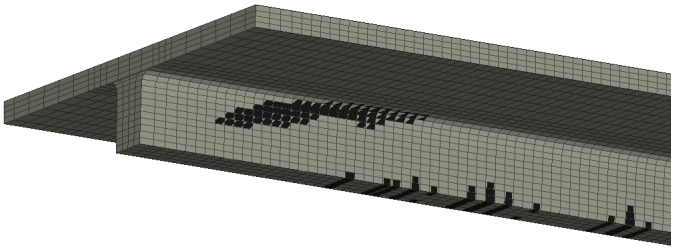

Crack pattern of numerical model and experimental test

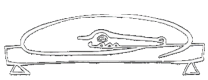

Stochastic material data calibration/identification

Material model of concrete:

- 3D Nonlinear Cementitious 2 (implemented in software ATENA Science)
- Four most sensitive material parameters were adjusted (*Fc, Ft, Gf, E*)

Parameters identified using ANN (using data obtained during fracture experiments):

Based on testing campaign-3point bending

Parameter	Mean	COV	PDF
Compressive strength	77 MPa	6.4%	GMB min EV1
Tensile strength	3.9 MPa	10.6%	GMB max EV 1
E - module	34.8 GPa	10.6%	WBL min (3par)
Fracture energy	219.8 Jm^{-2}	12.8%	GMB max EV 1

Parameters obtained from compression test of specimen with age of 41 days:

Based on experiment of girder

Parameter	Val. [MPa]	Obtained by
Compressive strength	69.7	Measurement
Tensile strength	04.IV	Calculated
E - module	35300	Cal. from LD curve

Stochastic material data calibration/identification

How to estimate material parameters of given realization with utilization of stochastic model of material?

- Use stochastic model to generate thousands of random vectors of material parameters using correct correlation matrix.
- Pick realization with F_c as close as possible to value directly measured before experiment.

Material parameters of given realization estimated using stochastic model:

f_c [MPa]	f_t [MPa]	G_f [MN/m]	E_c [MPa]
-69.7	3.3432	1.97E-04	28483

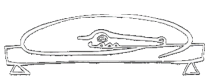

Load-displacement diagram (deterministic analysis)

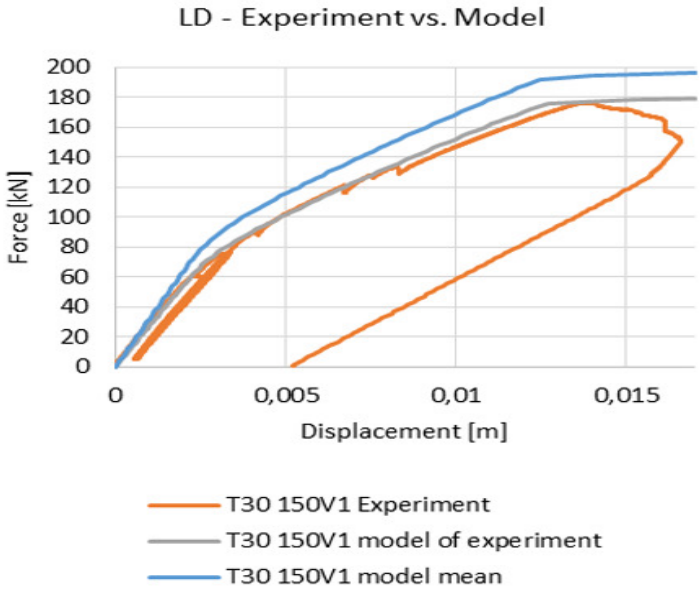

Comparison of load-displacement diagram

Experiments and simulation of scaled pre-stressed girders

Chosen strain monitors outputs:

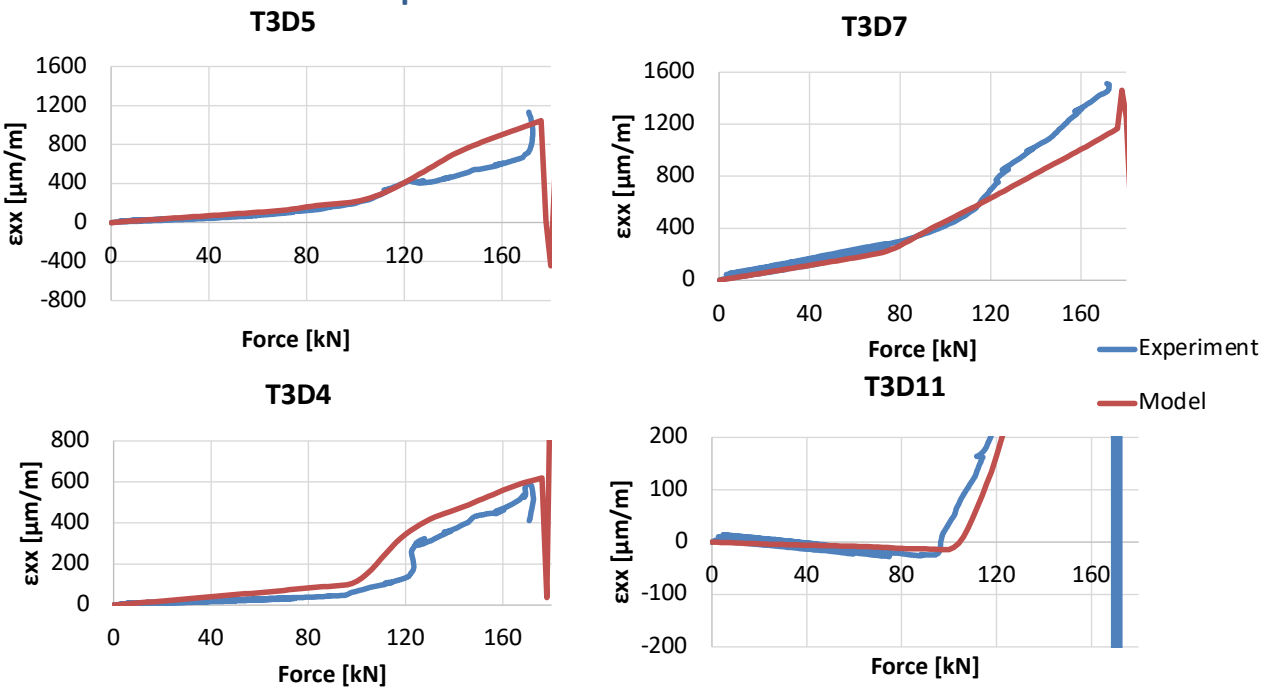

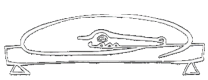

Random variables

Prameter	Mean	COV [%]	PDF	Unit	Source
Concrete (C50/60)					
E	34.8	20.6	WBL min (3 par)	[GPa]	(Řoutil et al. 2014)
f_t	3.9	20.6	GMB max EV I	[MPa]	(Řoutil et al. 2014)
f_c	-77	16.4	GMB min EV I	[MPa]	(Řoutil et al. 2014)
G_f	219.8	32.8	GMB max EV I	[J.m^{-2}]	(Řoutil et al. 2014)
ρ	0.0023	4	Normal	[kton/m^3]	(Řoutil et al. 2014)
Steel reinforcement (Bst 550B)					
E_s	200	2	Normal	[GPa]	(Ceresa et al. 2007)
f_{ys}	610	4	Normal	[MPa]	(Ceresa et al. 2007)
Tendons (Cables - St 1570/1770)					
E_t	195	2.5	Normal	[GPa]	(Ceresa et al. 2007)
f_{yt}	1387.88	2	Normal	[MPa]	(Ceresa et al. 2007)
Prestresing force					
P	0.0835	6	Normal	[MN]	(Ceresa et al. 2007)
Loss of prestresing (Uncertainties)					
I. L.	1	30	Lognormal	[-]	(Ceresa et al. 2007)
L. T. L.	1	30	Lognormal	[-]	(Ceresa et al. 2007)

Stochastic „bundle“ of load-displacemnet diagram

31 simulations (11 simulations extended in second run of hierarchical LHS method by another 20 simulations)

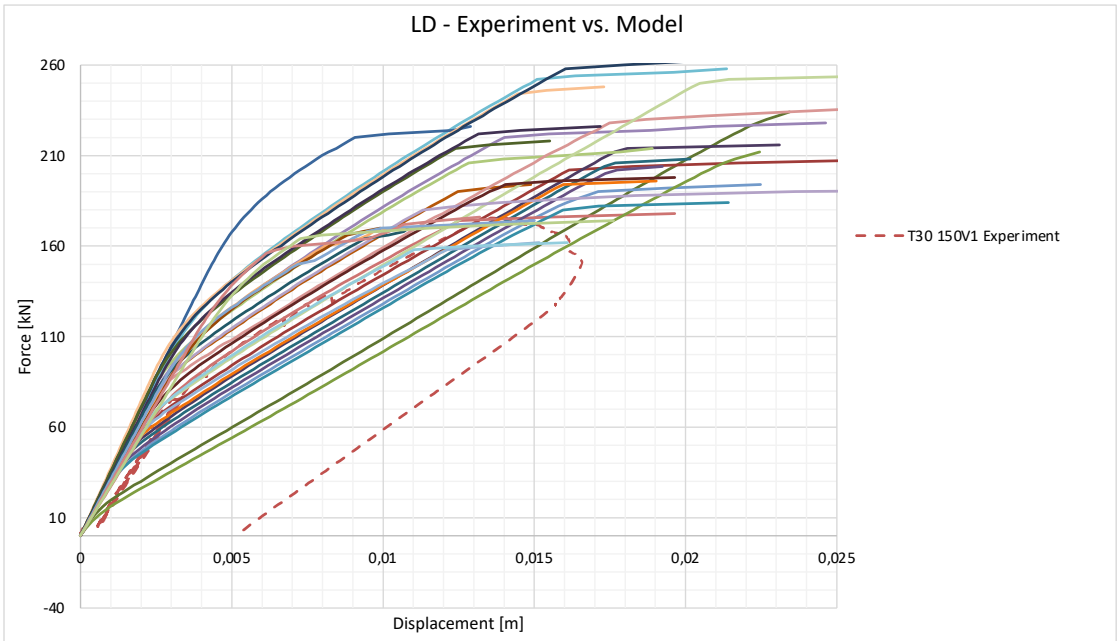

Ultimate limit state

- Ultimate limit state represented by critical value of force applied during experiment (peak of LD diagram)
- Design value by:
  - fully probabilistic approach – design value for Probability = 0.0012 (Eurocode)
  - classical calculation using partial safety factors
  - ECOV method

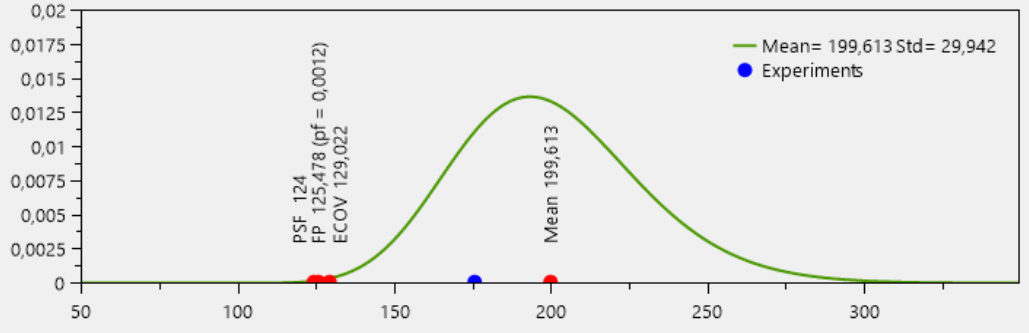

Conclusions

- Efficient techniques of employing stochastic simulation methods were combined in **FReET** software - an advanced tool for the probabilistic assessment of user-defined problems at ultimate capacity and serviceability limit states
- Degradation models implemented in **FReET-D** software can help users to choose appropriate models and assess the service life issue as applied to concrete structures - durability limit states
- **SARA** = complex integration of probabilistic engine (FReET) and nonlinear FEM (**ATENA**). Already hundreds applications/users worldwide, concrete structures, intensive development.
- <u>Theoretical development and application/promotion</u>

Project ATCZ190 – Advanced analysis of existing reinforced and pre-stressed concrete bridges: nonlinearity, reliability, safety formats, life-time aspects

awarded by European Regional Development Fund within the European Union program Interreg Austria–Czech Republic

- Project number: **ATCZ190**
- Project acronym: **SAFEBRIDGE**
- Duration: **01.09.2018–31.08.2021**
- URL: https://www.at-cz.eu/safebridge

- Lead partner: **Universität für Bodenkultur Wien**
- Project partner: **Brno University of Technology**
- Strategic partners: *public subjects*
  – national (BMVIT, ÖBB Infrastructure AG, ASFINAG, Ředitelství silnic a dálnic ČR, Správa železnic),
  – regional (Amt NÖ Landesregierung, Správa a údržba silnic Jihomoravského kraje),
  – local (MA29 a Brněnské komunikace a.s.)
  small and medium-sized companies (VILL ZT, KOB ZT, Schimetta ZT, Potyka & Partner ZT, Dopravoprojekt Brno a.s., EXprojekt s.r.o.)
  research institutions (Klokner Institute of the CTU in Prague)

EUROPEAN UNION

Interreg Austria-Czech Republic
European Regional Development Fund

- Main goal:
  – Design of advanced procedure of numerical assessment of bridge structures based on reliability theory (on the basis of EN 1990)

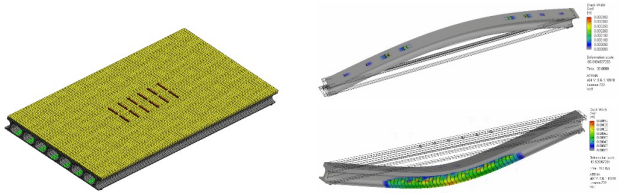

- Main outputs:
  – Ensuring the possibility of utilization of advanced reliability assessment of bridges based on combination of numerical and statistical methods
  – Creation of a Guideline for practical utilization of such methods (Appendix D of ÖN B 4008-2)
  – Design of sustainable training program focused on the assessment of structural reliability

Conclusions

Thank you for your attention!

www.freet.cz

www.cervenka.cz

Software tools: FReET, ATENA, SARA, FReET-D

http://www.freet.cz **http://www.cervenka.cz**

Annex C

Lars Erik Øi

Cost, size, and structure optimization of CO_2 absorber columns onshore and offshore

Cost, size, and structure optimization of CO2 absorber columns onshore and offshore

Brno, 23.5.2024 Lars Erik Øi,
Professor in Process Technology, USN

Department of Process, Energy and Environmental Technology

Universitetet i Sørøst-Norge

Energy and Carbon Capture research group (URGENT- USNs Research Group for Energy and Environmental Technology)

Subgroups:
Carbon Capture
Alternative fuels (gasification)
Environmental Biotechnology
Alternative power supply (wind)

Department of Process, Energy and Environmental Technology

Universitetet i Sørøst-Norge

USN Porsgrunn CO_2 capture group experience: http://www.co2-lab.com/

- Design of gas liquid absorption/desorption gas (e.g. CO_2) processes
- Process simulations
- Cost estimation
- Lab. determination of process design data (solvent data: physical, corrosion, degradation)
- Solvent management
- Industrial CO_2 safety
- Benchmarking of CO_2 capture technologies

Universitetet i Sørøst-Norge

PTP: Porsgrunn test pilot

- Background
  - Lab-scale solvent test pilot
    - 50 L solvent, Q=0,5-5 l/min; absorber: 1 bar, T_{max}: 70°C; desorber: 3 bar, T_{max}: 130°C; synthetic flue gas
    - Access to a complete support laboratory
- Possibility for
  - Low-threshold accelerated solvent testing
  - Validation of process models
  - Visual solvent monitoring, on-line speciation adsorb./desorb., off-line solvent analysis, etc.
  - Solvent degradadation, solvent management

Universitetet i Sørøst-Norge

CO2-concentration increases and the temperature increases

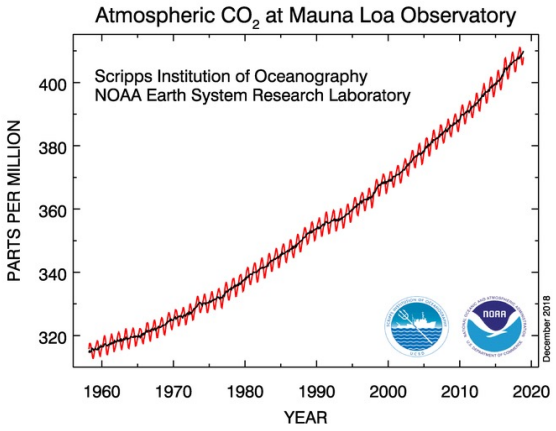

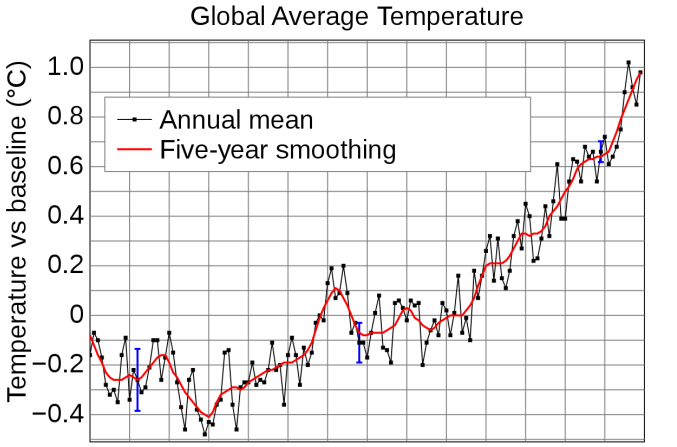

(Fra Wikipedia)

CO2-capture in IEA's 2-degrees scenario (2014)

CCS is a critical component of a sustainable energy system

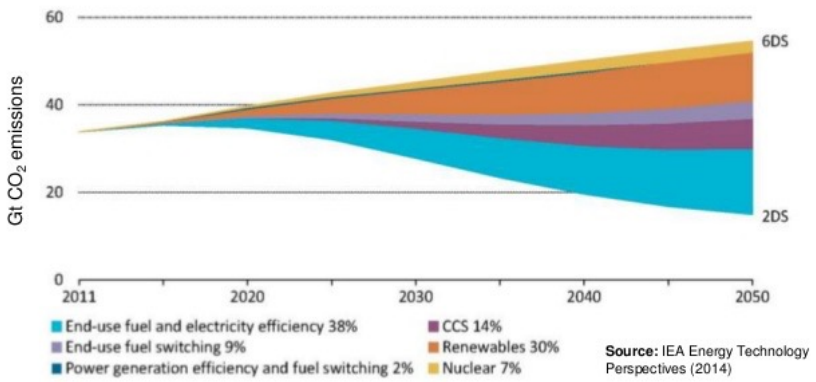

In a 2° scenario, CO_2 captured in 2030 is in excess of 1,500 Mt and 6,300 Mt in 2050. So how are we tracking?

Capture cost for CO_2-capture from industry in Norway Tel-Tek/Klimakur, Klif (MD), 2009

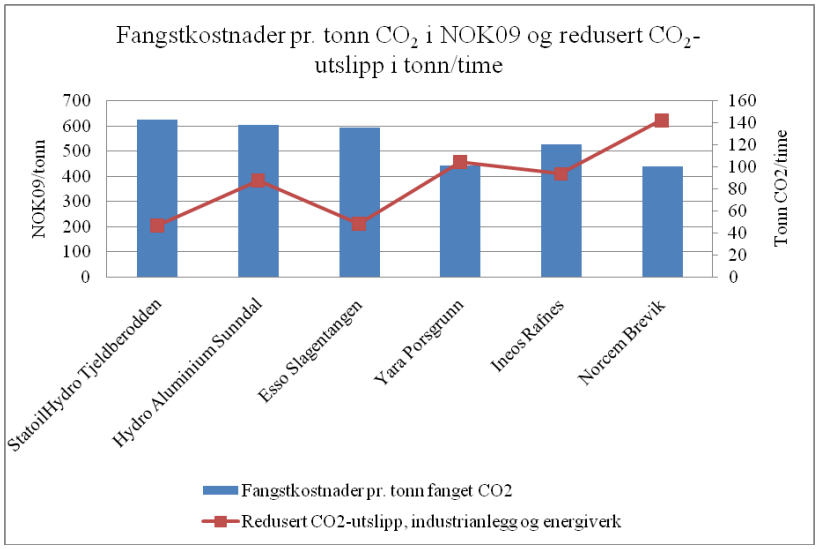

Storage of CO_2

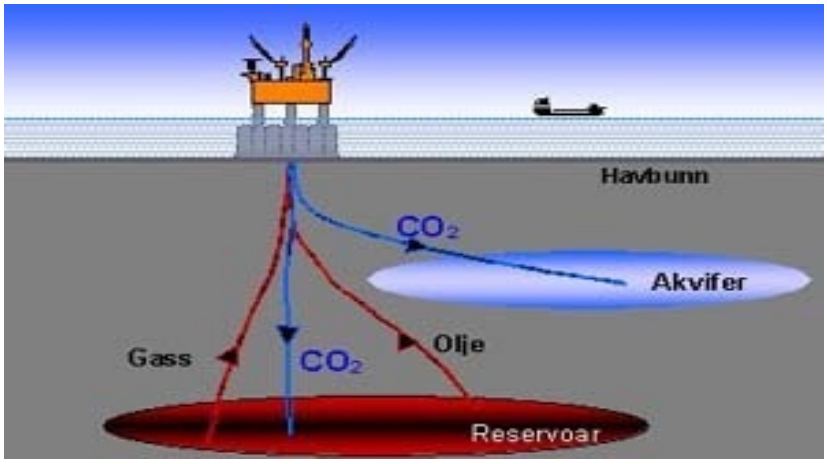

(Figure from Bellona)

Universitetet i Sørøst-Norge

Typical CO_2-capture-process based on absorption

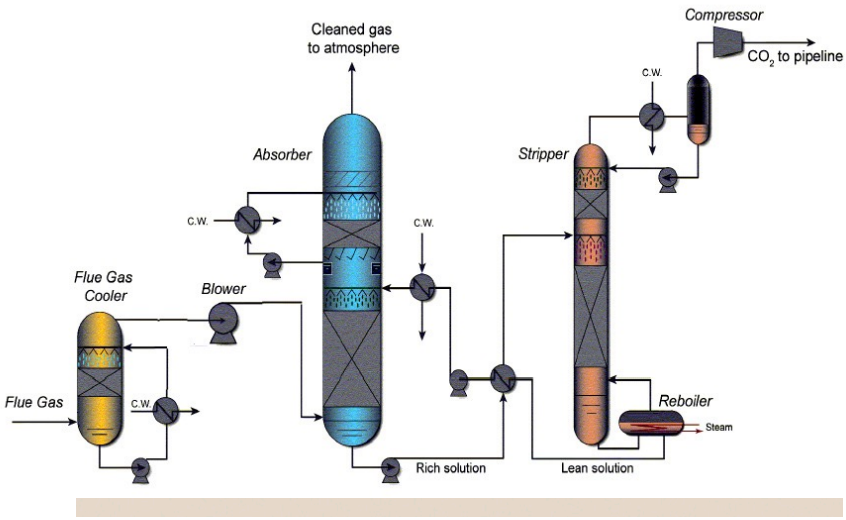

(Figure from SINTEF)

CO2-emmisions and capture at Yara in Porsgrunn

- Emissions of 900 000 CO_2 ton/yr (from ammonia plant)
- A fraction of this is absorbed in water under pressure in 4 blue absorption towers
- Some is sold as CO_2 (e.g. to Farris) and is exported by ship
- More of this CO_2 could be captured if it coould be stored

CO_2-fangst at the Sleipner field in the North Sea

- Absorption of CO_2 from natural gas
- To reduce unnecessary transport of CO_2 and to reduce CO_2 tax
- CO_2 is stored in the Utsira formation which is a salt water containing layer between the ocean bottom and the Sleipner oil and gas field

(Photo from Statoil)

Universitetet i Sørøst-Norge

Test Center Mongstad (TCM)

Test site for ca 80000 ton CO_2/yr (amine based absorption)

Have tested processes for Aker Solutions (ACC) and Cansolv (Shell)

On TCM also the Alstom chilled Ammonia prosess is tested

(Photo from TCM)

Universitetet i Sørøst-Norge

CO_2 capture on Boundary Dam in Saskatchewan in Canada

- Absorption of CO_2 from exhaust from coal based power plant
- CO_2 is used for enhanced oil recovery (EOR)

(Photo from SaskPower)

CO_2 emissions from Klemetsrud in Oslo

(Photo from Wikipedia)

CO_2 emissions from cement plant in Brevik

(Photo from Varden)

(Photo from Norcem)

Universitetet i Sørøst-Norge

CCS project in Norway (Northern Lights)

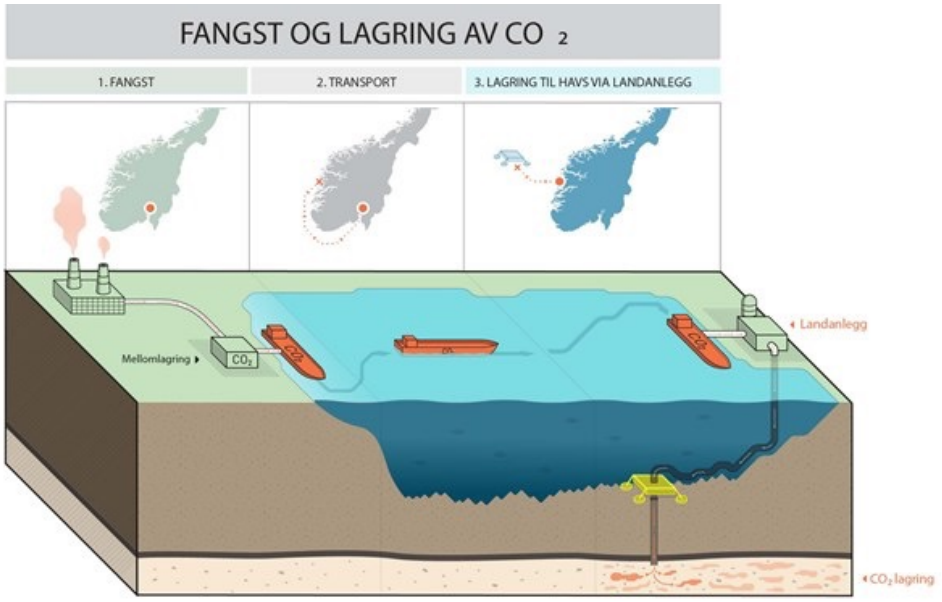

(Figure from Regjeringen.no)

Universitetet i Sørøst-Norge

SIMS EUROSIM 2021
First SIMS EUROSIM Conference on Modelling and Simulation
Virtual Conference on 21 - 23 September 2021

Offshore CO_2 Capture from gas turbine with low investment optimized using Aspen HYSYS

Lars Erik Øi, Fatemeh Fazli, Rajan Thapa
University of South-Eastern Norway

Federation of European Simulation Societies
SIMS - Scandinavian Simulation Society
UNIVERSITY OF OULU
FINNISH SOCIETY OF AUTOMATION
SUOMEN AUTOMAATIOSEURA RY

OUTLINE for paper

CO_2 capture from gas turbine exhaust gas is a possibility for CO_2 emission reduction on oil and gas production platforms.

A standard process is based on absorption in monoethanol amine (MEA).

A challenge for cost estimation and cost optimization is that the cost of size and weight for the process equipment is higher than on a land-based process.

UPSTREAM PROCESS AND A STANDARD CO_2 CAPTURE PROCESS

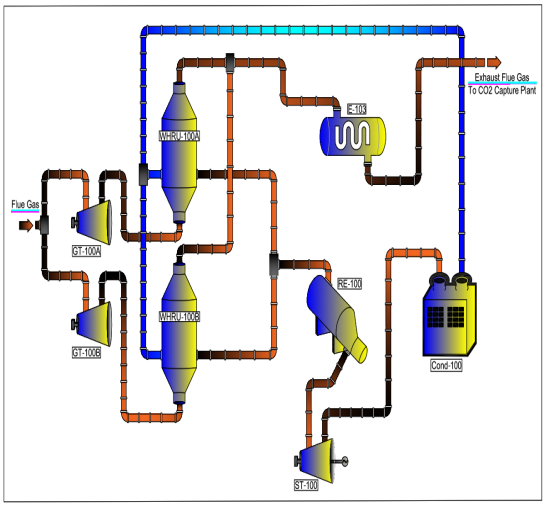

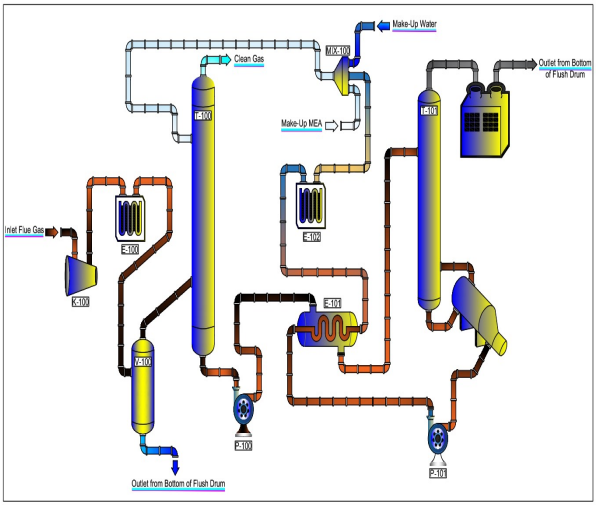

SIMULATION FLOWSHEET OF THE BASE CASE CO_2 CAPTURE PROCESS

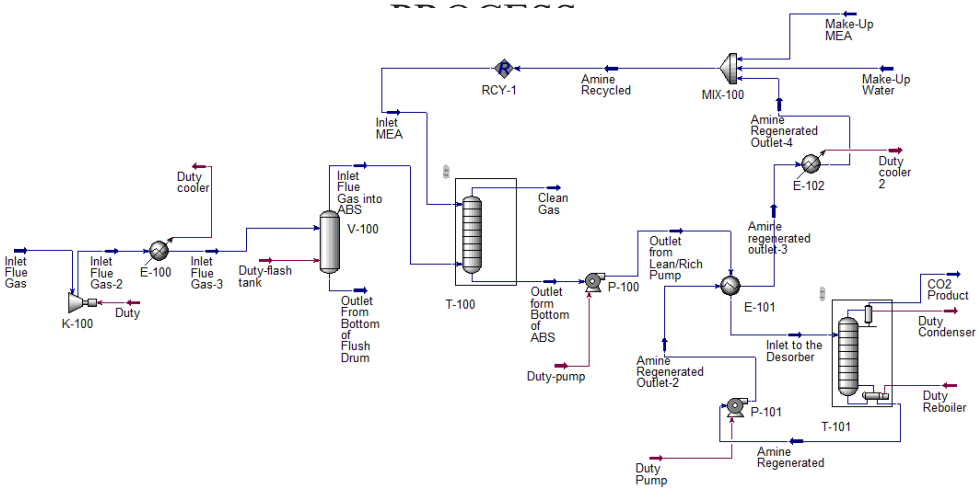

DIMENSIONING FOR COST ESTIMATION

For the absorber and desorber internals, a structured packing was chosen. Murphree efficiencies of 0.15 and 0.5 were specified for 1 meter of packing in the absorber and the desorber. The absorption and desorber column diameter was calculated based on a gas velocity of 2.0 m/s and 1 m/s.

Centrifugal pumps with 75 % adiabatic efficiency were specified.

Overall heat transfer coefficient was specified to 500 W/(m^{2}K)for the lean/rich exchanger.

COST SPECIFICATIONS FOR COST ESTIMATION

The equipment costs were taken fr the Aspen In-plant Cost Estimator (Version 10).

In the detailed factor method, each equipment cost (in carbon steel) was multiplied with its individual installation factor to get equipment installed cost.

Parameter	Value
Plant lifetime	25 years
Discount rate	8%
Maintenance cost	3 % of installed cost
Electricity price	0.078 Euro/kWh
Steam price	0.032 Euro/kWh
Annual operational time	8000 hours
Currency exchange rate 2021	9.78
Cost index 2020	301
Cost index September 2021	317

USN Universitetet i Sørøst-Norge

CONCEPTS FOR CO_2 ABSORPTION COLUMNS

Traditional: Circular steel columns (with structured packing)

Large structures: Concrete (cheap and robust)

New land-based CO_2 capture: Rectangular concrete shapes

Offshore: Compact circular steel columns. A challenge for cost optimization is that the cost of size and weight for the process equipment is higher than on a land-based process.

Universitetet i Sørøst-Norge

Large cooling towers

Universitetet i Sørøst-Norge Power plant in Dresden, H = 122 m. Modular version of cooling tower (Wikipedia)

Design of large scale CO_2 absorber column

Typical material: SS304/SS316
Typical wll thickness: 10 mm
Support structure

These factors may be optimized for offshore applications
- New optimization design criteria
- Specifications for equipment vendors

Universitetet i Sørøst-Norge

Design of CO_2 absorber column (from Thesis)

1.1 Absorber

To calculate the absorption column diameter, the gas velocity within the column must be determined, which is typically assumed to be between 2-2.5 m/s [29]. Equation (3.1) can then be utilized to calculate the cross-sectional area (A) of the column using the volumetric flow rate, $\dot{V}_{gas}$, and gas velocity, v_{gas}. Subsequently, Equation (3.2) can be used to determine the column diameter (D).

$$A = \frac{\dot{V}_{gas}}{v_{gas}} \tag{3.1}$$

$$D = \sqrt{\frac{4 \times A}{\pi}} \tag{3.2}$$

The gas flow and the dimensioning parameters for the absorber are shown in Table 3.1.

Table 3.1: Absorber diameter calculation for base-case, doubled feed gas and two-absorber case

Parameter	Base Case	Doubled Feed Gas	Two-ABS
Number of Absorbers	1	1	2
Column Packing Height, m	15	15	15
Column Height, m	30	30	30
Cross section area, m^2	266.02	531.9	266.02
Diameter, m	18.4	26.02	18.7

Universitetet i Sørøst-Norge

Cost estimatation of CO_2 absorber column

1.1.1 Aspen Process Economic Analyzer software for BEC estimation

Another approach to estimate BEC employed in this study is Aspen Process Economic Analyzer (APEA). Aspen Process Economic Analyzer relies on model-based estimation to generate project cost estimates. The user-defined data for estimation the cost is quite like the Aspen-In-Plant (AIP) cost estimator, while the APEA can calculate not only the equipment cost but also the installed direct cost (piping, civil, structural steel, insulation, etc.) for each process equipment. The equipment cost comparison for APEA and AIP cost estimator is presented in Table 4.3.

Equipment	Aspen Process Economic Analyzer (Euro)	Aspen In-Plant Cost Estimator (Euro)
Absorber	19957300	20175200

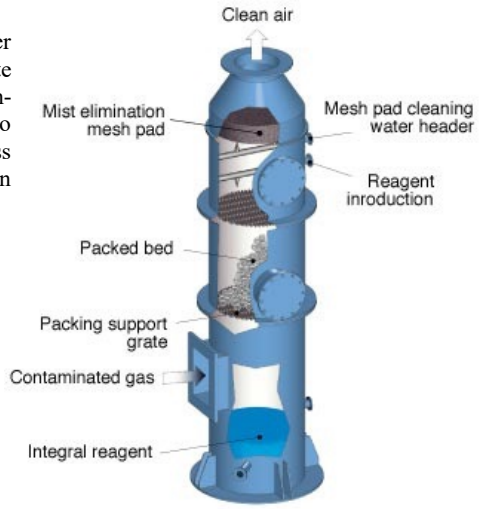

Universitetet i Sørøst-Norge

Improvement of design of large scale CO_2 absorber column, especially off-shore

Typical material: SS304/SS316
Typical wll thickness: 10 mm
Support structure

These factors may be optimized for offshore applications
- Simulation (e.g. CFD) and design (e.g. FEM) tools
- New optimization design criteria
- Specifications for equipment vendors

Universitetet i Sørøst-Norge

The End

Universitetet i Sørøst-Norge

Mer om CO_2-fangst, klimapolitikk og klimaforhandlinger kan finnes på nettsidene

- IPCC: http://www.ipcc.ch/
- IEA: http://www.iea.org/
- Miljødirektoratet: http://www.miljodirektoratet.no/
- Gassnova: http://www.gassnova.no/
- Bellona: http://bellona.no/
- Cicero:http://cicero.uio.no/no/posts/klima/parisavtalen-hva-ble-egentlig-vedtatt?
- COP21: http://www.cop21paris.org/

Universitetet i Sørøst-Norge

Annex D

David Lehký

Determination of mechanical fracture parameters using machine learning-based inverse analysis

Determination of mechanical fracture parameters using machine learning-based inverse analysis

David Lehký

Brno University of Technology, Czech Republic

BRNO UNIVERSITY OF TECHNOLOGY
FACULTY OF CIVIL ENGINEERING

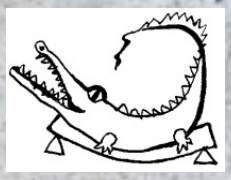

Outline

1. Introduction and motivation.
2. Methods for determining mechanical fracture parameters.
   - Direct evaluation of fracture test data
   - Inverse analysis
3. Identification of statistical characteristics of parameters
4. Methodology of inverse analysis
   1. Artificial neural network
   2. Stratified sampling
   3. Software
5. Hybrid NNE-based identification system for fine-grained composites
6. Example of identification: shear wall failure
7. Summary and conclusions

Introduction and motivation

Why do we determine material parameter values?

The main reasons include:

1. Verification of the material properties of existing structures to ensure their reliability and durability.
2. Studying the material properties of newly developed composites (recycled materials, high strength materials, etc.)
3. Numerical modeling of structures – advanced material models.

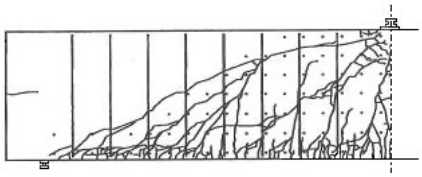

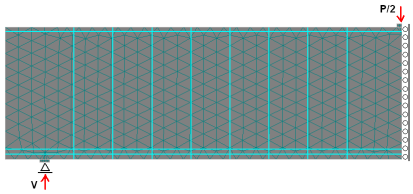

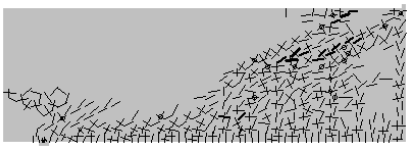

Introduction and motivation

Not only mechanical properties (strength, stiffness) but also fracture properties (resistance to the initiation and propagation of cracks) are of interest.

Important parameters of concrete and other quasi-brittle materials are modulus of elasticity, tensile and compressive strength, effective crack elongation, effective fracture toughness, etc.

Key parameter for computational modeling is fracture energy.

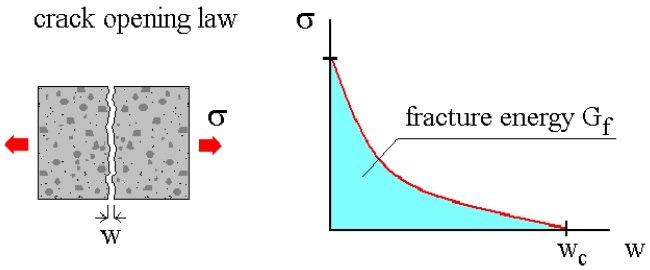

Computational modeling – a typical procedure

Numerical model of structure

appropriate material model
(e.g. 3D Nonlinear Cementitious 2, Microplane model, etc.)
– many material parameters

Information about parameters:

- Experimental data
- Code recommended formulas
- Engineering estimation

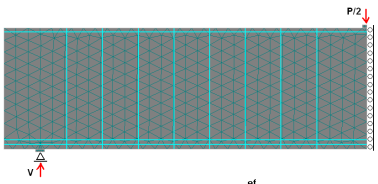

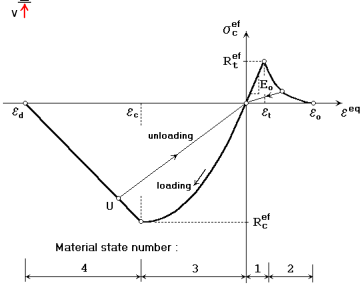

Computational modeling – a typical procedure

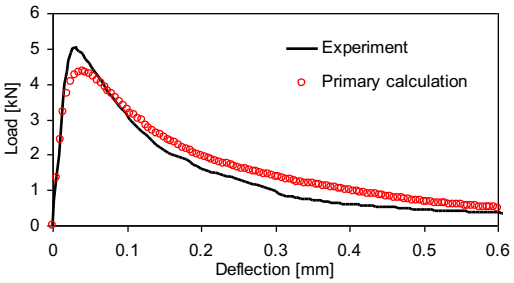

Primary calculation:

Correction of parameters:

- „Trial–and–error“ method
- Model updating via inverse analysis

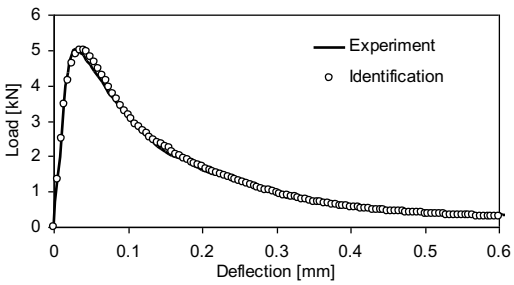

How do we determine the parameter values?

Experimental measurements need to be carried out – *in situ* or in the laboratory.

Laboratory fracture tests of specimens with stress concentrators loaded in a suitable test configuration, e.g. three-point bending test, wedge splitting test, etc., are used to determine the mechanical fracture parameters of composites with quasi-brittle matrix.

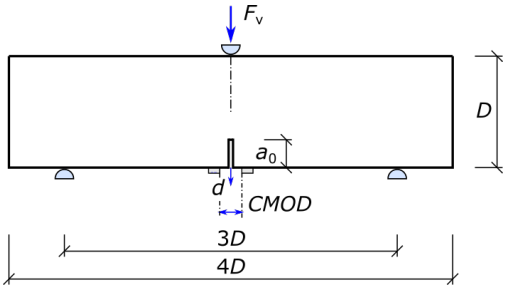

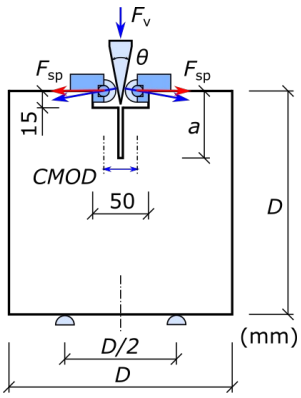

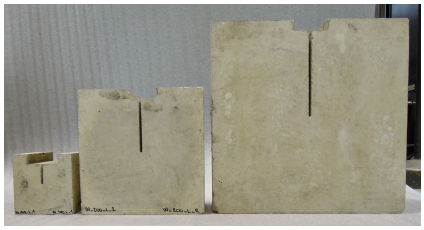

How do we determine the parameter values?

During the test, the specimen is loaded with an increment of deformation and the values of applied load and displacement (deflection or crack mouth opening displacement) are recorded.

The result of the measurement is a test record in the form of a force vs. displacement (*F–d*) or force vs. crack mouth opening displacement diagram (*F–CMOD*).

The (*F–d*) diagram carries a lot of information about the properties of the studied specimen.

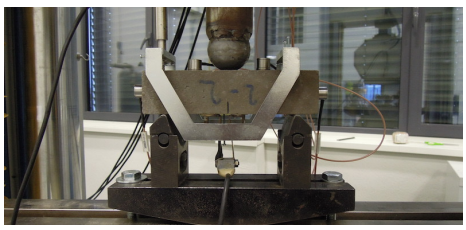

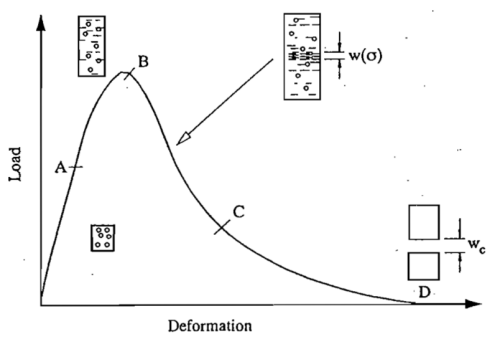

How do we determine the parameter values?

When carrying out the test, it is necessary to ensure that the test is carried out correctly and that the correct data is recorded. It is necessary to eliminate phenomena such as:

- Seating of the specimen + pushing into the supports – leads to incorrect recording of deformation. A special steel frame is used to measure deformation.
- Loss of measurement stability due to insufficient test machine stiffness in relation to the specimen stiffness. It can be detected from a deflection time series. Incorrect part must be removed and could be replaced by a suitable approximation.

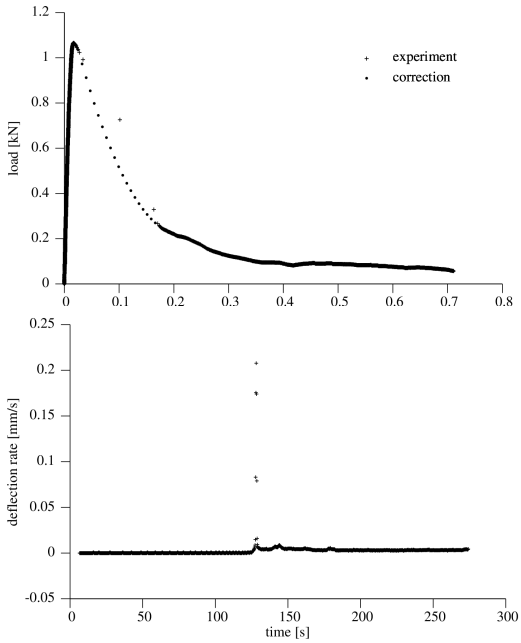

How do we determine the parameter values?

The mechanical fracture parameters can be obtained from the test record data by:

1. Direct evaluation of the *F–d* diagram using the Work-of-fracture method, Effective Crack Model, Double-*K* model.
2. Inverse analysis using the computational model.

Direct evaluation of *F–d* diagram

Static modulus of elasticity

It can be obtained from the initial branch of the *F–d* diagram. E.g. for 3PBT:

$$E_{\mathrm{B}} = \frac{F_{\mathrm{v},i}}{4Bd_i}\left(\frac{S}{D}\right)^3\left[1 - 0.387\frac{D}{S} + 12.13\left(\frac{D}{S}\right)^{2.5}\right] + \frac{9}{2}\frac{F_{\mathrm{v},i}}{Bd_i}\left(\frac{S}{D}\right)^2 F_1(\alpha_0)$$

$$F_1(\alpha_0) = \int_0^{\alpha_0} xY^2(x)dx \qquad \alpha_0 = \frac{a_0}{D} \qquad S = 3D$$

$$Y(\alpha_0) = A_0 + A_0\alpha_0 + A_2\alpha_0^2 + A_3\alpha_0^3 + A_4\alpha_0^4 A_i \ldots \text{see Karihaloo (1985)}$$

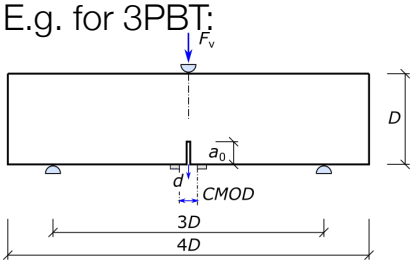

Direct evaluation of *F–d* diagram

Effective fracture toughness

It is based on the effective crack model. It represents a quantitative expression of the material's resistance to crack propagation. It is the specific energy that a material is able to absorb locally before unrestricted crack propagation occurs.

$$K_{\mathrm{I}ce} = \frac{6M_{\max}S}{BD^2}Y(\alpha_e)\sqrt{a}_e \qquad \alpha_{\mathrm{e}} = \frac{a_e}{D}$$

a_e, $M_{\max}$ … effective crack length and maximum moment, both corresponding to $F_{v,\max}$

Fracture energy

It represents the total energy required to create two new surfaces. It is evaluated from the entire *F–d* diagram – the fracture work is calculated = area under the curve divided by the size of the intact ligament. Then the fracture energy:

$$G_{\mathrm{f}} = \frac{1}{(D-a_0)B}\left(\int F_v \mathrm{d}d + m_g d_{\max}\right)$$

m_g … mass of the specimen
$d_{\max}$ … maximum deflection
B … specimen width

Direct evaluation

True fracture energy

- The fracture energy obtained from the tests is dependent on the size of the specimens – it is affected by the size of the fracture process zone, which is affected by the free end of the specimen.
- Hu & Wittman assume a bilinear distribution of the local fracture energy g_{f} over the depth.
- The value obtained from the tests is the average fracture energy G_{f}.
- The real fracture energy G_{F} (material constant) can be determined from a set of at least two tests on the same size specimens with different initial notch depths a_0 – a system of two equations with unknowns G_{F} a a_{l}.

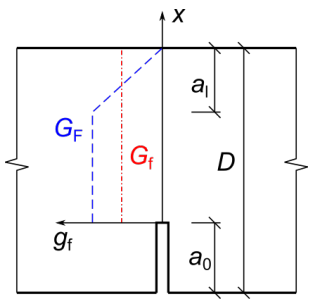

$$G_{\mathrm{f}}\left(\frac{a_0}{D}\right) = \begin{cases} G_{\mathrm{F}}\left(1 - \frac{1}{2}\frac{\frac{a_l}{D}}{1-\frac{a_0}{D}}\right) & 1-\frac{a_0}{D} > \frac{a_l}{D} \\ G_{\mathrm{F}}\frac{1}{2}\frac{\left(1-\frac{a_0}{D}\right)}{\frac{a_l}{D}} & 1-\frac{a_0}{D} \le \frac{a_l}{D} \end{cases}$$

Inverse analysis

The values of the selected mechanical fracture parameters can be determined by inverse analysis, where we try to use the measured response **R** to obtain information about the input parameters **P** which lead to the given response.

Inverse analysis can be performed in two ways:

1. Using optimization – an iterative search for input parameters under the condition of minimizing the difference between the obtained (from the model) and the desired response (from the experiment). A direct forward relationship (model) between the input parameters **P** and the output response **R** (**P**→**R**) is used.
2. Using direct inversion – the inverse relationship between **P** and **R** (**R**→**P**) is used. This must first be expressed/defined.

Inverse analysis

Both methods use a nonlinear computational model.
E.g. ATENA software – CC3D Nonlinear Cementitious 2 material model.

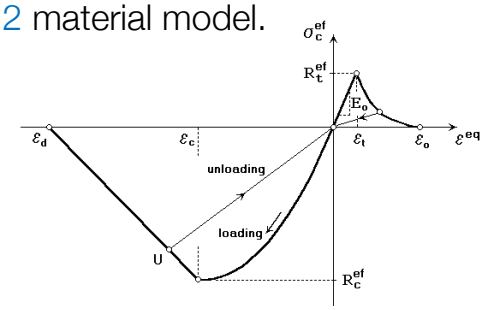

Parameters to be identified from 3PBT:

- Modulus of elasticity E_c
- Tensile strength f_t (R_t)
- Fracture energy G_f

Tensile softening model according to Hordijk:

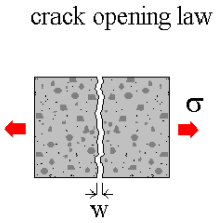

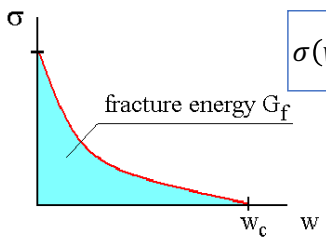

$$\sigma(w_c) = \left\{1 + \left(c_1 \frac{w}{w_c}\right)^3\right\} \exp\left(-c_2 \frac{w}{w_c}\right) - \frac{w}{w_c}(1 + c_1^3)\exp(-c_2)$$

$$c_1 = 3;\ c_2 = 6.933;\ w_c = \frac{5.14 G_f}{f_t}$$

Identification using direct inversion

The inverse relationship between the input material parameters **P** and the response of the test sample **R** is sought.

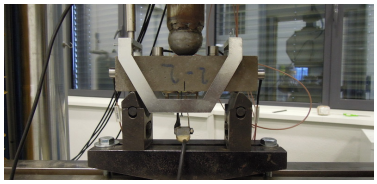

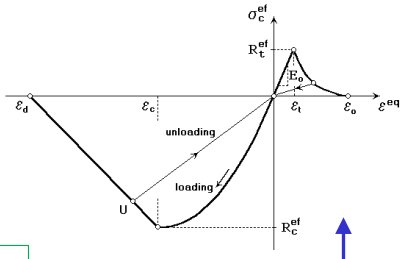

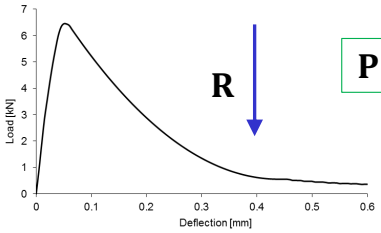

R

$$\mathbf{P} = f^{-1}(\mathbf{R})$$

P

Identification using direct inversion

The inverse relationship between the input material parameters **P** and the response of the test sample **R** is sought, e.g. in the form of an artificial neural network (ANN).

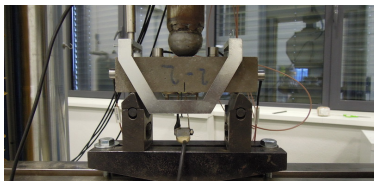

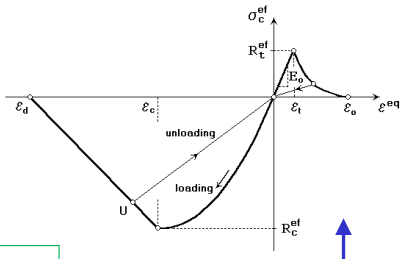

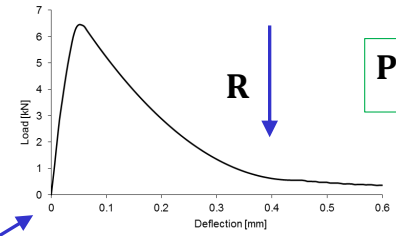

R

$$\mathbf{P} = f_{\mathrm{ANN}}^{-1}(\mathbf{R})$$

P

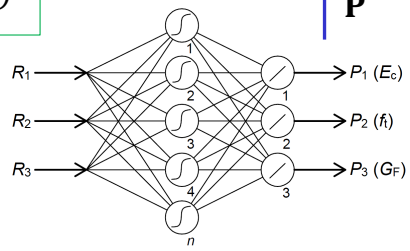

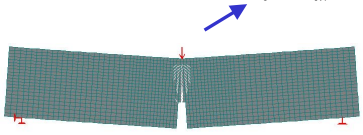

Identification of statistical characteristics of parameters

Two approaches:

- Load-deflection "one-by-one" identification approach

  Material parameters are identified individually for each specimen (individual *L–d* diagram is used as an input of ANN). Subsequently, statistical assessment of parameters of all specimens is carried out.

- Direct statistical parameters identification

  Random response of a structure is available in form of histograms and statistical moments (set of random *L–d* diagrams is used as an input of ANN). Statistical parameters are direct output of inverse analysis (ANN).

Direct statistical parameters identification

This approach offers the possibility of direct identification of random material parameters based on the random response.

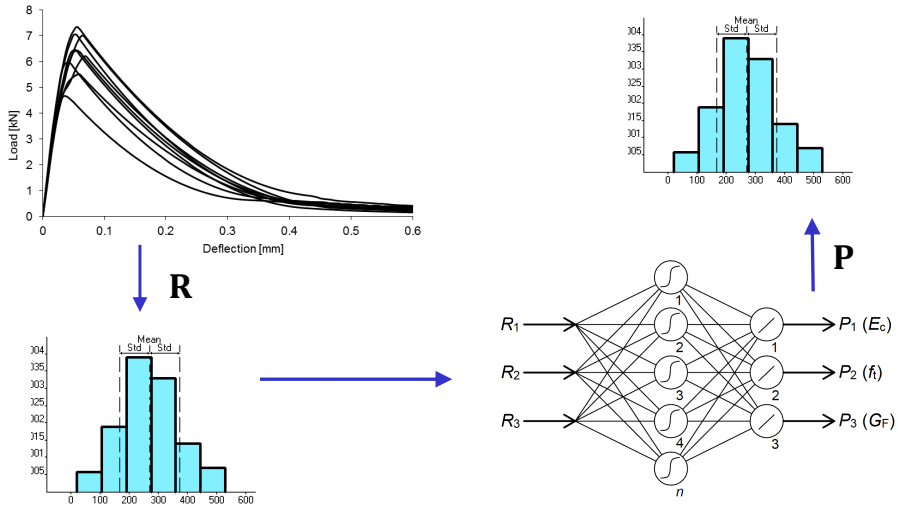

Methodology: artificial neural network

Neuron:

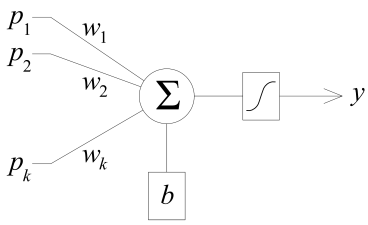

Feed-forward multilayer network:

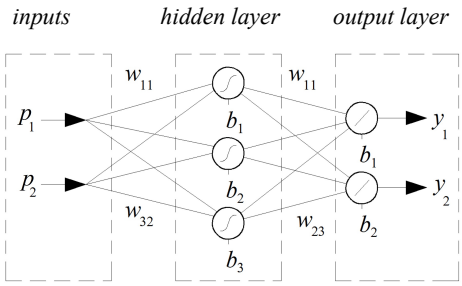

Output from a neuron:

$$y = f(x) = f\left(\sum_k (w_k p_k) + b\right)$$

k – number of input (1,...,K)
w_k – synaptic weight of connecting path from kth neuron of previous layer
p_k – input signal from kth neuron of previous layer
b – bias
f – transfer function of neuron

Methodology: artificial neural network

2 phases of ANN activity → Active phase (simulation)
2 phases of ANN activity → Adaptive phase (training)

ANN training – adjustment of synaptic weights and biases:

To train the feed-forward ANN, a training set is required, i.e. a set of ordered pairs of inputs and corresponding outputs of the network.

$$\begin{bmatrix} p_{11} & \cdots & p_{1i} & \cdots & p_{1N} \\ \vdots & & \ddots & & \vdots \\ p_{j1} & \cdots & p_{ji} & \cdots & p_{jN} \end{bmatrix} \leftrightarrow \begin{bmatrix} y_{11} & \cdots & y_{1i} & \cdots & y_{1N} \\ \vdots & & \ddots & & \vdots \\ y_{k1} & \cdots & y_{ki} & \cdots & y_{kN} \end{bmatrix}$$

Minimizing network error – it's an optimization task:

$$E = \frac{1}{2}\sum_{i=1}^{N}\sum_{i=1}^{K}\left(y_{ik}^{s} - y_{ik}^{p}\right)^2$$

N – set size (number of input–output vectors);
y_{ik}^{s} – the real output of kth output neuron for ith input;
y_{ik}^{p} – the required output of kth output neuron for ith input.

Methodology: Latin hypercube sampling simulation

Preparation of a training set by performing random virtual experiment via stratified statistical simulation.

- One p_i is chosen from each of N_{sim} intervals
- High accuracy at low N_{sim}

Alternatives:

- LHS median
- LHS random
- LHS mean

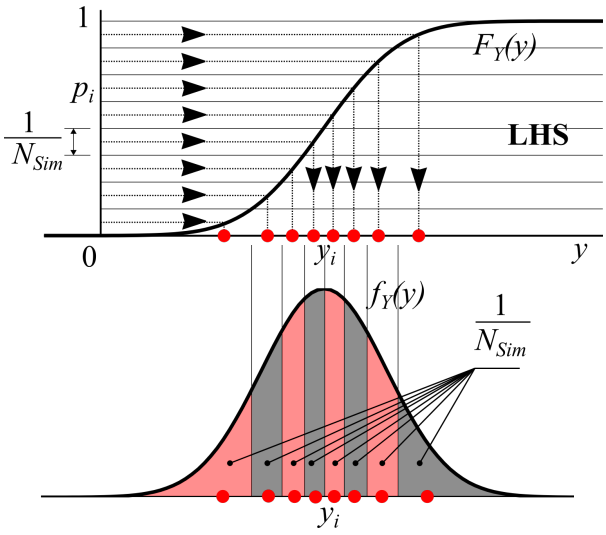

Software: FraMePID-3PB

- Developed for fully automatic and easy to use ANN based identification using 3PB experimental data (*L–d* diagrams).
- Designed for concretes of various strength and ages (large training set with relatively high variability of material parameters).
- Prepared for testing of specimens with various notch depth – study of fracture process zone development and corresponding changes of fracture energy.
- Implemented experimental data filtering.

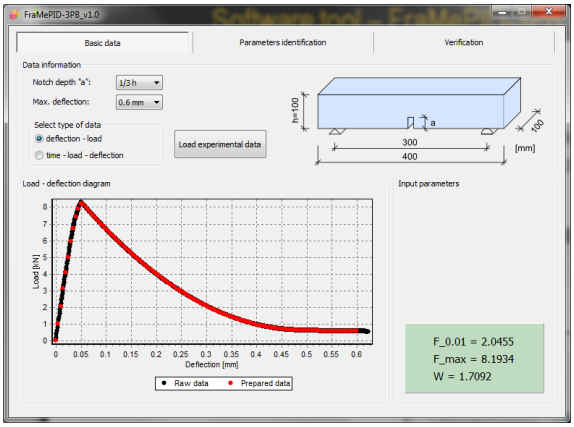

Software: FraMePID-3PB

- Robust ANN implemented and trained – significant time reduction compared to general identification tasks.
- FEM computational model implemented (ATENA software) – 3D Nonlinear Cementitious 2 material model.
- Subject of identification:
  - modulus of elasticity E_c
  - tensile strength f_t
  - fracture energy G_f
- Export of identified parameters to clipboard, text file, ATENA .ccm file.
- Direct transfer to ATENA for verification via ATENA interface (in preparation).

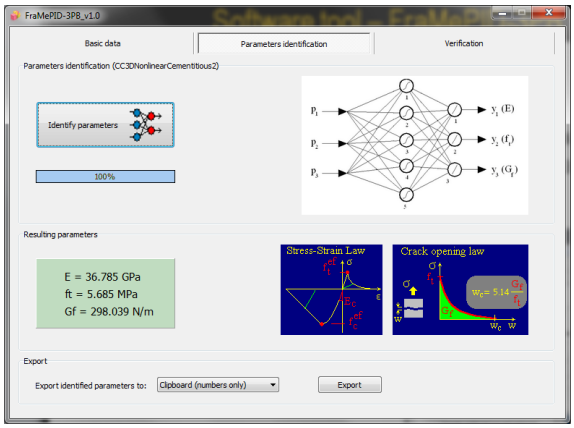

Fine-grained composites

Extensive research efforts in developing new types of binders, environmental-friendly building materials such as alkali-activated materials (AAMs) which are a promising alternative to traditional Portland cement.

Major disadvantage:

- Increased shrinkage → volume contraction, microcracking and the deterioration of tensile and bending properties.

Solution:

- The addition of different types of fiber to alkali-activated matrix. E.g., hemp fibers can be used as a sustainable alternative to the steel and synthetic fibers.

Coarse- vs. fine-grained composites

Coarse-grained composites
(concrete)

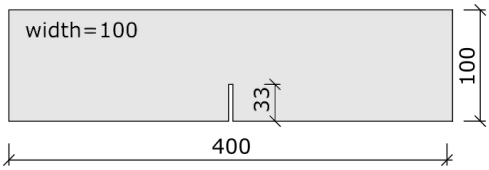

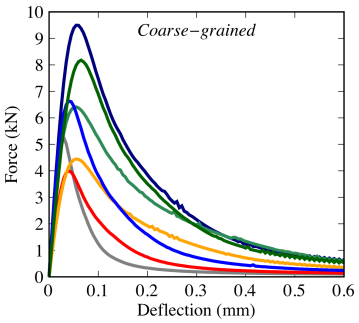

Fine-grained composites
(mortars)

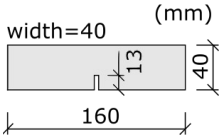

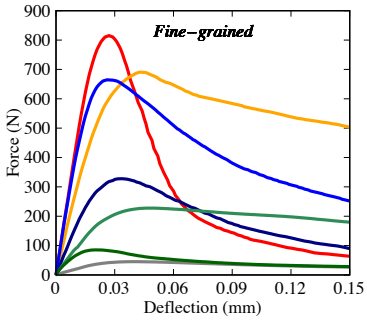

Hybrid NNE-based identification system

Properties of a Hybrid neural network ensemble-based system:

- E_c – f_t – G_f space divided into subspaces with a single ANN in each.
- Limited range of parameters for a single network.
- One or more ANNs activated based on an initial analysis of response data.
- Robust, accurate and easily expandable system.

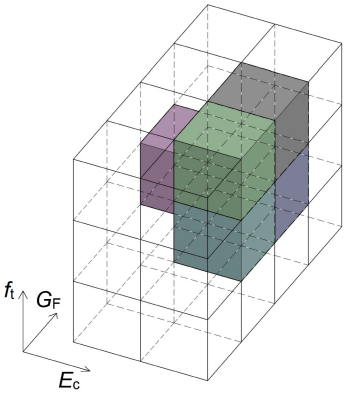

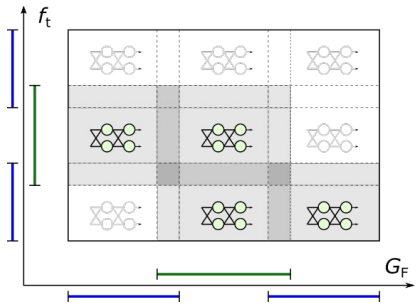

Hybrid NNE-based identification system

Weighted parameters from ANN ensemble in overlapping parts

$$p = \sum_{i=1}^{n} w_i p_i$$

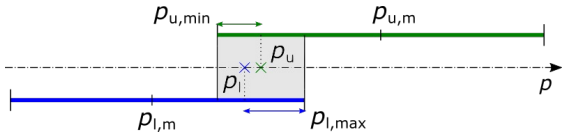

$n = 2^k$ overlapping subspaces for k parameters

Weighting coefficients: $w_i = \dfrac{\lambda_i}{\sum_{i=1}^{n} \lambda_i}$

Relative distance: $\lambda_i = \dfrac{p_{l,max} - p_i}{p_{l,max} - p_{l,m}}, \quad \lambda_i = \dfrac{p_i - p_{u,min}}{p_{u,m} - p_{u,min}}.$

Example of identification 2: Shear wall failure

Identification of material model parameters of constitutive law for concrete failure (shear wall)

Experiment

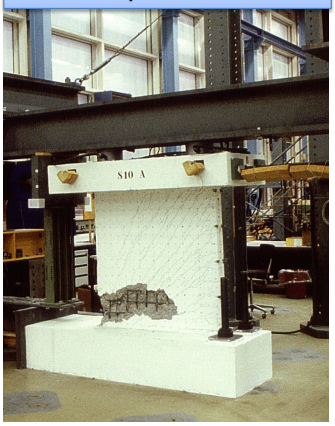

Experiment: Maier a Thürliman, 1985

Simulation

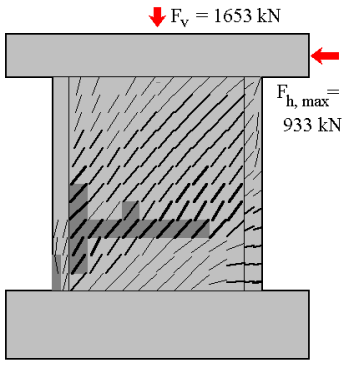

Example of identification 2: Shear wall failure

Experimental failure

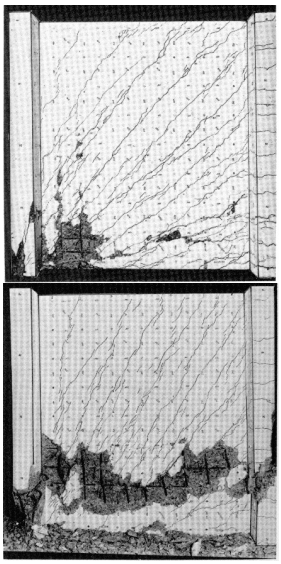

FEM model in ATENA software

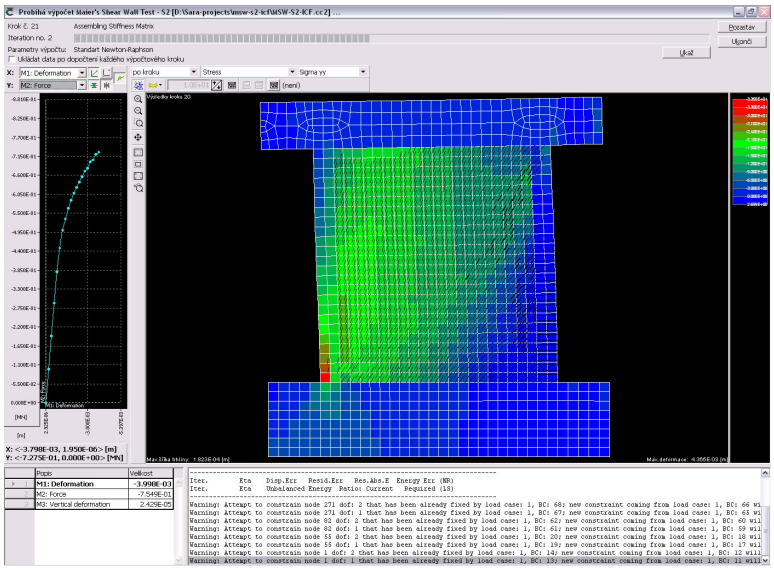

Example of identification 2: Shear wall failure

20 random realizations (LHS) – training set

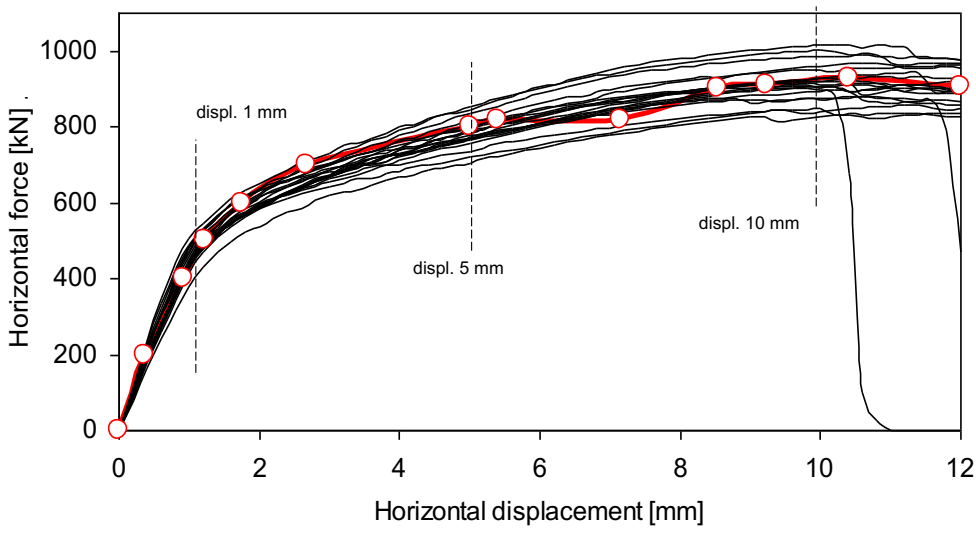

Example of identification 2: Shear wall failure

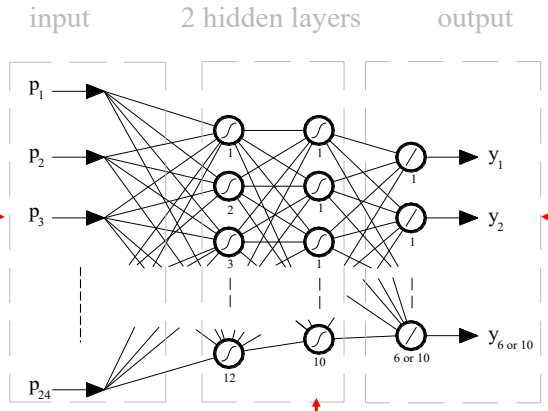

24 points on l-d diagram

6 or 10 neurons in output layer – linear transfer function

12 and 10 neurons in 2 hidden layers – nonlinear transfer function

Example of identification 2: Shear wall failure

Spearman	E	f_t	f_c	G_f	ε_c	w_d	x_1	fx_1	x_2	fx_2
F_1	0.753	0,123	0.453	0.045	-0.335	-0.108	-0.167	0.015	-0.087	-0.107
F_5	0.262	0.513	0.460	0.014	-0.263	-0.081	-0.516	0.311	-0.051	0.045
F_{10}	0.158	0.382	0.608	0.081	-0.080	-0.027	-0.344	0.490	0.005	0.104
F_{max}	0.129	0.341	0.636	0.054	-0.042	-0.053	-0.307	0.537	-0.009	0.171

Sensitivity of material model parameters:

- 6 parameters identified
- 10 parameters identified

Parameters obtained from simulation of neural network:

DLNNET	6 par.	10 par.
E [MPa]	29.9	33.0
f_t [MPa]	2.47	2.47
f_c [MPa]	34.51	35.3
G_f [MN/m]	75.0	77.85
ε_c [-]	2.51E-03	2.57E-03
w_d [m]	3.00E-03	3.10E-03
x_1	2.72E-03	2.74E-03
fx_1	566.9	570.7
x_2	1.50E-02	1.47E-02
fx_2	764	768.8

Example of identification 2: Shear wall failure

L-d diagrams obtained with identified parameters

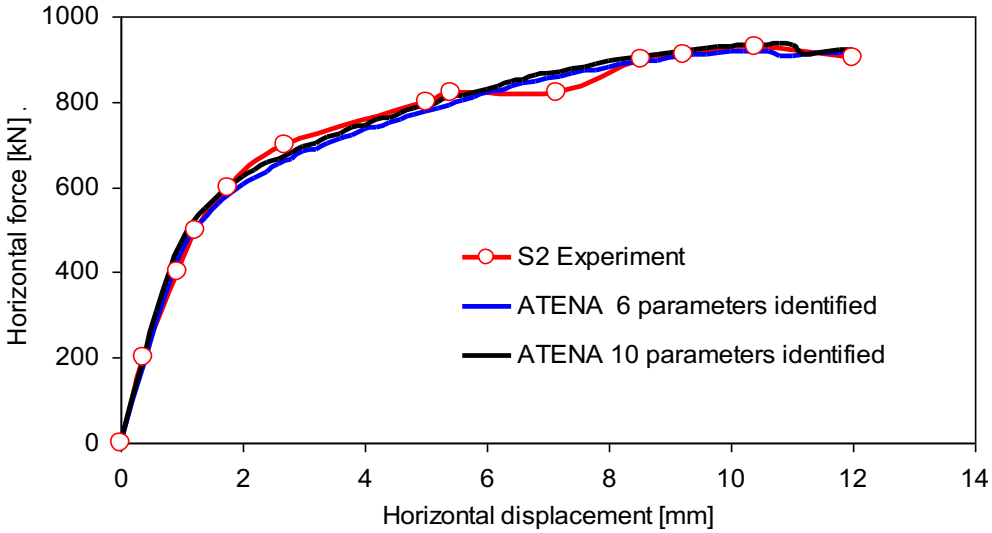

Summary and conclusions

- The determination of mechanical fracture parameters is important in many structural and materials engineering tasks.
- The combination of laboratory fracture testing, direct evaluation of the test data and inverse analysis provides comprehensive information, especially for nonlinear modelling of structures made of quasi-brittle materials.
- Inverse analysis can provide information on additional parameters of constitutive models that cannot be determined directly from test records or have no physical meaning.
- ANN-based identification method can be used to directly identify the statistical characteristic of mechanical fracture parameters.
- When testing strength and fracture parameters, it is necessary to keep in mind their dependence on the size of the tested specimens.
- To automate the identification of heterogeneous groups of materials such as fine-grained composites, fiber-reinforced concretes, etc., it is appropriate to use a hybrid NNE-based identification system.

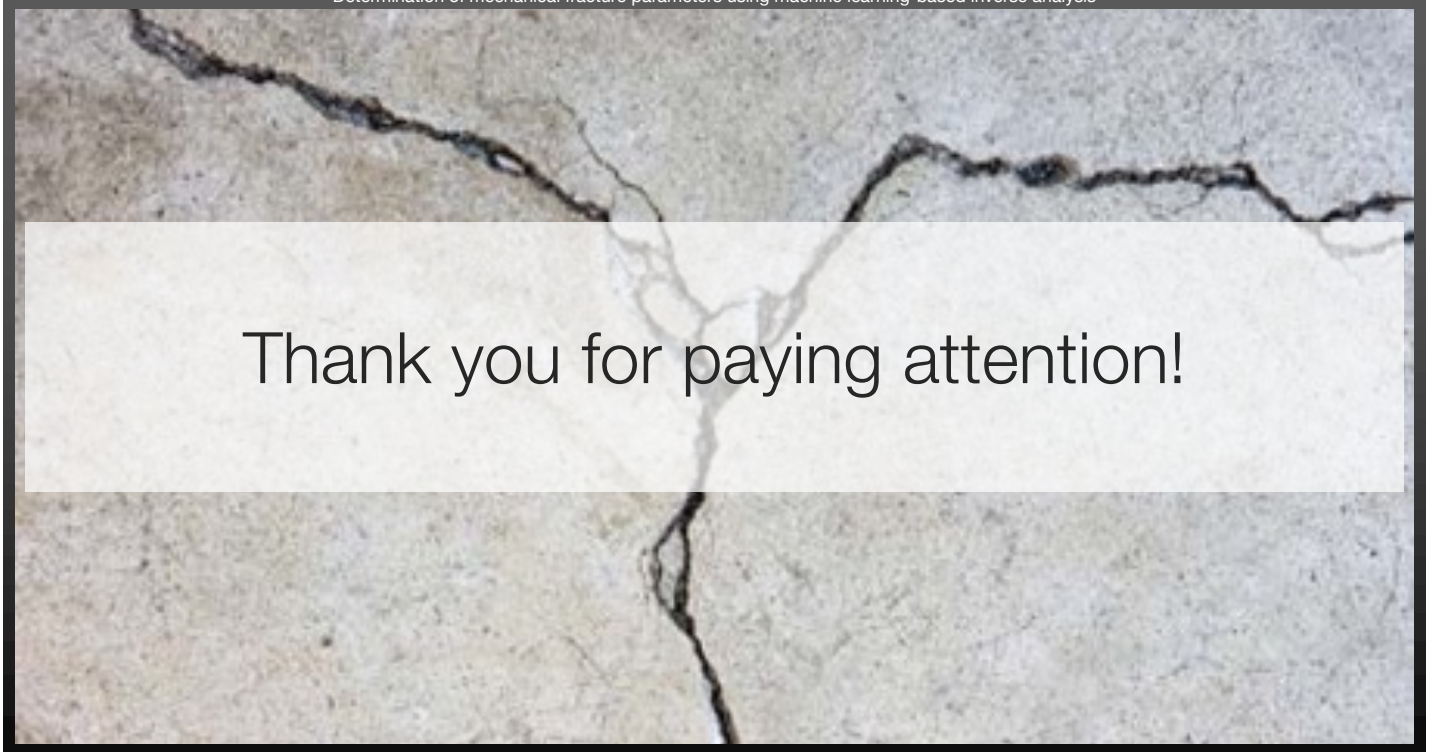

Thank you for paying attention!

Annex E

Mequanent M. Alamnie

Mechanistic asphalt pavement damage prediction and modelling for Sustainable roads

Permanent deformation and fatigue damage analysis of asphalt concrete

Mequanent Mulugeta Alamnie
Department of Process, Energy and Environmental Technology
University of Southeastern Norway

May 23, 2024
Brno University of Technology (BUT)
Brno, CZ

Outline

- Asphalt concrete damage
- Permanent deformation & Fatigue
- Damage interaction
- Way forward
- Conclusion

Asphalt concrete mixtures

- Asphalt concrete is an *engineered heterogenous* mixture (***Aggregates***, ***sand*** *(and fillers)*, ***binder*** *and/or modifiers*).
- Over 90% of paved roads are asphalt concrete
- Mixing temperature: *Hot, warm, cold*

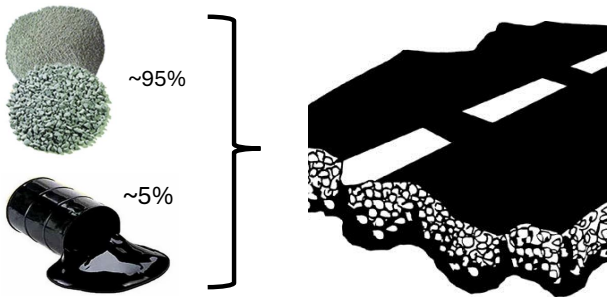

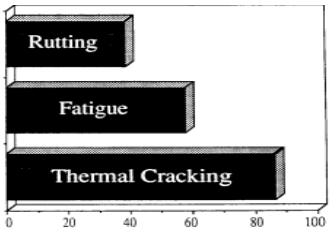

Effect of binder on asphalt mixture performance

- Roberts, F. L., Mohammad, L. N., & Wang, L. B. (2002). History of Hot Mix Asphalt Mixture Design in the United States. Journal of Materials in Civil Engineering, 14(4), 279-293.
- European Asphalt Pavement Association (EAPA), Asphalt in Figures, 2022

Asphalt concrete mixture

- An engineered material
- subjected to high loading cycle (in 10^6) i.e., *short service life*
- Main objectives of service life prediction;
  - Critical strain due to deformation, ε_{cr}
  - Number of cycles to fatigue failure, N_f

Traditional design criteria

- Tensile strain at bottom of AC layer, ε_t
- Vertical stress on top of subgrade

Tire pavement interaction ?

Top-down cracking?

shear surface deformation?

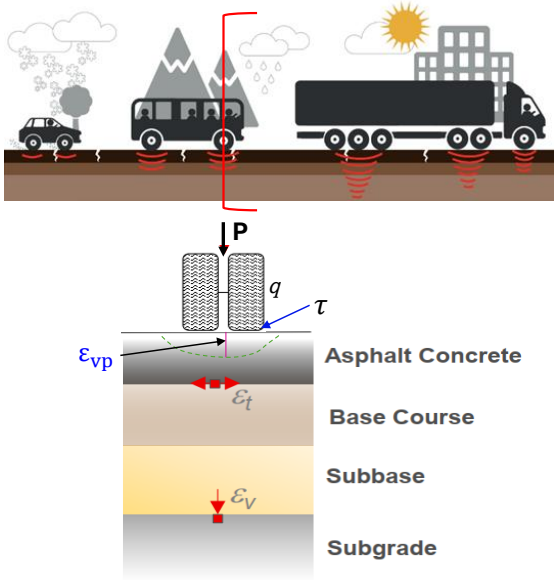

Stress distribution Under Tire

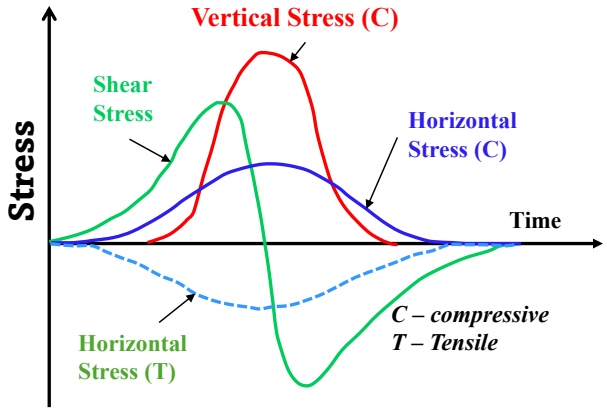

Observations →
- ✓ Sharp shear stresses cause surface cracks
- ✓ Rutting accompanied cracking

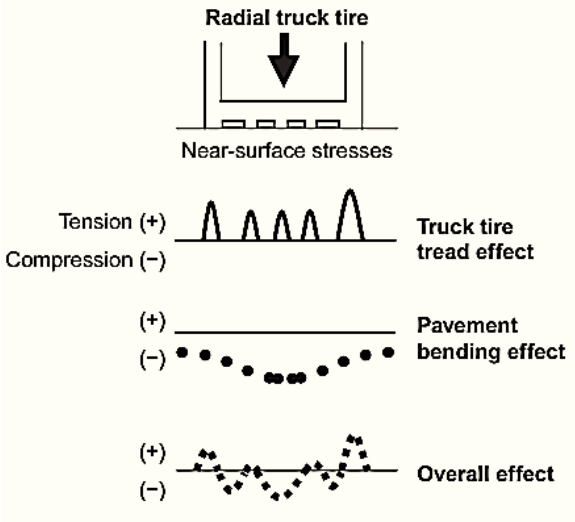

L. Ann Myers, et al., Measurement of Contact Stresses for Different Truck Tire Types To Evaluate Their Influence on Near-Surface Cracking and Rutting, Journal of the Transportation Research Board 1999 Vol. 1655 Issue 1

Asphalt Mixture Performance

Factors affecting performance

- constituent materials,
- load,
- environmental conditions
- construction

Required performances

- *Ability to* distribute stresses
- *Resistance to:*
  - permanent deformation
  - cracking (*fatigue, thermal, etc.*)
  - freeze-thaw and moisture damage.

Di Benedetto, et al., 2013. Mechanical Testing of Bituminous Mixtures, in: Progress of Recycling in the Built Environment. Progress of Recycling in the Built Environment, 143–256.

Asphalt Mixture Performance

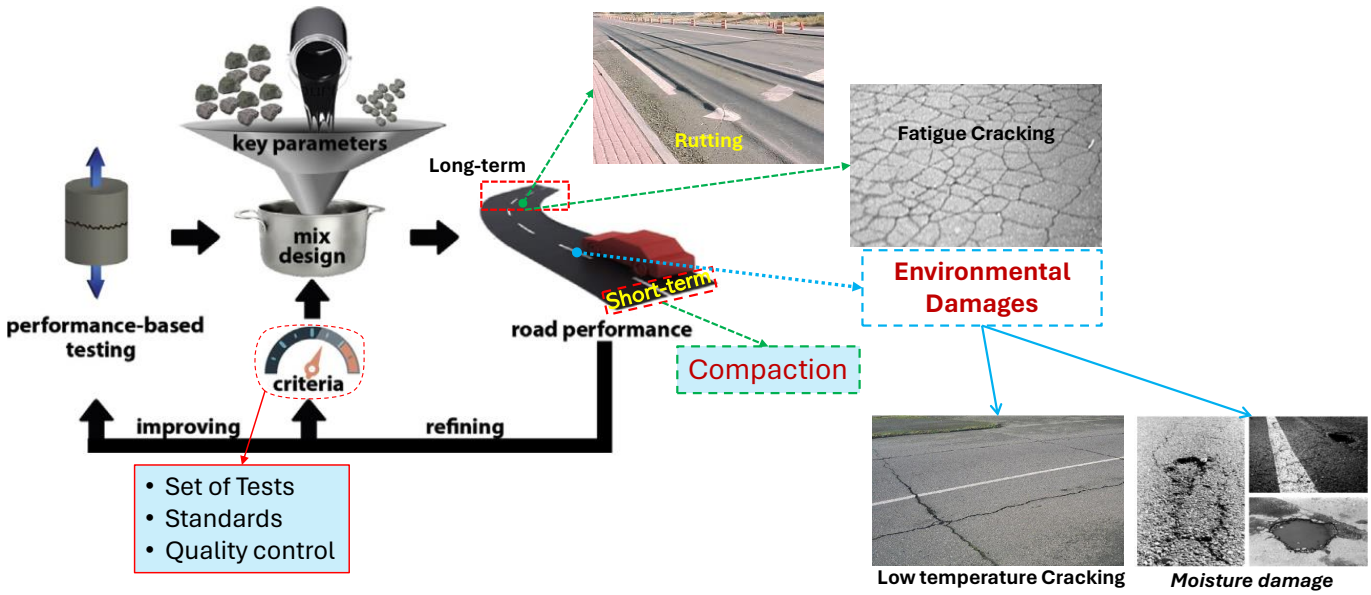

Notani, M.A. et al.,. Performance Evaluation of Using Waste Toner in Bituminous Material by Focusing on Aging and Moisture Susceptibility. J. Mater. Civ. Eng. 2021, 33, 4020405

Common Pavement damages

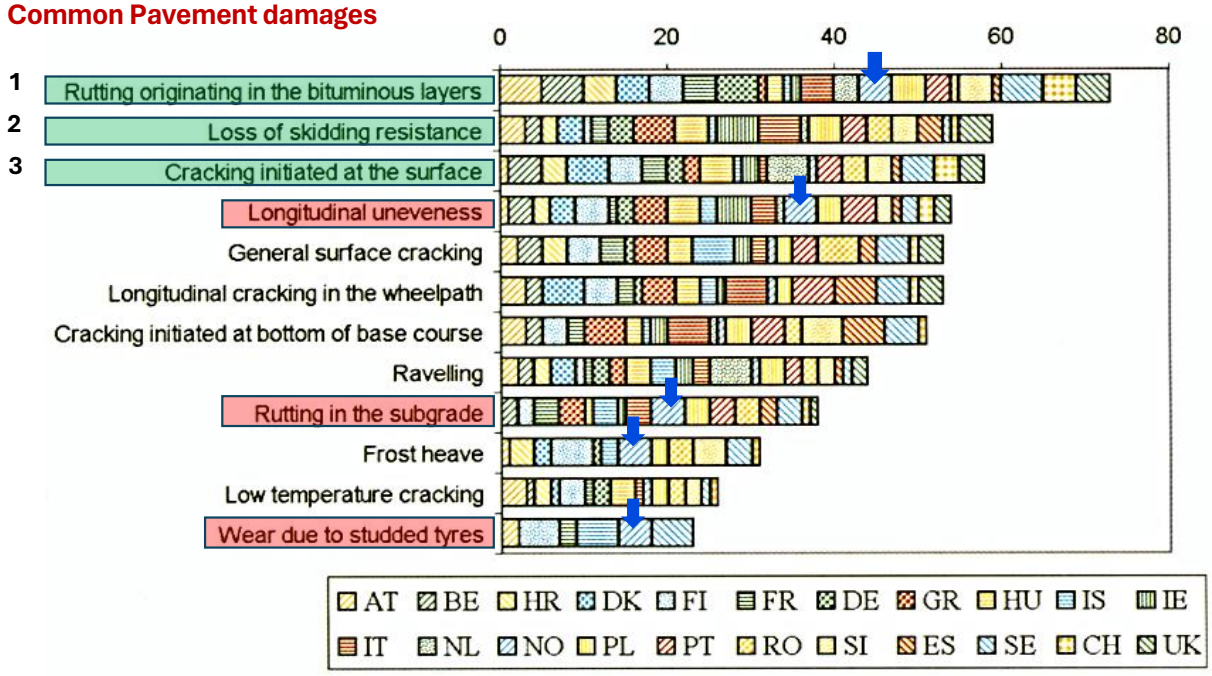

European Commission: *COST 333: Development of New Bituminous Pavement Design Method: Final Report of the Action*, volume 18906. European Communities, 1999

Domains of Asphalt mixture behavior

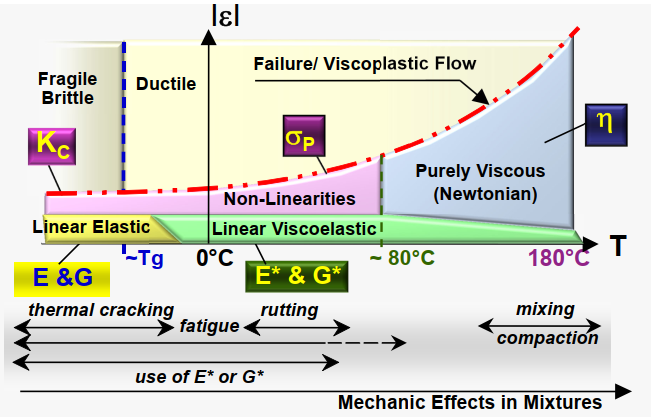

- **Small vs Large strain**
- **Low vs High cycle fatigue**
- **Influence of temperature**

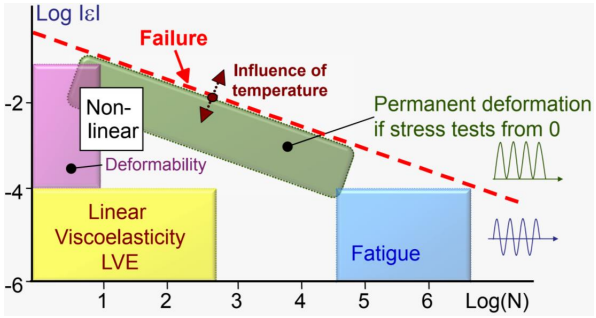

Di Benedetto, H., Yan, X.L.: Comportement me´canique des Enrobe´s bitumineux et mode´lisation de la contrainte maximale. Mater. Struct. 27, 539–547 (1994)
Olard, F., Di Benedetto, H., Dony, A., Vaniscote, J.-C., 2005. Properties of bituminous mixtures at low temperatures and relations with binder characteristics. Materials and Structures 38, 121–126.

Fundamental Response

Viscoelastic damage

- *Viscoelastic Continuum damage model At Low Temperature*

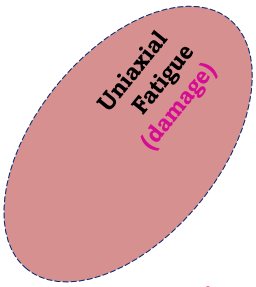

Interaction

Fatigue – rutting interaction

- Intermediate temperature
- Visco-damage, Visco-fracture

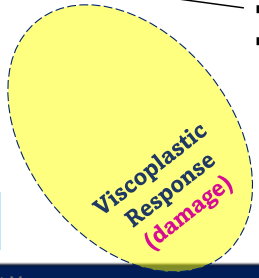

Viscoelastic-Viscoplastic damage

- Viscoplasticy- strain hardening
- Creep-recovery test at *intermediate-high temperature*

$$R_{\varepsilon,\sigma} = f(T_o, \varepsilon_o, \sigma_{ij}, P_o, P_{atm}, \dot{\varepsilon})$$

Permanent deformation

The permanent deformation of asphalt pavement are caused by

- asphalt mixture instability (shear instability rutting) – Mode 1
- structural deficiency, – Mode 2
- *Wear due to studded tyre**

Rut Depth: $\mathrm{RD} = \sum_{i=1}^{i} h_i \varepsilon_{vp,i}$

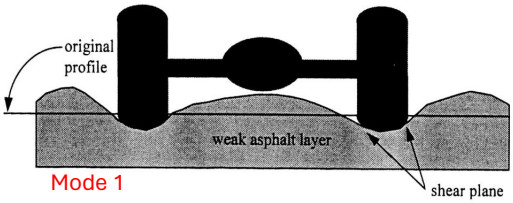

Mode 1

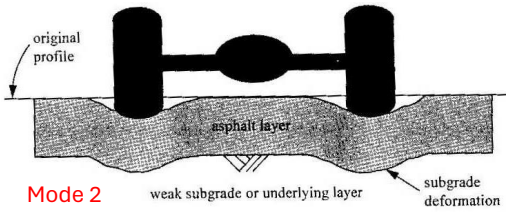

Mode 2

McGennis, R.B., Anderseon, R.M., Kennedy, T.W., and Solaimanian, M. (1994), Introduction to Superpave asphalt mixture design, Federal Highway Administration, Office of Technology Applications, W, DC.

Permanent deformation

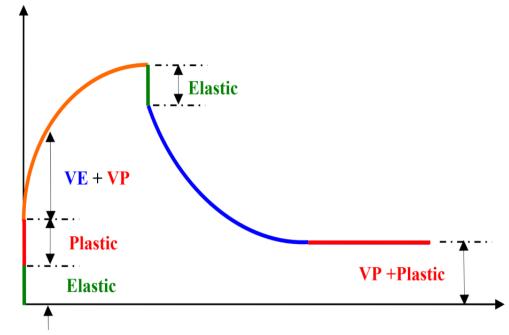

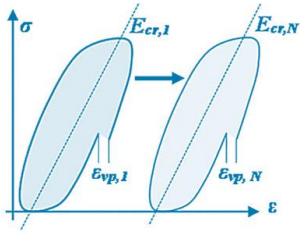

$\varepsilon_{vp} = AN^{B} + C(e^{DN} - 1)$

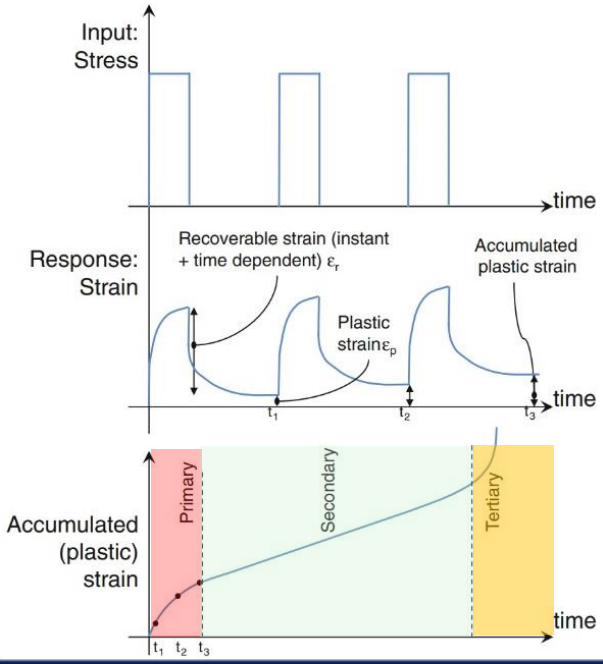

Fatigue Damage

- Fatigue is manifested as stiffness deterioration and cracking
- Strain controlled or stress controlled, T-T or T-C

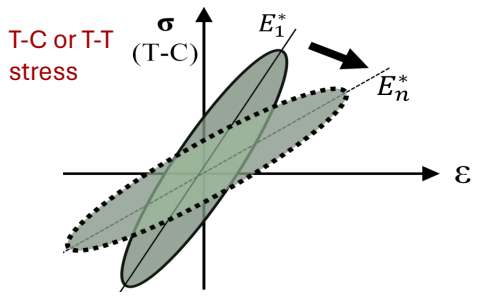

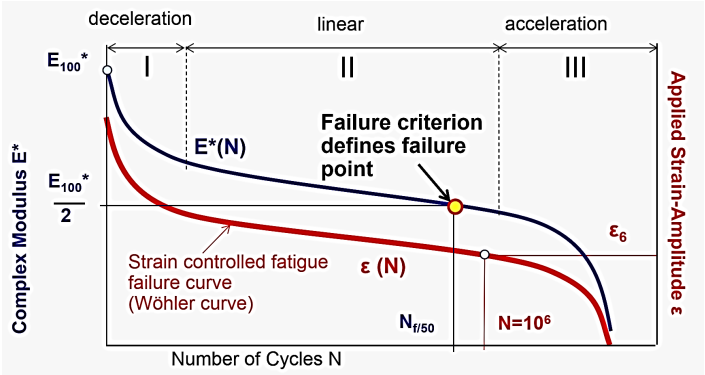

Viscoelasticity

- **Uniaxial stress-strain ($\sigma - \varepsilon$)** relationship for linear viscoelastic (LVE) material given by Boltzmann integral,

$$\sigma(t) = \int_0^t E(t-\tau)\frac{d\varepsilon}{d\tau}d\tau,$$ t – physical time; τ – integral variable;

- $E(t)$ – relaxation modulus using generalized Maxwell model;

$$E(t) = E_\infty + \sum_{n=1}^{N} E_n\left[exp\left(-\frac{t}{\lambda_n}\right)\right]$$

E_∞ - *Long-term (equilibrium) modulus*

- Time-Temperature-pressure Superposition (TTPS):

→ $E*(T, P, f) = E*(T_0, P_0, f_R)$

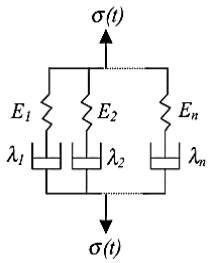

Maxwell model

Damage Modeling

1. The dissipated energy (DE)

$$DE = \int_0^{\tau} \sigma(t) \frac{\partial \varepsilon(\tau)}{\partial \tau} d\tau$$

- Sinusoidal fatigue (strain-controlled),

$$DE_F = \pi E_i^* \varepsilon_i^2 \sin(\varphi_i)$$

- Creep-recovery deformation

$$DE_{PD} = \sigma_o * \varepsilon_{cr}$$

  - DE failure criteria: $\boldsymbol{DER = n \frac{DE_1}{DE_n}}$

2. Continuum damage mechanics

- Damage density, $\omega \in [0,1)$; $\omega = 1 - \frac{\sigma^A}{\sigma^T}$
- Viscoelastic Continuum Damage
  - (elastic-viscoelastic corresp. principle and work potential theory)

$$\frac{d(S)}{d(t)} = \left(-\frac{dW^R}{dS}\right)^{\alpha} \qquad W^R = \frac{1}{2}\sigma\varepsilon_i^R = \frac{1}{2}C(S)(\varepsilon_i^R)^2$$

$$C = \frac{\sigma(t)}{\varepsilon_i^R} \qquad \varepsilon_i^R = \frac{1}{E_R}\int_0^t E(t-\tau)\frac{d\varepsilon}{d\tau}d\tau$$

$$\Delta S = \left[-\frac{DMR}{2}\left(\varepsilon_i^R\right)^2 (C_i - C_{i+1})\right]^{\alpha/(1+\alpha)} (\Delta t_R)^{1/(1+\alpha)}$$

Asphalt concrete Testing Options

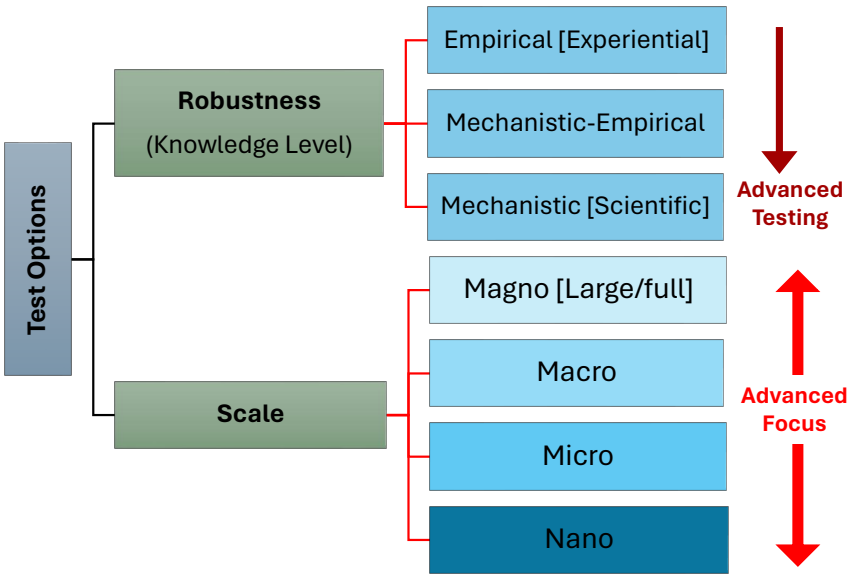

Multiscale Investigation;

- **Nano** (nm. . .mm),
- **Micro** (mm. . .mm),
- **Meso** (mm. . .dm),
- **Magno** (dm. . .dam)
- **Mega** (dam. . .km)

Multiscale Testing of Asphalt Mixtures

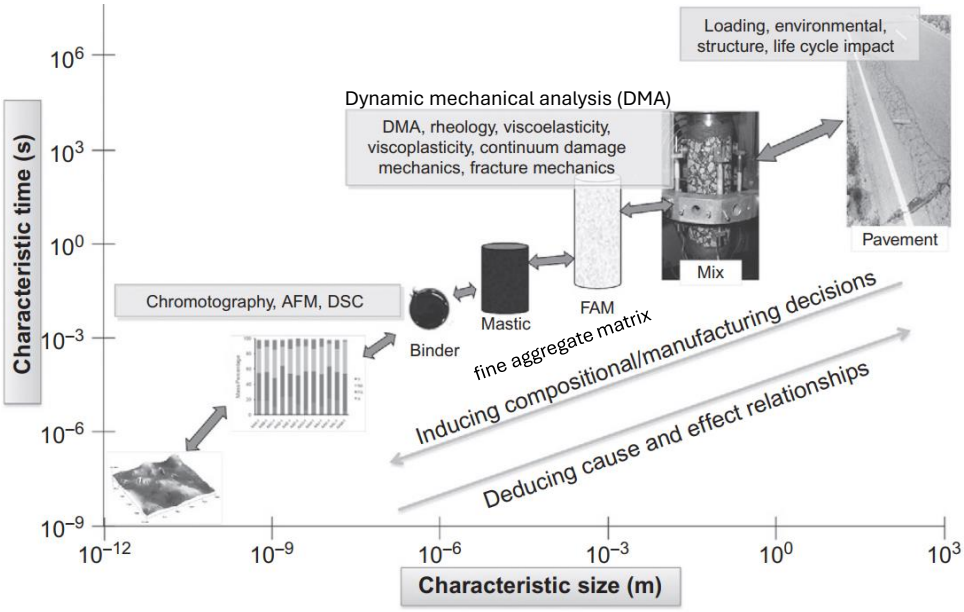

Scale dependencies involved in a multiscale interpretation of asphalt concrete

***AFM**-Atomic Force Microscopy,*

***SPM**-scanning probe microscopy*

***CFM**-chemical force microscopy,*

***DSC**-differential scanning calorimetry,*

B.S. Underwood, Multiscale modeling approach for asphalt concrete and its implications on oxidative aging, Ed.(s): Shin-Che Huang, Hervé Di Benedetto, Advances in Asphalt Materials, Woodhead Publishing, 2015, 273-302.

Full scale Asphalt Performance tests

National Academies of Sciences, Engineering, and Medicine. 2012. Significant Findings from Full-Scale Accelerated Pavement Testing. Washington, DC: The National Academies Press.

Some Laboratory Asphalt concrete mixture tests

Performance	Asphalt Mixture Test	Verdict	Indicator	Remark
1. Stiffness	**Dynamic Modulus**	• **Homogenous**	**Stiffness, Fatigue, rutting**	**Fundamental**
	Resilient Modulus	• Non-homogenous	Stiffness	
2. Permanent deformation	Repeated creep recovery	• Realistic traffic, Complicated, costly	Rutting, relaxation	
	Superpave shear test	• **Complex, costly**	**Shear Modulus, Shear Rutting**	**Accurate shear rutting**
	Wheel tracking	• Simulative, costly	Rutting and stripping	
3. Fatigue Cracking	Uniaxial T-C fatigue	• Homogenous, complex	Fatigue	
	IDT fatigue	• Non-homogenous, Effective	Fatigue, fracture	
4. Low temperature	Thermal Stress Restrained Specimen Test (TSRST)	• Homogenous, complex	Thermal cracking	

Dynamic Modulus tests

- Sinusoidal stress and strain waves in complex domain,
- Dynamic Modulus, E^* is a complex number (with real and imaginary components)

$$E^* = |E^*|(cos\varphi + isin\varphi) = |E^*|e^{i\varphi}$$

  - Storage/real Component → $E' = |E^*|(cos\varphi)$
  - Loss/imaginary Modulus → $E'' = |E^*|sin(\varphi)$

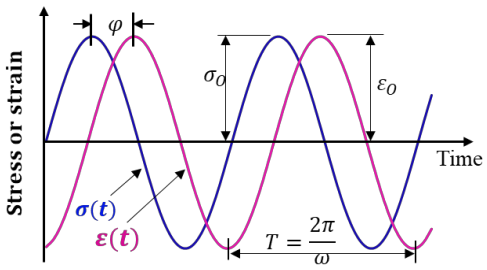

$\varepsilon(t) = \varepsilon_0 \sin(\omega t) = \varepsilon_o e^{i\omega t}$

$\sigma(t) = \sigma_o sin(\omega t + \varphi) = \sigma_o e^{i(\omega t+\varphi)}$

φ - the phase angle
ω - Pulsation frequency

Dynamic Modulus master curves

- Effect of confining stress on dynamic modulus

$$\log E^* = \delta + \frac{\alpha - \delta}{1 + \exp(\beta - \gamma \log f_R)} \qquad \log(a_T) = -\frac{C_1(T - T_r)}{(T - T_r) + C_2}$$

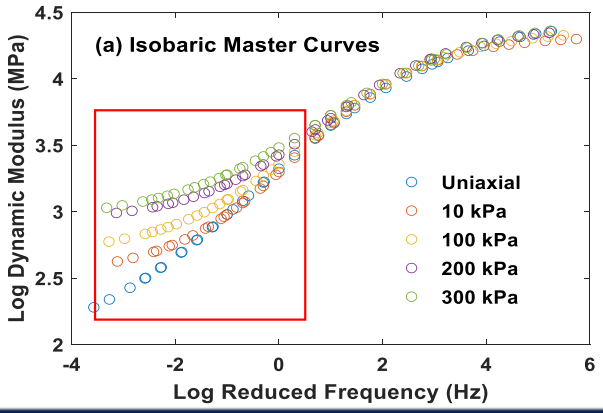

- Relaxation modulus

$$E(t) = E_\infty + \sum_{n=1}^{N} E_n \left[\exp\left(-\frac{t}{\lambda_n}\right)\right]$$

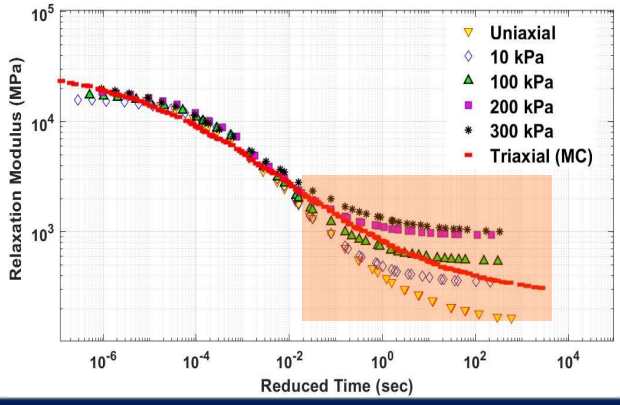

Linear Viscoelastic Analysis

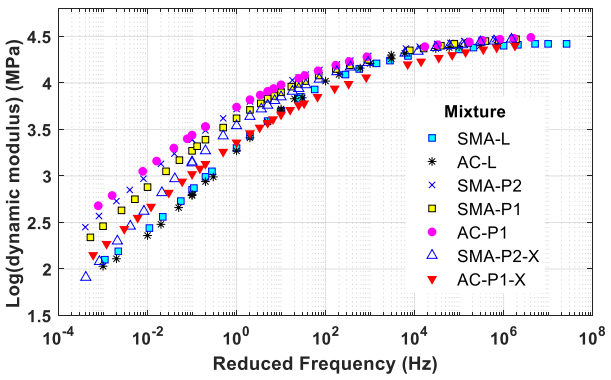

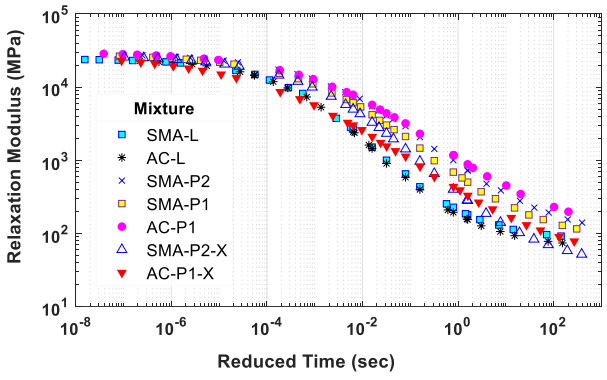

Mixture	AC-L	SMA-L	AC-P1	SMA-P1	SMA-P2	AC-P1-X	SMA-P2-X
E_∞	61.92	87.88	172.48	101.74	127.12	72.20	38.78
S_o	0.70	0.69	0.52	0.59	0.53	0.50	0.65
α	2.43	2.45	2.91	2.69	2.90	3.02	2.54

$$S_o = \max\left\{\frac{\Delta \log(E(t))}{\Delta \log(t)}\right\}$$

$$\alpha = \frac{1}{S_o} + 1$$

Repeated Creep-recovery Test

- EN 12697-25
- Temperature: 30, 40, 50 °C
- Loading/Rest time : 0.1/0.9, 0.4/0.6 …
- Axial stress: 200 – 2000 kPa
- Confining stress: 0 – 300 kPa

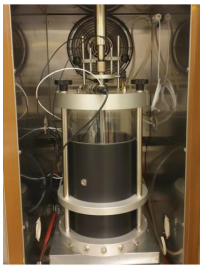

Haversine and block

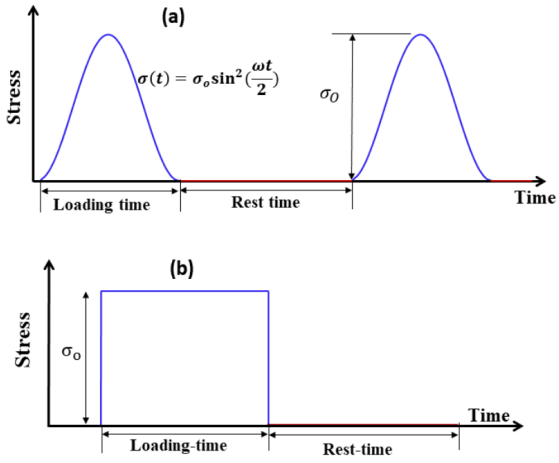

Repeated Creep-recovery test

- Effect of *triaxial stress* on PD evolution

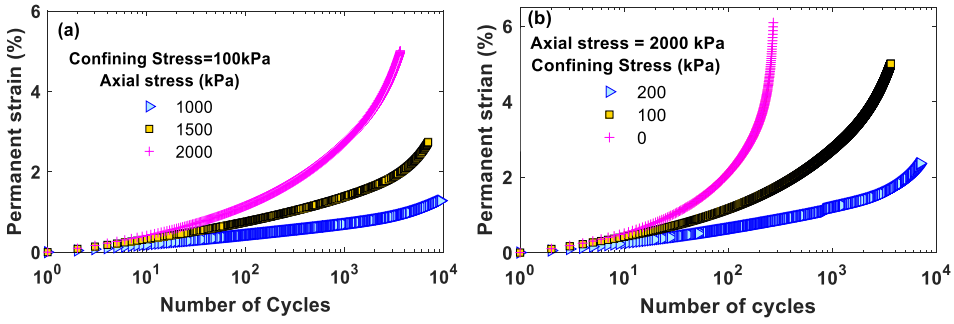

Effect of stress on permanent deformation and hardening rate – (T= 50 °C)

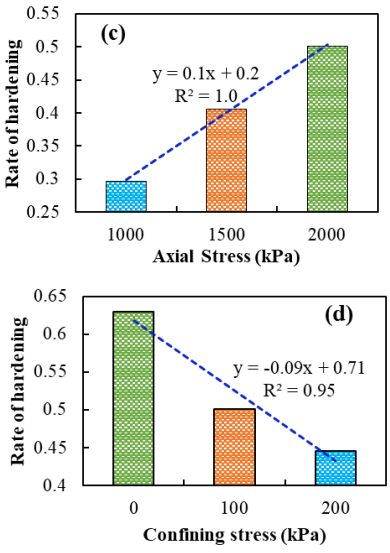

Repeated Creep-recovery test

- Three-stage creep evolution is based on strain rate
- **Defining a new criterion using DER** (Post FN, shear deformation)

$$DER_{PD} = N\left(\frac{A + C(e^{D} - 1)}{AN^{B} + CD(e^{DN} - 1)}\right) = N\left(\frac{K}{\varepsilon_{vp}}\right)$$

- Deformability rates:

$\varepsilon_{FN}/_{FN}$, $\varepsilon_{PV}/_{N_{PV}}$ and $\varepsilon_{SEL}/_{SEL}$

$$\varepsilon_{vp} = AN^{B} + C(e^{DN} - 1)$$

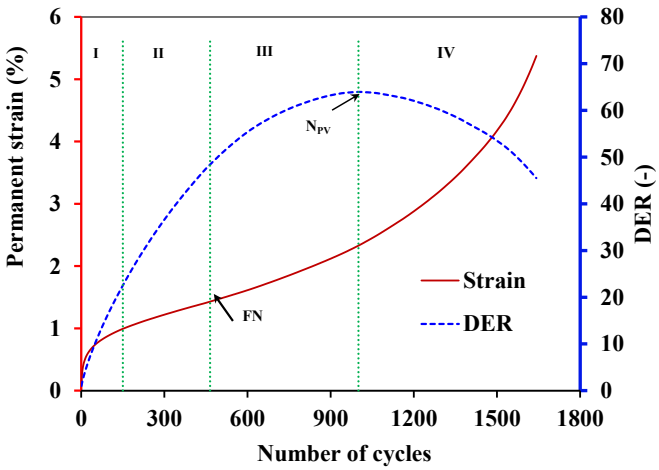

Uniaxial Fatigue Test

Test conditions

- **AASHTO TP107**
  - **Strain controlled:** 300, 400 με
- **Temperature:** 10, 15, 21 and 30°C
- **Frequency:** 10 Hz
- **Pulse:** Sinusoidal (in tension-Tension, Tension-compression)
- **Failure Criterion:** 50% dynamic modulus reduction

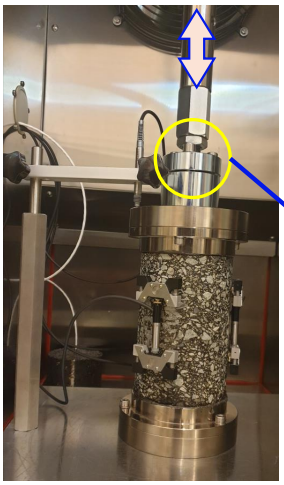

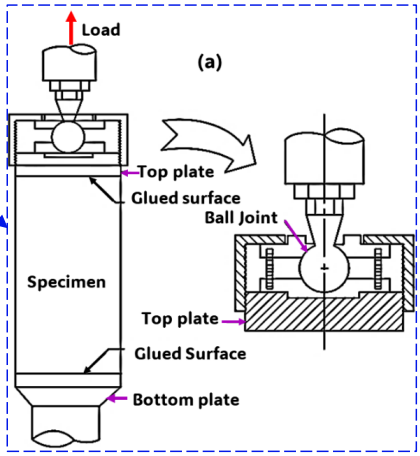

Fatigue damage

VECD Model

- Damage characteristics curve, ***S***

$$\Delta S = \left[-\frac{DMR}{2}\left(\varepsilon_{a,i}^{R}\right)^{2}\left(C_i^{*} - C_{i+1}^{*}\right)\right]^{\frac{\alpha}{1+\alpha}} \left(\Delta t_R\right)^{\frac{1}{1+\alpha}}$$

$$DMR = \frac{|E^*|_{fingerprint}}{|E^*|_{LVE}}, \Delta t_R = \frac{1}{a_T}\left[\frac{\Delta N}{10}\right]$$

$$C = 1 - as^b$$

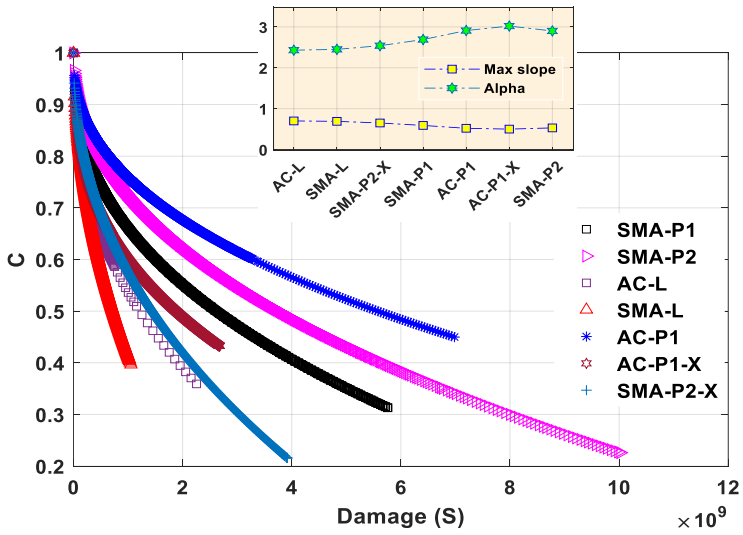

Fatigue damage (T= 10 °C and Target strain = 300με)

Proposed Test Procedure for fatigue and rutting performance

Assumption

- Sequential damage evolution
- post compaction or strain hardening can cause of fatigue cracking.

Damage interaction

Permanent deformation-Fatigue (PD-F) Sequence

- early service life of asphalt concrete pavements, which is dominated by volumetric densification.

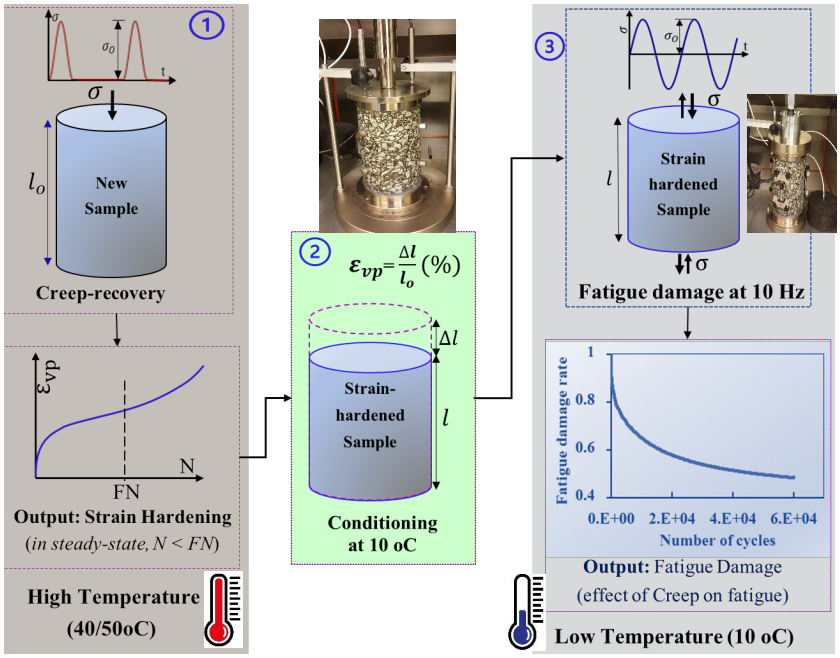

Damage Interaction

Fatigue – Permanent deformation (F-PD) sequence

- to simulate the effect of fatigue cracking on permanent deformation
- Or the development of PD due to prior fatigue cracking
- Perpetual/thick pavements

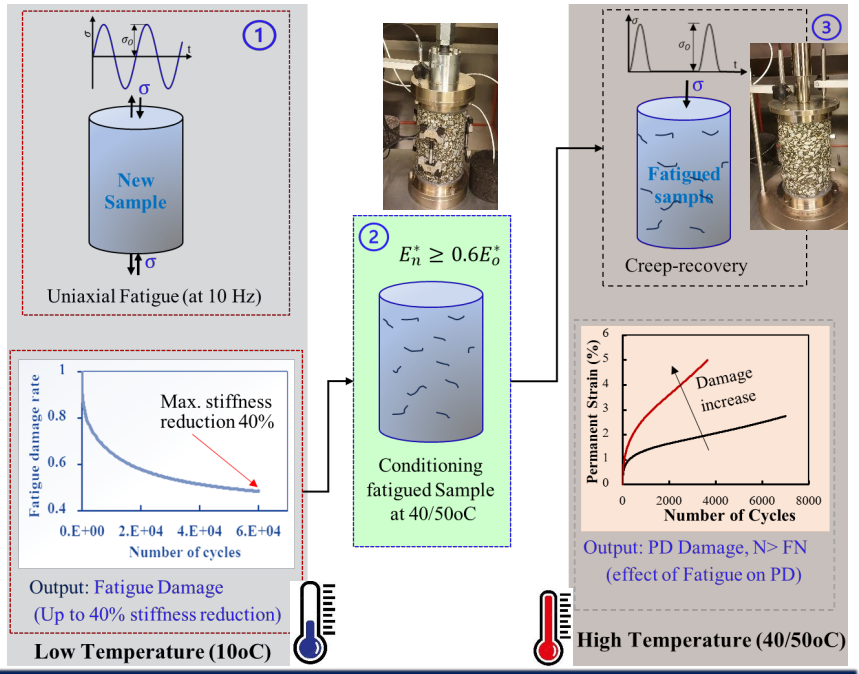

The PDF Sequence

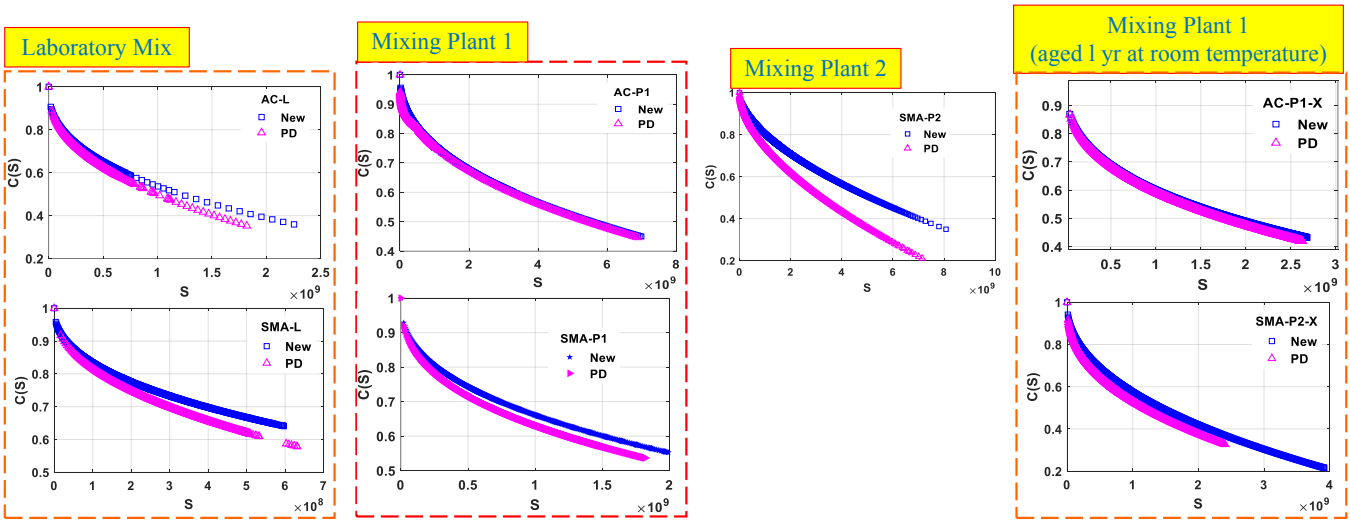

PDF sequence – fatigue (T=10 ºC, strain 300με) on new and per-deformed (PD) samples

The PDF Sequence

Effect of pre-deformation on fatigue damage response

$$C = 1 - as^b$$

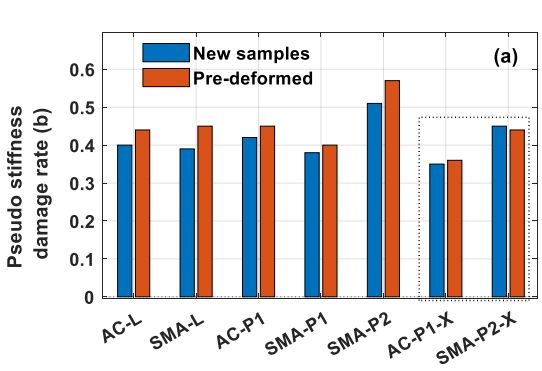

(a) parameter b

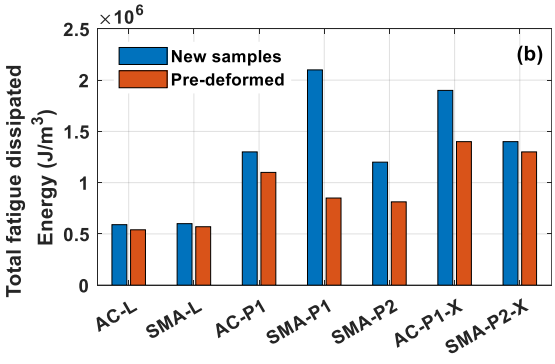

(b) total fatigue dissipated energy until failure (50% pseudo stiffness)

The F-PD Sequence

- The effect of Fatigue on Permanent Deformation
  - *the strain rate in the steady-state stage, FN and the DE.*

$$\varepsilon_{vp} = AN^B + C\left(e^{DN} - 1\right) \qquad DER_F = n \times \frac{\pi E^*_1 \varepsilon_1^2 \sin\varphi_1}{\pi E^*_i \varepsilon_i^2 \sin\varphi_i} \approx n\left(\frac{E_1}{E_i}\right)\left(\frac{\varphi_1}{\varphi_i}\right) \qquad DER_{PD} = N\left(\frac{A + C(e^D - 1)}{AN^B + CD(e^{DN} - 1)}\right) = N\left(\frac{K}{\varepsilon_{vp}}\right)$$

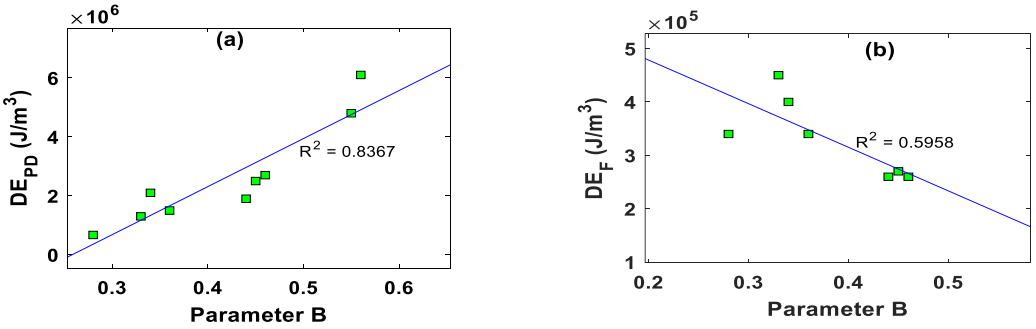

F-PD sequence (a) DE_{PD} of pre-fatigued samples (b) initial DE_F of samples used for PD test

The F-PD Sequence

- *DE_PD* and *DE_F* energy quantities are not consistent with FN.
- DE depends on mixture type, specimen, and temperature.

$$\frac{DE_T}{FN} = DE\ rate$$

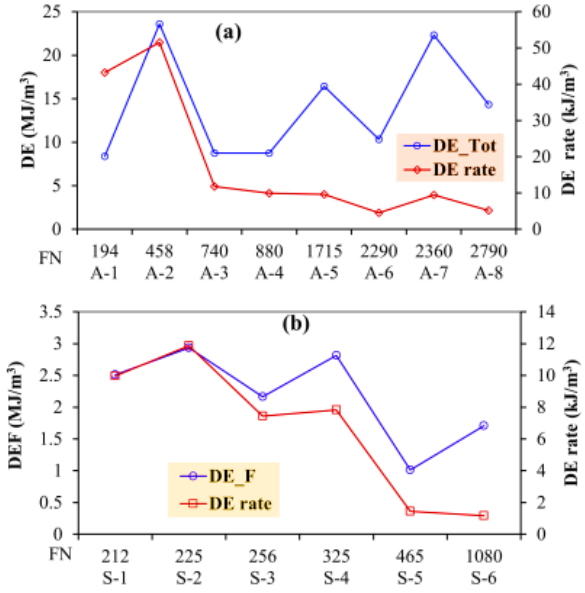

Correlation of DE_T, $DE\ rate$ vs FN in FPD sequence

Towards Mechanistic approach

- Based on fundamental material theories
  - *Rely on material constitutive models*
- Unlimited scope for model refinement
  - *New materials, parameters etc.*
- Realistic Pavement Response Model
  - *Evaluate change in loading to pavement performance*
- More integrated one-step model

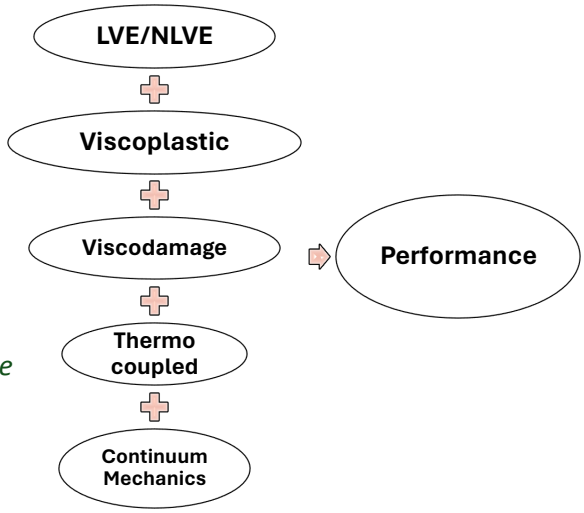

Way forward

Mechanistic method of asphalt design require advanced performance testing.

- *Performance-Engineered* Mix design *(PEMD)* approach

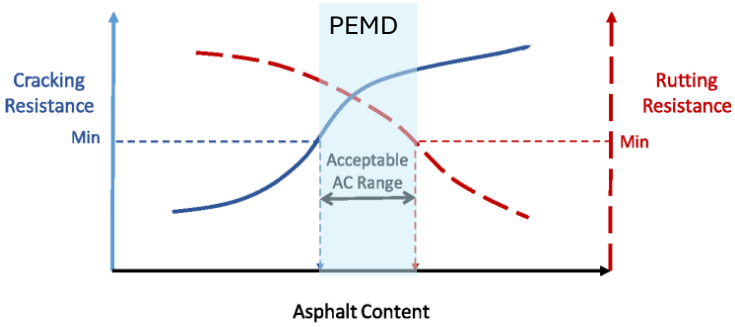

Coupled testing

- *Performance tests that can evaluate different damages*

Unified damage modeling

- *Temperature coupled models*

Conclusion

- The LVE properties of AC is stress-dependent shift models – *the long-term relaxation modulus and viscoelastic damage parameter*.
- *In a sequential test, the PD-F sequence was found to be more realistic damage sequence, where Strain hardening is the primary cause of fatigue damage.*
- In the F-PD sequence, effect of pre-fatigue cracking (up to 40 % stiffness) on PD was found to be marginal, which can be related to the healing and relaxation.
- The shear endurance limit (fourth creep stage) marks the macro-crack formation – important to estimate pavement life.
- Coupling different asphalt concrete damages opens up the possibility of unified asphalt damage modeling using the benefits of a mechanistic approach.

Outlook

- Existing test protocols for AC are insufficient to evaluate different damage modes simultaneously.
- The validity of time-temperature-pressure superposition principle can be extended to assess the interaction of permanent deformation and fatigue damages at intermediate temperatures.
- Towards a unified damage model which entails innovative testing methods and fundamental theory.

Thank you for your attention!

Annex F

Lukáš Novák

Uncertainty quantification in structural mechanics: point estimates and surrogate models

UQ in structural mechanics: point estimates and surrogate models

Lukáš Novák

Novak.L@fce.vutbr.cz

Brno University of Technology
Czech Republic

Reliability and sustainability of structures

Outline

Uncertainty Quantification

Acknowledgments

GAČR
CZECH SCIENCE FOUNDATION

DEFENSE THREAT REDUCTION AGENCY
UNITED STATES OF AMERICA

MINISTRY OF EDUCATION, YOUTH AND SPORTS

MSEE
MATERIALS SCIENCE IN EXTREME ENVIRONMENTS
UNIVERSITY RESEARCH ALLIANCE

Uncertainty quantification

- quantity of interest of a physical system is represented by a costly mathematical model $Y = \mathcal{M}(\mathbf{X})$
- behavior of **real** physical system is **non-linear**
- input variables should be considered as **random** variables $\mathbf{X}$
- uncertainty quantification of $Y = \mathcal{M}(\mathbf{X})$: statistical moments, PDF, sensitivity analysis, estimation of quantiles etc.

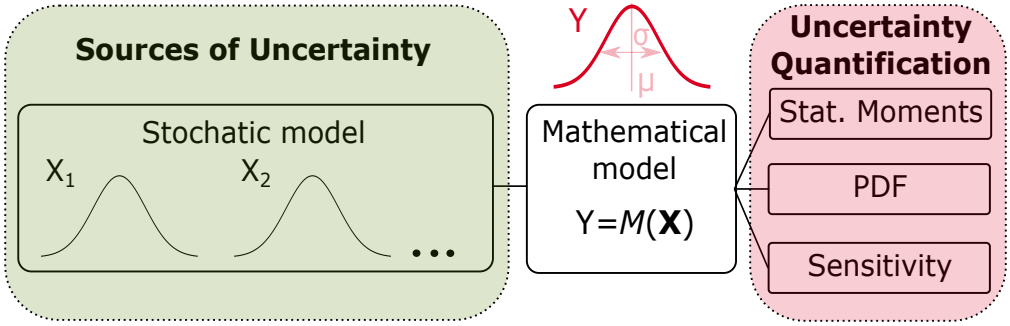

ECoV: Point Estimates

Semi-probabilistic approach

How to determine design value of resistance R_d?

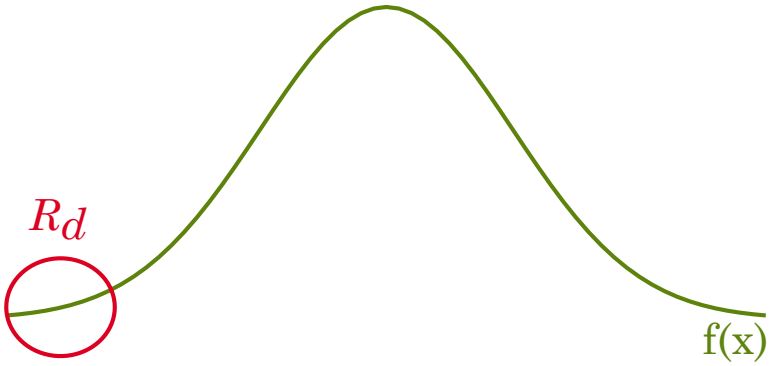

$$R_d = \mu_R \cdot exp(-\alpha_R \beta v_R)$$

Task Definition

- slightly non-linear function solved by NLFEM
- separation of Resistance and Load (α_R)
- assumption of 2 parametric Lognormal distribution (Gaussian)
- simplified task: estimation of mean value and variance (V_R)
- coefficient of variation v_R can be decomposed as:

$$V_R = \sqrt{\cancel{V_g^2} + \cancel{V_m^2} + V_f^2},$$

ECoV methods in 2D

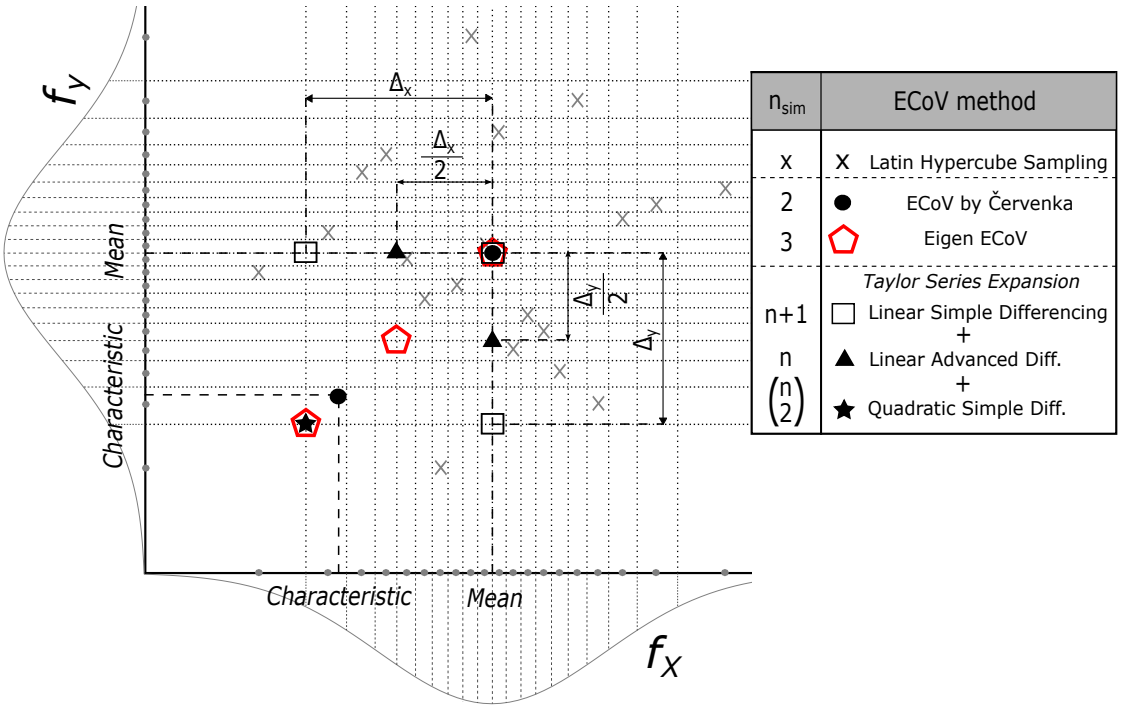

ECoV by Červenka

- determination of global safety factor is based on sensitivity factor α_R and reliability index β (JCSS)
- **2** simulations are needed for estimation of coefficient of variation v_R
- implemented in *fib* ModelCode 2010

$$R_d = \frac{R(X_m)}{\gamma_R \gamma_{R_d}} \; ; \; v_R = \frac{1}{1.65} \, ln\left(\frac{R_m}{R_k}\right)$$

$$\gamma_R = exp(\alpha_R \beta v_R)$$

ČERVENKA, V.: Reliability-based non-linear analysis according to fib Model Code 2010. Struct Concr J fib, 2013, 14:19-28.

JCSS, JCSS Probabilistic Model Code, Joint Committee on Structural Safety (2001), iSBN 978-3-90938679-6.

Walraven, J., (editor), fib Model Code for Concrete Structures 2010, September 2013. ISBN: 978-3-433-03061-5.

Linear TSE (TSE I)

- based on Taylor series expansion for uncorrelated variables
- closed formula for variance and mean value
- simple one-sided differencing

$$CoV_R = \frac{1}{r_\mu}\sqrt{\sum_i^n \left(\frac{r_\mu - r_{X_{i\Delta}}}{\Delta_{X_i}}\sigma_{X_i}\right)^2}$$

$$X_{i\Delta} = F_i^{-1}(\Phi(-c)) \approx \mu_{Xi}\cdot[1 - exp(-c\cdot\sigma_{X_i})]$$

$$\frac{\partial r(X)}{\partial X_i} = \frac{r_\mu - r_{X_{i\Delta}}}{\Delta_{X_i}}$$

H. SCHLUNE, K. GYLLTOFT, and M. PLOS, "Safety formats for non-linear analysis of concrete structures," in Mag Concrete Res (2012) 64:563-74.

Advanced differencing (TSE II)

- based on Taylor series expansion
- closed formula for variance and mean value
- adapted second order backward differencing

$$\mathrm{VAR}[R] = \sum_i^n \left(\frac{\partial r(\mathbf{X})}{\partial X_i}\sigma_{X_i}\right)^2$$

$$\frac{\partial r(\mathbf{X})}{\partial X_i} = \frac{3R_m - 4R_{Xi\frac{\Delta}{2}} + R_{X_{i\Delta}}}{\Delta_{X_i}}$$

$$R_{Xi\frac{\Delta}{2}} = r(\boldsymbol{X}_{\boldsymbol{i}\frac{\Delta}{2}}) = r(X_1, ..., X_{i\frac{\Delta}{2}}, ..., X_N)$$

$$X_{i\frac{\Delta}{2}} = \mu_{Xi} - \Delta_{X_i}/2$$

TSE sampling in 2D

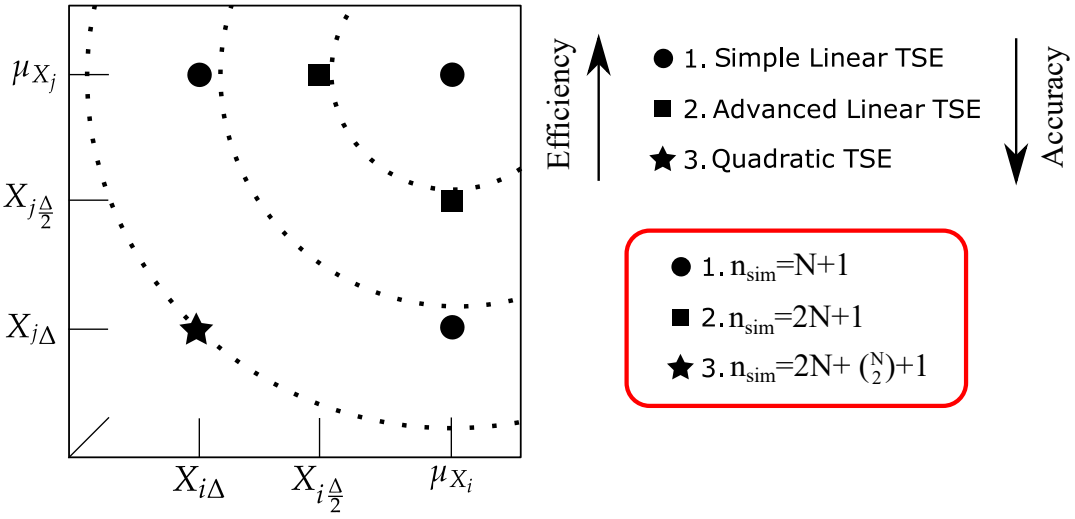

L. Novák, D. Novák "On Taylor Series Expansion for Statistical Moments of Functions of Correlated Random Variables" Symmetry 2020, 12(8), 1379

Eigen ECoV (derived from TSE)

$$v_R \approx \frac{3R_m - 4R_{\Theta\frac{\Delta}{2}} + R_{\Theta\Delta}}{\Delta_\Theta} \cdot \frac{\sqrt{\lambda_1}}{R_m},$$

where $R_{\Theta\Delta} = r(X_{1\Delta}, \ldots, X_{N\Delta})$ and $R_{\Theta\frac{\Delta}{2}} = r\left(X_{1\frac{\Delta}{2}}, \ldots, X_{N\frac{\Delta}{2}}\right)$

The Eigen distribution of the input random vector $\Theta \sim (\mu_\Theta, \sigma^2_\Theta)$ is described by:

$$\sigma^2_\Theta = \sum \sigma^2_{X_i} = \lambda_1,$$

$$\mu_\Theta = \sqrt{\sum_{i=1}^{N} (X_{mi})^2}$$

$$\Delta_\Theta = \mu_\Theta - \mu_\Theta \cdot exp\left(-c \cdot \frac{\sqrt{\lambda_1}}{\mu_\Theta}\right)$$

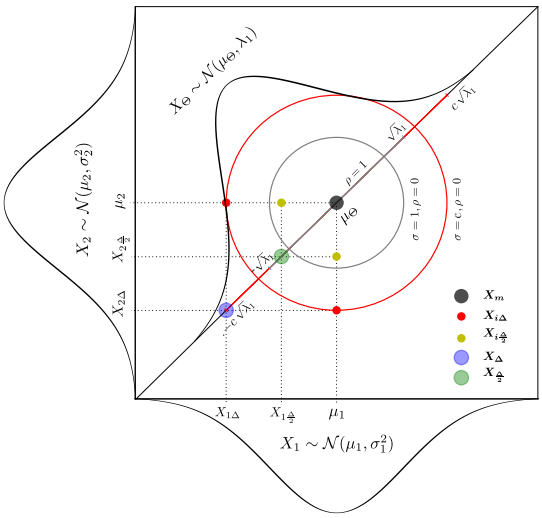

L. Novak, D. Novak "Estimation of coefficient of variation for structural analysis: The correlation interval approach" *Structural Safety*, 2021, vol. 92, 102101.

Surrogate models for UQ

Polynomial Chaos Expansion

$$Y = \mathcal{M}(\mathbf{X}) = \sum_{\alpha \in \mathbb{N}^M} \beta_\alpha \Psi_\alpha(\mathbf{X})$$

- deterministic **coefficients** to be computed - β_α
- orthonormal **basis** of multivariate polynomials - $\Psi_\alpha(\mathbf{X})$
- M represents number of input random variables
- multi-index $\alpha = \{\alpha_1, ..., \alpha_M\}$, $\mathcal{A} = \{\alpha \in \mathbb{N}^M\}$

GHANEM R.G., SPANOS P.D. Stochastic finite elements—a spectral approach. Berlin: Springer; 1991

Orthonormal basis

$$\langle \psi_\alpha, \psi_\beta \rangle = \int \psi_\alpha(\xi)\psi_\beta(\xi)p_\xi(\xi)d\xi = \delta_{\alpha\beta}$$

- multivariate basis functions are orthonormal with respect to the joint PDF p_ξ.
- normalized Hermite polynomials are orthonormal to Gaussian probability measure in the Wiener-Hermite PCE.
- common distributions can be associated to specific type of polynomial (Wiener-Askey scheme).

XIU, D.; KARNIADAKIS, G.: The Wiener-Askey polynomial chaos for stochastic differential equations. J Sci. Comput., 2002, 24(2):619-44.

Orthonormality of PCE

- generally statistical moment of any order is defined as:

$$\langle y^m \rangle = \int [f(\mathbf{X})]^m p_\xi(\xi)d\xi = \int [\sum_{\alpha\in\mathbb{N}^M} \beta_\alpha \Psi_\alpha(\xi)]^m p_\xi(\xi)d\xi =$$
$$= \int \sum_{\alpha_1\in\mathbb{N}^M} \dots \sum_{\alpha_m\in\mathbb{N}^M} \beta_{\alpha_1}\dots\beta_{\alpha_m}\Psi_{\alpha_1}(\xi)\dots\Psi_{\alpha_m}(\xi)p_\xi(\xi)d\xi =$$
$$= \sum_{\alpha_1\in\mathbb{N}^M} \dots \sum_{\alpha_m\in\mathbb{N}^M} \beta_{\alpha_1}\dots\beta_{\alpha_m} \int \Psi_{\alpha_1}(\xi)\dots\Psi_{\alpha_m}(\xi)p_\xi(\xi)d\xi$$

- it might be computationally demanding to employ MC
- PCE leads to dramatic simplification of equation due to the orthonormality of basis polynomials

Non-intrusive PCE

- PCE basis is made of polynomials up to a certain degree p
- coefficients by OLS $\rightarrow \mathcal{Y} = \mathcal{M}(\mathbf{X})$ for n_{sim}
- $n_{sim} \geq 3 - 5P$, where $P = \text{card } \mathcal{A}$

$$\boldsymbol{\beta} = (\boldsymbol{\Psi}^T \boldsymbol{\Psi})^{-1} \boldsymbol{\Psi}^T \mathcal{Y}$$

$$\boldsymbol{\Psi} = \left\{ \Psi_{ij} = \Psi_j(\boldsymbol{\xi}^{(i)}), i = 1, ..., n, \quad j = 0, ..., P-1 \right\}$$

Tensor product Total pol. order Hyperbolic Sparse solution

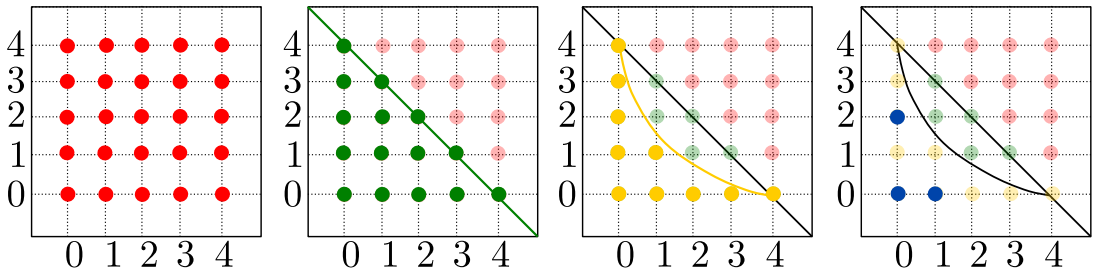

Sensitivity analysis: Sobol' indices

- Hoeffding-Sobol' decomposition - Sobol' indices (ANOVA)
- highly efficient derivation of Sobol' indices from PCE
- first order indices

$$S_i = \sum_{\alpha \in \mathcal{A}_i} \frac{\beta_\alpha^2}{Var\left[\tilde{\mathcal{M}}^{PCE}\right]} \qquad \mathcal{A}_i = \left\{ \alpha \in \mathbb{N}^M : \alpha_i > 0, \alpha_{j \neq i} = 0 \right\}$$

- total indices

$$S_i^T = \sum_{\alpha \in \mathcal{A}_i^T} \frac{\beta_\alpha^2}{Var\left[\tilde{\mathcal{M}}^{PCE}\right]} \qquad \mathcal{A}_i^T = \left\{ \alpha \in \mathbb{N}^M : \alpha_i > 0 \right\}$$

SUDRET, B.: Global sensitivity analysis using polynomial chaos expansions. Reliab Eng and System Safety, 2008, 93: p. 964-979.

SOBOL, I.: Global sensitivity indices for nonlinear mathematical models and their Monte Carlo estimates. Math and Comput in Simulation 55, 2001, p. 271-280.

Higher moments and Sensitivity

- Sobol indices consider only the first 2 moments
- Higher statistical moments: shape of PDF
- Monte Carlo (LHS) needs thousands of simulations
- Efficient alternative? → Polynomial Chaos Expansion

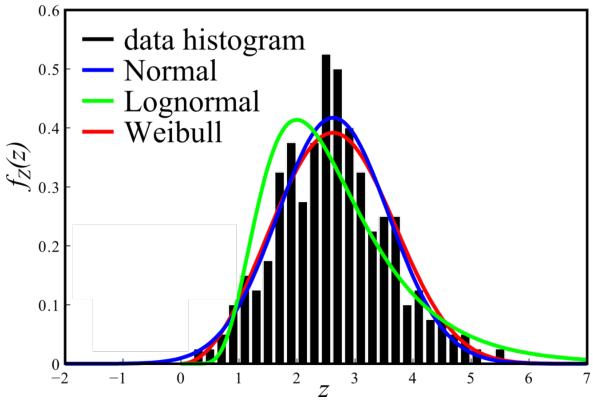

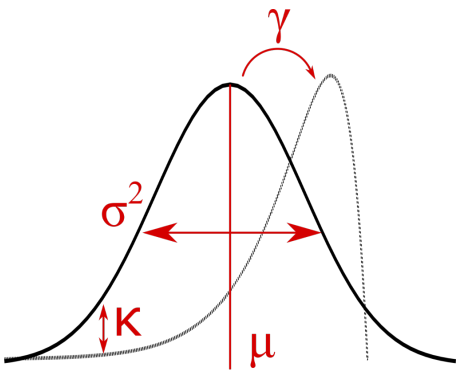

NOVÁK, L. On Distribution-Based Global Sensitivity Analysis by Polynomial Chaos Expansion. *Computers & Structures*, 2022

Distribution-based SA

- Conditional moments → conditional CDFs
- Generalization of Sobol indices for PCE

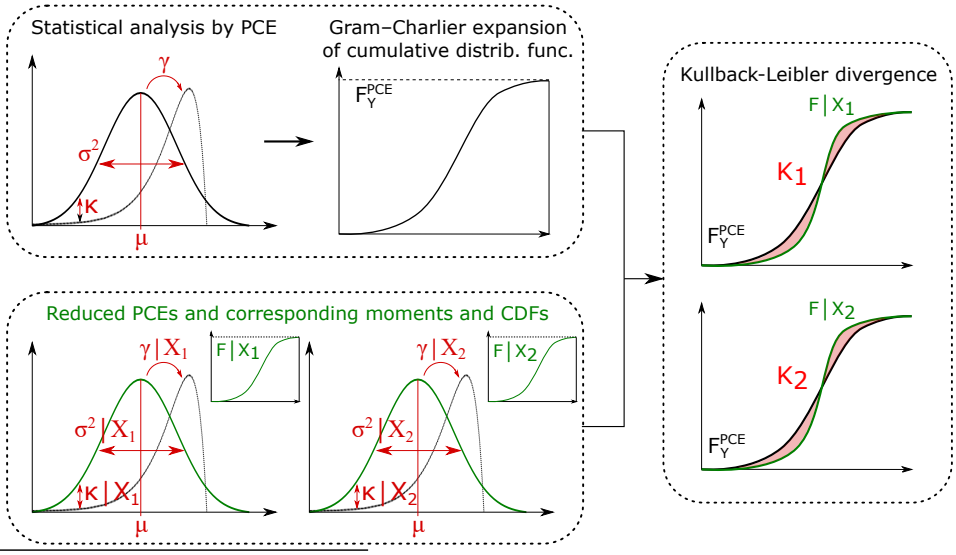

NOVÁK, L. On Distribution-Based Global Sensitivity Analysis by Polynomial Chaos Expansion. *Computers & Structures*, 2022

Industrial Application & Comparison

NLFEM of prestressed bridge

length 19.98m and total width 16.6m (midspan)
16 prefabricated bridge girders
NFEM in ATENA, including construction process
5 random variables
1 simulation takes approx. 24 hours

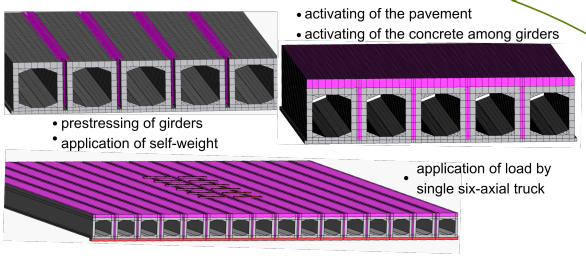

Polynomial Chaos Expansion

Complex stochastic models

Negligible comp. req. per simulation
Statistical & sensitivity analysis
Higher number of simulations

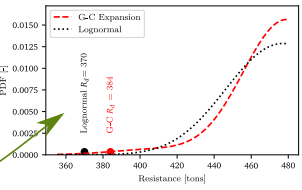

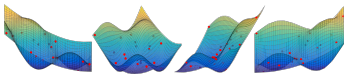

Semi-probabilistic approach

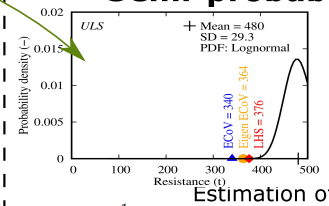

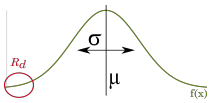

Simplified models

$$R_d = \phi_{Ln}^{-1}(p_f)$$

Estimation of the first two statistical moments
Assumptions on correlation and distribution
Negligible number of simulations

Recent Developments

Scientific Machine Learning

- Machine learning & Scientific Computations → SciML
- Foundations: Domain-aware, Interpretable, Robust
- Recent breakthrough: Physics-informed Neural Networks (PINNs) by Raissi et al. 2019 (7750 citations)
- Uncertainty quantification in SciML?

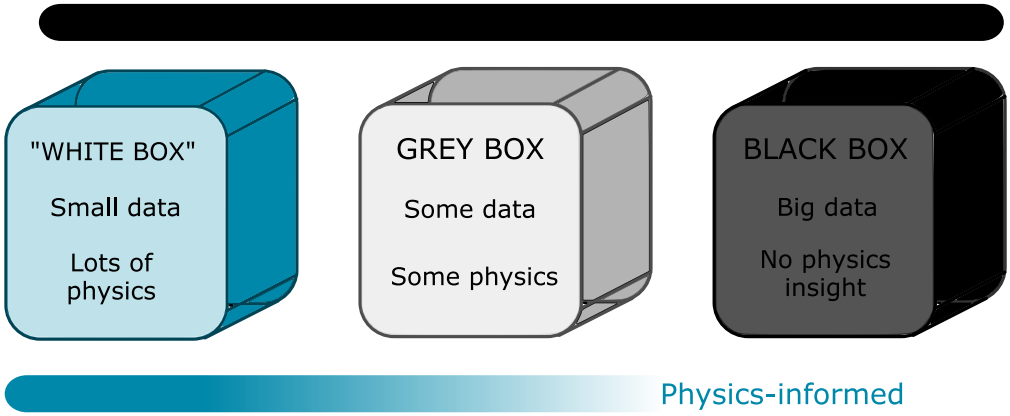

PC²: Physically Constrained PC

- Orthonormal basis in PCE
  - Analytical form (fast evaluation) → easy derivation
  - Efficient for UQ (statistical and sensitivity analysis)
- Physical constraints
  - Combination of data ($\mathbf{X}$, $\mathcal{M}(\mathbf{X}) = \mathcal{Y}$) and equality constraints
  - Boundary conditions: Dirichlet, Neumann, Mixed, etc.
  - constrained by PDE/ODE in virtual samples (discrete)
- Efficient optimization?
  - Karush–Kuhn–Tucker conditions & Lagrange multipliers
  - Normal equations → constrained least squares

NOVÁK, L., SHARMA, H., SHIELDS, M. Physics-Informed Polynomial Chaos Expansions. Journal of Computational Physics 506, 2024

Lagrange multipliers, KKT

- P unknown deterministic coefficients β
- n_{sim} samples in experimental design $\Psi(\mathbf{X})$, $\mathcal{Y}$
- n_{BC} boundary conditions $\mathcal{B}[\Psi(\mathbf{X}_b)]$,$\mathbf{c}_b$
- $n_{\text{v}} = P - n_{\text{BC}}$ virtual samples $\mathcal{L}[\Psi(\mathbf{X}_v)]$,$\mathbf{c}_v$

$$\begin{aligned} \min \quad & \|\Psi(\mathbf{X})\beta - \mathcal{Y}\|^2 \\ \text{s.t.} \quad & \mathcal{B}[\Psi(\mathbf{X}_b)]\beta = \mathbf{c_b} \\ & \mathcal{L}[\Psi(\mathbf{X}_v)]\beta = \mathbf{c_v} \end{aligned}$$

$$\underbrace{\begin{bmatrix} \boldsymbol{\Psi}^T\boldsymbol{\Psi} & \boldsymbol{A}^T \\ \boldsymbol{A} & \mathbf{0} \end{bmatrix}}_{\text{KKT matrix}} \begin{bmatrix} \beta \\ \lambda \end{bmatrix} = \begin{bmatrix} \boldsymbol{\Psi}^T\mathcal{Y} \\ \boldsymbol{c} \end{bmatrix}$$

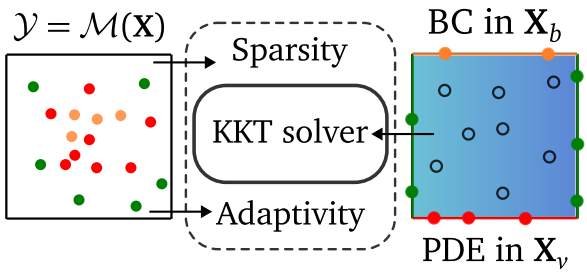

Wave Equation

- Solution of the model $\mathcal{M}(\mathbf{X})$

- Dirichlet $\begin{cases} y(0,t) = y(1,t) = 0 \\ y(x,0) = \sin(\pi x) \end{cases}$

- Neumann $\dfrac{\partial y(x,0)}{\partial t} = 0$

- Virtual $\dfrac{\partial^2 y(x,t)}{\partial t^2} = 4\dfrac{\partial^2 y(x,t)}{\partial x^2}$

The code is available here.

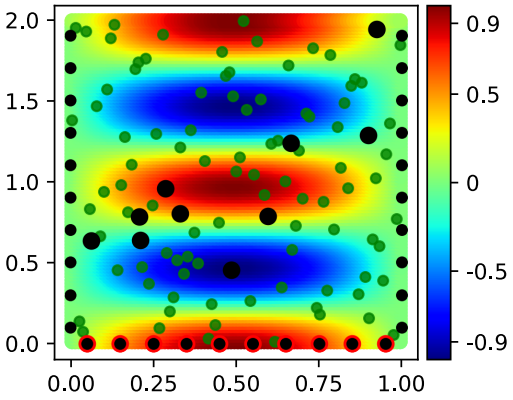

●● standard LAR PCE

●●●● PC^2 based on KKT (LAR)

→ iterative algorithm
$p \in [12, 14]$

Heat Equation with Random $\mathcal{D}$

$$\frac{\partial f(x,t)}{\partial t} = \mathcal{D}\frac{\partial^2 f(x,t)}{\partial x^2}, \qquad x \in [0,1], \quad t \in [0,1], \quad \mathcal{D} \sim \mathcal{U}[0.2, 0.8]$$
$$f(0,t) = f(1,t) = 0, \qquad f(x,0) = \sin(\pi x)$$

- PC^2 based on 90 $\mathbf{X}_{\mathrm{BC}}$ and $\mathbf{X}_{\mathrm{v}}$ ($n_{sim} = 0$)

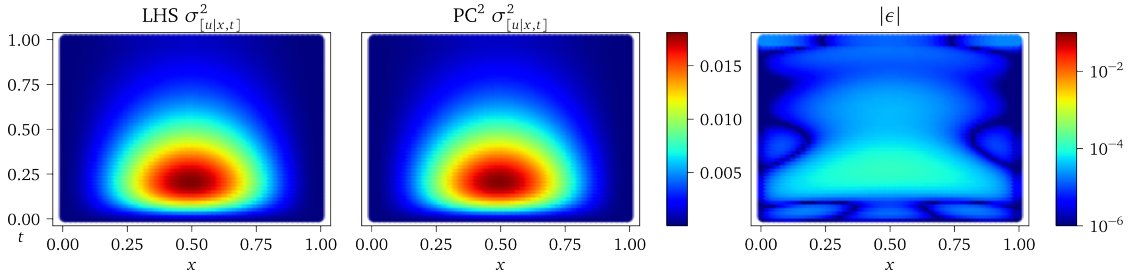

Mean and Quantiles

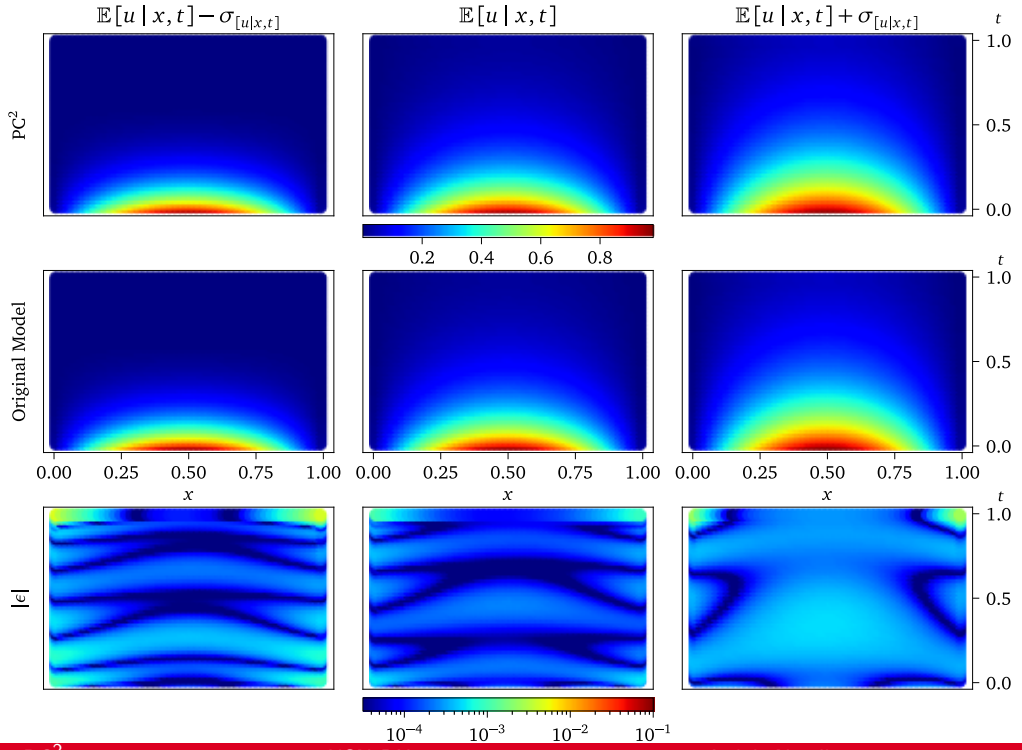

Stochastic Euler Beam

- $EI = const. = 1$, KLE: $q(x) = \sum_{i=1}^{N} \sqrt{\lambda_i}\theta_i(\omega)f_i(x)$
- truncation: $N \in [1, 2, .., 5]$
- PC^2 based on only $\mathbf{X}_{\mathrm{BC}}$ and $\mathbf{X}_{\mathrm{v}}$ ($n_{sim} = 0$)

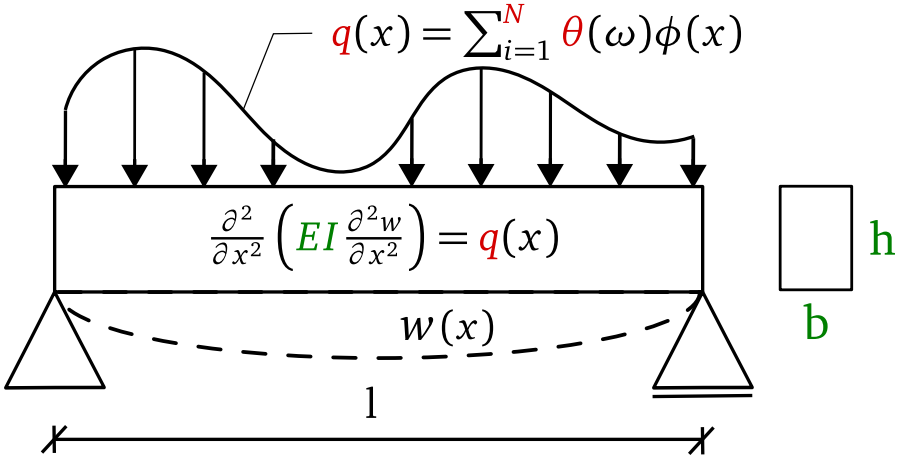

PC^2 random realizations

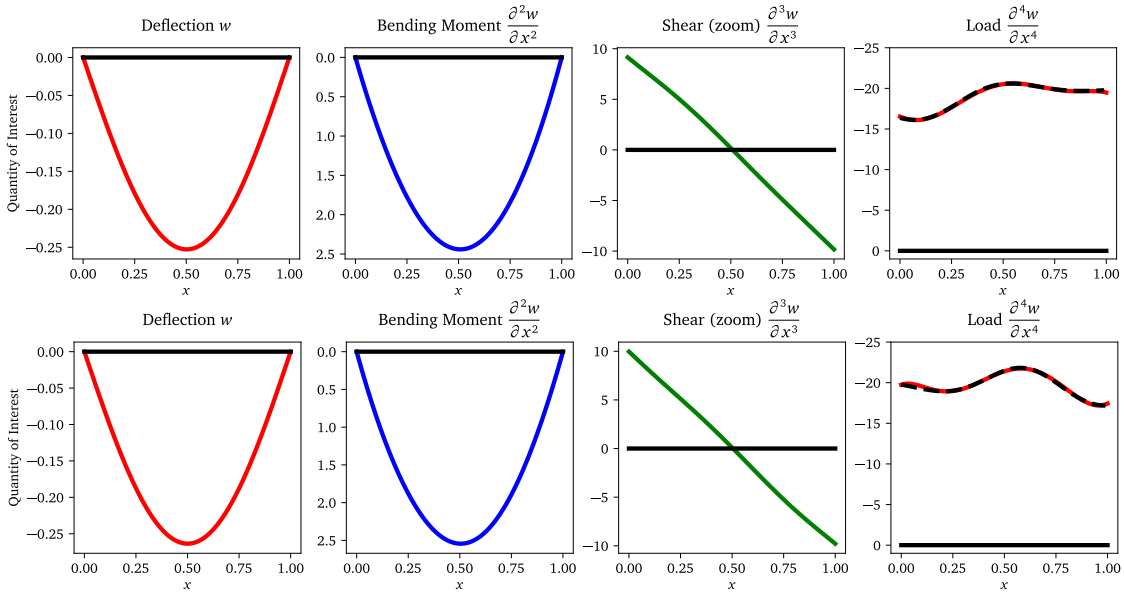

PC^2 UQ & Derivatives

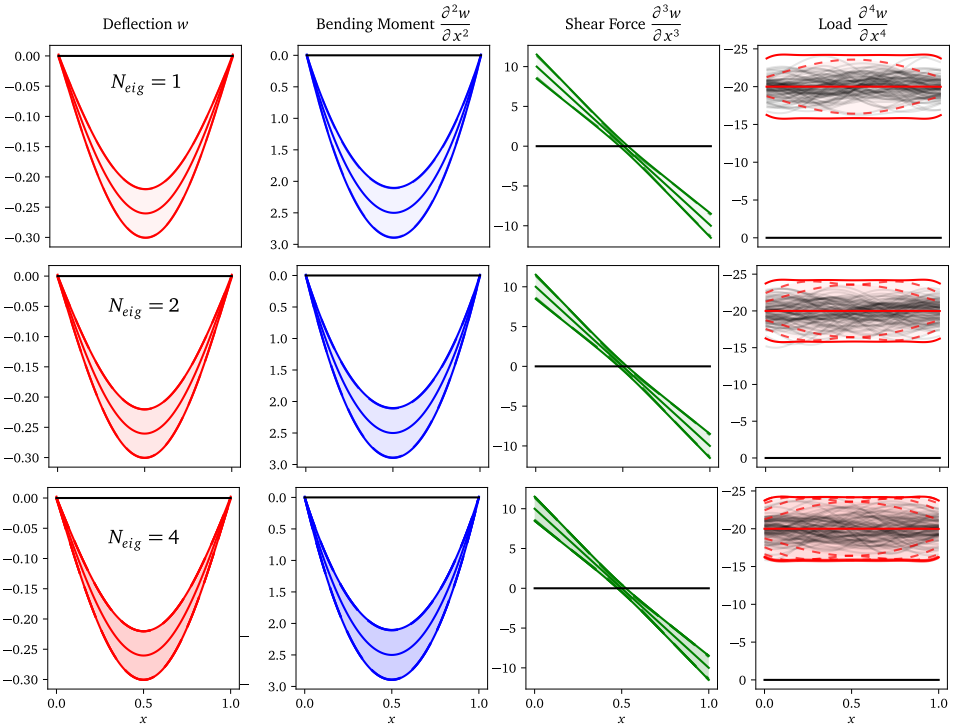

PC^2 is available in UQPy!

- available on the Python Package Index (PyPI) and Conda:
  Quick Guide for Installation of Jupyterlab and Anaconda
- version control through git (requires Python 3):
  https://github.com/SURGroup/UQpy
- Examples & Documentation:
  https://uqpyproject.readthedocs.io/en/latest/

TSAPETIS, D.; SHIELDS, M.; GIOVANIS, D.; OLIVIER, A.; NOVÁK, L.; CHAKROBORTY, P.; SHARMA, H.; CHAUHAN, M.; KONTOLATI, K.; VANDANAPU, L.; LOUKREZIS, D.; GARDNER, M. UQpy v4.1: Uncertainty quantification with Python. SoftwareX, 2023

Conclusions

- UQ plays an important role in engineering
- simplified point-estimates: ECoV methods
- complex analysis: surrogate models (PCE)
- PC^2 for UQ of random and stochastic PDEs
- PC^2 is available in UQPy!

Thank you for your attention!

SHARMA, H., NOVÁK, L., SHIELDS, M. Physics-constrained polynomial chaos expansion for scientific machine learning and uncertainty quantification. arXiv, 2402.15115, 2024